

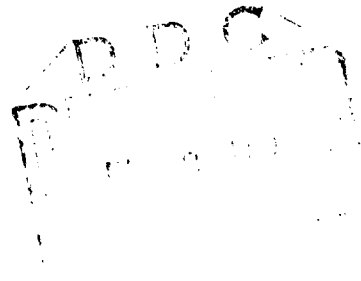
AD 701902



AD

Technical Report 46-TR
**USE OF SIDE-LOOKING AIRBORNE RADAR (SLAR)
IMAGERY FOR ENGINEERING SOILS STUDIES**
by
Dr. David J. Barr
September 1969

This document has been approved for public
release and sale; its distribution is unlimited.



Reproduced by the
CLEARINGHOUSE
Federal Scientific & Technical
Information, Springfield, Va. 22151

**U.S. ARMY ENGINEER TOPOGRAPHIC LABORATORIES
FORT BELVOIR, VIRGINIA**

123

**U. S. ARMY ENGINEER TOPOGRAPHIC LABORATORIES
FORT BELVOIR, VIRGINIA**

Technical Report 46-TR

**USE OF SIDE-LOOKING AIRBORNE RADAR (SLAP)
IMAGERY FOR ENGINEERING SOILS STUDIES**

Project 4A623501A854

September 1969

Distributed by

**The Commanding Officer
U. S. Army Engineer Topographic Laboratories**

Prepared by

**Dr. David J. Barr
for the
Geographic Information Systems Branch
Geographic Sciences Division**

**This document has been approved for public
release and sale; its distribution is unlimited.**

SUMMARY

This report is concerned with the development and evaluation of techniques of utilizing Side-Looking Airborne Radar (SLAR) imagery for engineering soils studies. The primary objective was the development of a systematic SLAR image interpretation technique. Secondary objectives included an evaluation of methods for quantification of SLAR image textures and radar shadows. SLAR images from a variety of physiographic regions within the United States were evaluated. Systems operating at several wavelengths were represented in the study. Field checking was performed for several of the study sites. Major conclusions from the quantitative analysis and evaluation of the various SLAR images are as follows:

1. It is possible to interpret regional engineering soil types by means of an inference technique based on recognition and evaluation of repetitive, characteristic patterns.
2. "Brute force" SLAR imagery allows a more detailed interpretation than does "synthetic aperture" SLAR imagery.
3. At the wavelengths utilized for the study imagery, the pattern elements were derived as a function of microwave reflection from the first surface of the terrain.
4. The relatively small scale at which SLAR imagery is obtained and the resolution of typical imagery are considered advantageous for regional engineering soils interpretations. SLAR imagery provides a synoptic view of terrain unconfused by minor tonal contrast.

FOREWORD

Authority for performing the research and for preparing this report is contained in Project 4A623501A854, "Military Geographic Intelligence."

The research carried out in the preparation of this report was accomplished by David J. Barr as a doctoral thesis under the direction of Professor Robert D. Miles, School of Civil Engineering, Purdue University. The study was prepared under the supervision of Everard G. A. Barnes, Project Engineer; Marvin Gast, Chief, Geographic Applications Branch; and Dr. Kenneth R. Kothe, Chief, Geographic Sciences Division, U. S. Army Engineer Topographic Laboratories, Fort Belvoir, Virginia.

CONTENTS

<u>Section</u>	<u>Title</u>	<u>Page</u>
	SUMMARY	ii
	FOREWORD	iii
	ILLUSTRATIONS	vi
	TABLES	viii
I	INTRODUCTION	
	1. Subject	1
	2. Purpose and Scope	2
II	RADAR PRINCIPLES AND BASIC ELECTROMAGNETIC ENERGY CONSIDERATIONS	
	3. Definition and History of Radar	3
	4. The SLAR System Components	4
	5. Frequencies of Operation	5
	6. Resolution of SLAR	5
	7. Radar Image Geometry	10
	8. Image Presentation	10
	9. Scales	10
	10. Terrain Elevations	15
	11. Radar Equation	19
	12. Scattering Theories	21
	13. General Considerations of the Reliability of SLAR Imagery as a Record of Terrain Reflectance Data	25
III	PREVIOUS INVESTIGATION	
	14. Early Research	26
	15. Research from 1962 to 1965	28
	16. Recent Research	32
IV	RESEARCH APPROACH	
	17. Introduction	36
	18. Acquisition of Imagery	36
	19. Qualitative Analysis of SLAR Imagery	37
	20. Quantitative Analysis of SLAR Imagery	40
	21. Collection of Ground-Truth Information	40

CONTENTS (cont'd)

<u>Section</u>	<u>Title</u>	<u>Page</u>
V	QUALITATIVE ANALYSIS OF SLAR IMAGERY	
	22. Introduction	42
	23. Evaluation of Pattern Elements	42
	a. Analysis of Element of Tone	42
	b. Analysis of Element of Image Texture	53
	24. Detailed Analysis of SLAR Image Patterns	54
	a. SLAR Image Patterns of Drainage	57
	b. SLAR Image Patterns of Topography	58
	c. SLAR Image Patterns of Land Use	63
	25. Interpretation of Landforms	64
	26. Interpretation of Local, Land-Surface Conditions	68
	27. Systematic SLAR Image Interpretation Technique	69
	28. Effect of System Design, Image Resolution, and Degradation on Interpretation	71
	29. Evaluation of the Systematic Interpretation Technique	71
	30. Comparison Between SLAR Image and Aerial Photograph Interpretation	72
	31. Summary of Qualitative SLAR Image Analyses	73
VI	QUANTITATIVE ANALYSIS OF SLAR IMAGERY	
	32. Introduction	95
	33. Image Texture Analysis	95
	a. Selection of Sample Areas	95
	b. Generation of Probability/Density Curves	96
	c. Analysis of Probability/Density Curves	99
	d. Interpretation of Results	100
	34. Radar Shadow Analysis	103
	a. Selection of Sample Locations	103
	b. Collection of SLAR Image Data	103
	c. Determination of a Terrain-Roughness Parameter	104
	d. Analysis of Data	107
	e. Interpretation of Results	107
	f. Potential Application of the Roughness Model	109
VII	CONCLUSIONS	
	35. Conclusions	111
	LITERATURE CITED	113
	APPENDIX	123

ILLUSTRATIONS

<u>Figure</u>	<u>Title</u>	<u>Page</u>
1	SLAR-System Diagram	4
2	Technique of Producing Map-Like Display with SLAR	6
3	Geometry of Range Resolution	9
4	Geometry of Azimuth Resolution	9
5	Slant Range Image Geometry	11
6	Image Scale Geometry	13
7	Terrain Elevation Geometry	17
8	Terrain Feature Types	18
9	Stereo Configurations	20
10	Variation of Backscattering Coefficients at X-Band	24
11	Dynamic Range of Terrain Parameter at K- and X-Band	24
12	Discrete Tonal Elements	49
13	Average Areal Tones	51
14	SLAR Image Textures	55
15	Basic Patterns of Drainage	59
16	Patterns of Topography	61
17	Patterns of Land Use	65
18	Systematic Interpretation Flow Diagram	70
19	Example Interpretation: Mississippi Valley	75-77
20	Example Interpretation: Arizona	79-81
21	Example Interpretation: Wyoming	83-85
22	Example Interpretation: Pennsylvania	87-89

ILLUSTRATIONS (cont'd)

<u>Figure</u>	<u>Title</u>	<u>Page</u>
23	Example Interpretation: Northern Indiana	91-93
24	Equipment for Generating Probability/Density Curves	96
25	Representative Probability/Density Curves Obtained with 1-Millimeter Densitometer Aperture	97
26	Roughness Experiment Sampling Techniques	105

TABLES

<u>Table</u>	<u>Title</u>	<u>Page</u>
I	Radar Frequencies	7
II	SLAR Image Study Sites	38-39
III	Ground-Truth Information Sources	41
IV	Study Site Ground Truth and Environment	43-46
V	Terrain Factors and Representative Tonal Ranges	48
VI	Discrete Tonal Elements Related to SLAR Image Drainage Pattern	58
VII	Radar Characteristics of Cultural Features	67
VIII	Inferred Image Textures and Corresponding Probability/Density Curve Data	101
IX	Correlation Matrix: Probability/Density Curve Parameter Versus Inferred and Measured SLAR Image Parameters	102
X	Summary of Sample Locations and Data Used in the Terrain Roughness Experiment	106
XI	Variables Considered in Final Regression Analysis for Determination of Terrain Roughness from SLAR Imagery	108
XII	Typical Landforms and Corresponding Measured Roughness (Log K)	110

USE OF SIDE-LOOKING AIRBORNE RADAR (SLAR)

IMAGERY FOR ENGINEERING SOILS STUDIES

I. INTRODUCTION

1. Subject. Techniques for interpreting engineering soils information from aerial photography were developed at Purdue University in the early 1940's. Since that time, continued research has proved the value of the technique for engineering site selection and preliminary engineering soils investigations (66, 79).¹ The airphoto technique, which utilizes photography obtained in the visible range of the electromagnetic spectrum, is limited to the interpretation of reflections of visible light. It has been shown by many investigators that additional information concerning the materials of the earth's surface can be obtained from reflections produced by the interaction of earth materials and energy in other regions of the spectrum, such as, ultraviolet, infrared, and microwave (79, 90, 100).

Advancements in the enhancement and recording of reflected, microwave energy have produced a high-resolution, side-looking airborne radar (SLAR) system capable of producing imagery of possible value in engineering soils investigations. Side-looking radar of selected wavelengths will image a terrain surface and present a film record containing patterns of land use, drainage, land-water contacts, and cultural features. Studies have revealed that landform interpretation is possible with SLAR (7, 8, 11, 56, 87).

Remote-sensing systems operating at wavelengths other than in the visible range should facilitate the interpretation of engineering soils from remote images by identifying significant soil parameters in addition to those parameters obtained from visible photography. Surface configuration and drainage pattern as portrayed on the SLAR image might be good indicators of erodibility which, in turn, could lead to the interpretation of engineering soil types. It is hypothesized that certain microwave wavelengths may penetrate the soil and be reflected by subsurface layers (29). The evaluation of these radar potentials with respect to engineering soils interpretation will better define the worth of microwave imagery for civil engineering and geological endeavors.

Sufficient evidence exists to justify applied research aimed at determining and developing a technique of engineering soils interpretation from SLAR imagery. Furthermore, inasmuch as it pertains to soils and terrain, a capability for engineering site selection from SLAR imagery should be developed.

1. Numbers in parentheses refer to items in *Literature Cited*, p. 113.

2. Purpose and Scope. The primary objective of this study was to evaluate the potential of SLAR imagery as a means of defining and mapping engineering soils. A necessary part of this evaluation was the development of a logical, systematic technique for interpreting engineering soil types from SLAR imagery. Secondary objectives included: (1) an evaluation of methods for quantification of SLAR image textures and radar shadows; (2) an evaluation of the advantage of using SLAR imagery in combination with aerial photography; and (3) a literature survey of the techniques of interpreting the imagery obtained by various SLAR systems in varying environments.

Radar systems operate at wavelengths of a few centimeters to several meters and are active systems which generate their own source of "illumination." Consequently, the radar-system parameters and the parameters of terrain which affect the returned energy are significantly different from those of conventional, photographic systems. An understanding of these differences is essential for the correct evaluation of radar returns from terrain. Section II covers the electronic characteristics and imaging geometry of typical, side-looking, airborne radar systems and the basic energy considerations involved in the imaging of terrain by radar.

Section III reviews previous investigations concerned with the evaluation of terrain and earth conditions by means of radar-imagery analysis. Investigations utilizing the concept of pattern analysis and the inference technique are evaluated in terms of their potential for engineering soils mapping and regional engineering site investigation.

The remaining sections of the report deal with methods of investigation and specific qualitative and quantitative experiments. In addition, conclusions and a systematic radar interpretation procedure are presented. Section IV presents the methods of investigation, selection of imagery, and a field and literature investigation of the study sites. Sections V and VI deal with specific qualitative and quantitative experiments leading to the development of a technique for the extraction of engineering soils information from SLAR imagery. Section VII presents the conclusions derived from this study. The Appendix is a summary of landforms and their image characteristics used for this study presented as a manual for the interpretation of engineering soils from SLAR imagery.

This study, supported under Contract DA-44-009-AMC-1847(X), was performed for the U. S. Army Engineer Topographic Laboratories (ETL), Fort Belvoir, Virginia. Radar imagery was provided by ETL; the U. S. Army Electronics Command; Autometric Corporation; and the Rome Air Development Center. During the course of the study, many research groups were visited for discussions concerning the present state-of-the-art of terrain and materials interpretation from SLAR imagery. Research groups of the United States Geological Survey at Flagstaff, Arizona; Denver, Colorado; Menlo Park, California; and Silver Spring, Maryland, were visited. Meetings were also

held with researchers working for the Autometric Corporation and the Goodyear Aerospace Corporation.

II. RADAR PRINCIPLES AND BASIC ELECTROMAGNETIC ENERGY CONSIDERATIONS

3. Definition and History of Radar. Radar, an acronym for the words *RA*dio *D*etection *A*nd *R*anging, can be defined as a device to determine the presence and location of an object or objects by sensing an echo of radio energy from that object. By the measurement of the time interval between transmission of radio energy and reception of reflected energy, the range of an object from a radar antenna can be determined. Azimuth of the object is determined by the direction from which the energy is reflected. The velocity of a moving object can be determined by measuring the Doppler shift in frequency of the reflected energy. A common analogy to describe the operation of radar is sound. The foghorn on a ship transmits energy at audio frequencies in all directions. If a land mass is near enough, an echo will be reflected to the ship. The direction from which the echo is heard establishes the azimuth of the land mass; while the time it takes for the echo to return is proportional to the range of the land mass.

The practical effect of radar was first observed in 1922 when Naval Research Laboratory engineers noted that a ship passing between a radio transmitter and a receiver caused radio energy to be reflected to the transmitter (2). Research conducted before and during World War I established the value of radar for a variety of military applications. Radar was used extensively during World War II for fire control, navigation of ships and planes, and target detection. Since World War II, the potential of radar for nonmilitary applications has been investigated. Imaging radar has been of special interest to cartographers, earth scientists, and photo interpreters.

Plan-Position-Indicator (PPI) radar and SLAR are the two systems which produce a visible display capable of being used for the study of terrain conditions. PPI display airborne radar, operational since World War II, is the most common radar which produces a map-like display of the earth's surface. PPI displays consist of a cathode ray tube (CRT) which indicates range and azimuth of targets for a full 360 degrees. Antennas for PPI radar systems are highly directional in the horizontal plane, rotate a full 360 degrees, and are synchronized with the circular deflection of the CRT indicator. The CRT can be photographed by a conventional camera to produce a permanent record of the land-surface image. The SLAR system, on the other hand, designed especially for producing a radar image of terrain, has a strip film as its form of display. The SLAR system and basic radar principles are described in detail.

4. The SLAR System Components. The typical radar system consists of a pulse-generating device, transmitter, duplexer, receiver, antenna, and a CRT indicator. In the SLAR system, the antenna is fixed to an aircraft and the indicator consists of a strip-film camera which photographs radar returns on a CRT. Figure 1 illustrates these components in a typical SLAR system.

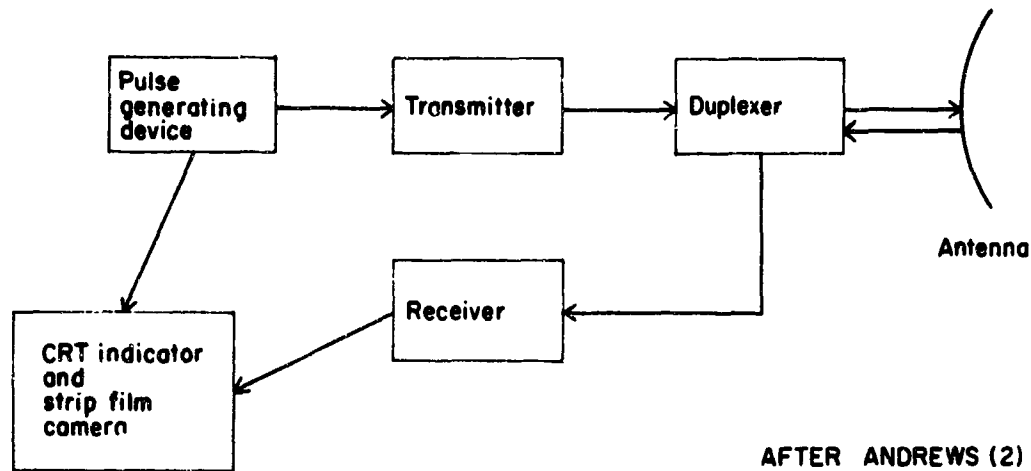


Fig. 1. SLAR-System diagram.

Pulses of electromagnetic energy are generated by an oscillator circuit which produces timing or synchronizing pulses. Because they have a small amplitude, the timing pulses are modulated by an amplifier system before being acted upon by the transmitter. Modulation also serves to determine the width or duration of the transmitted pulse by controlling the width of the keying pulse applied to the transmitter oscillator. The oscillator circuit also triggers the sweep of the CRT recording device.

The transmitter converts each pulse of energy from the generating circuit into a burst of radio-frequency (RF) energy. Special tubes, such as magnetrons or klystrons designed for high-frequency operation, are required for this transformation of energy.

SLAR systems utilize the same antenna for both transmitting and receiving the radio energy. Thus, an electronic switch is required to prevent interference between the transmitted and received pulses. The duplexer accomplishes this task by blocking the receiver during periods of transmitting and blocking the transmitter during periods of receiving.

The radar antenna is simply a reflector which focuses the RF energy into the desired shape for transmission and which also collects the returned, reflected radio waves. The physical shape of the antenna greatly affects the quality and extent of coverage of the radar image.

A superheterodyne radio receiver, basically similar to a home radio, amplifies the weak, attenuated, reflected radio waves collected by the antenna. Receivers are designed to preserve the pulse shape and phase of the reflected energy. This is of vital concern because the time relationship of the reflected energy determines its position as a resolution element on the final image.

In the case of brute force SLAR systems, reflections are amplified and displayed on a CRT as resolution elements of varying intensity. The intensity of each resolvable element on the CRT is proportional to the strength of the reflected energy from the corresponding area on the ground, while the relative position of the area is determined by the time interval between transmission of energy and its reflection back to the antenna. Figure 2 illustrates the principles involved in transforming energy reflections into a map-like display of terrain. A permanent record of the terrain display is obtained by continuously passing a photographic film, synchronized with the speed of the aircraft, across the face of the CRT. The display of a "synthetic antenna" SLAR system (more completely described in later paragraphs) is a film record of many separate return signals from each point on the ground and as such is not directly interpretable as a terrain image.

5. Frequencies of Operation. Radar frequencies range from 25 to 70,000 Megacycles (7). The common frequencies utilized for radar sensing and corresponding letter codes and wavelengths are shown in Table I. Radar frequencies generally lying within the K-band have been further sub-divided because of their general use in terrain-imaging systems. In general, radar-system components, including the antenna, must be larger for lower frequency operation in order to maintain a specified level of competence (2).

6. Resolution of SLAR. Most photographic and image-producing instruments are evaluated and compared on the basis of photograph or image resolution. For photographic purposes, resolution is defined as "the ability of the entire photographic system, including lens, exposure, processing, and other factors, to render a sharply defined image. It is expressed in terms of lines per millimeter recorded by a particular film under specified conditions." (14) For radar-imagery applications, resolution has been defined as "the ability to discriminate between two adjacent ground objects in the radar record." (7) However, according to this definition, the reflecting nature of the objects themselves in addition to the effects of the system design can affect the resolution. It has been found that two objects producing return intensities of different magnitudes may require a greater resolution distance for detection than will objects producing

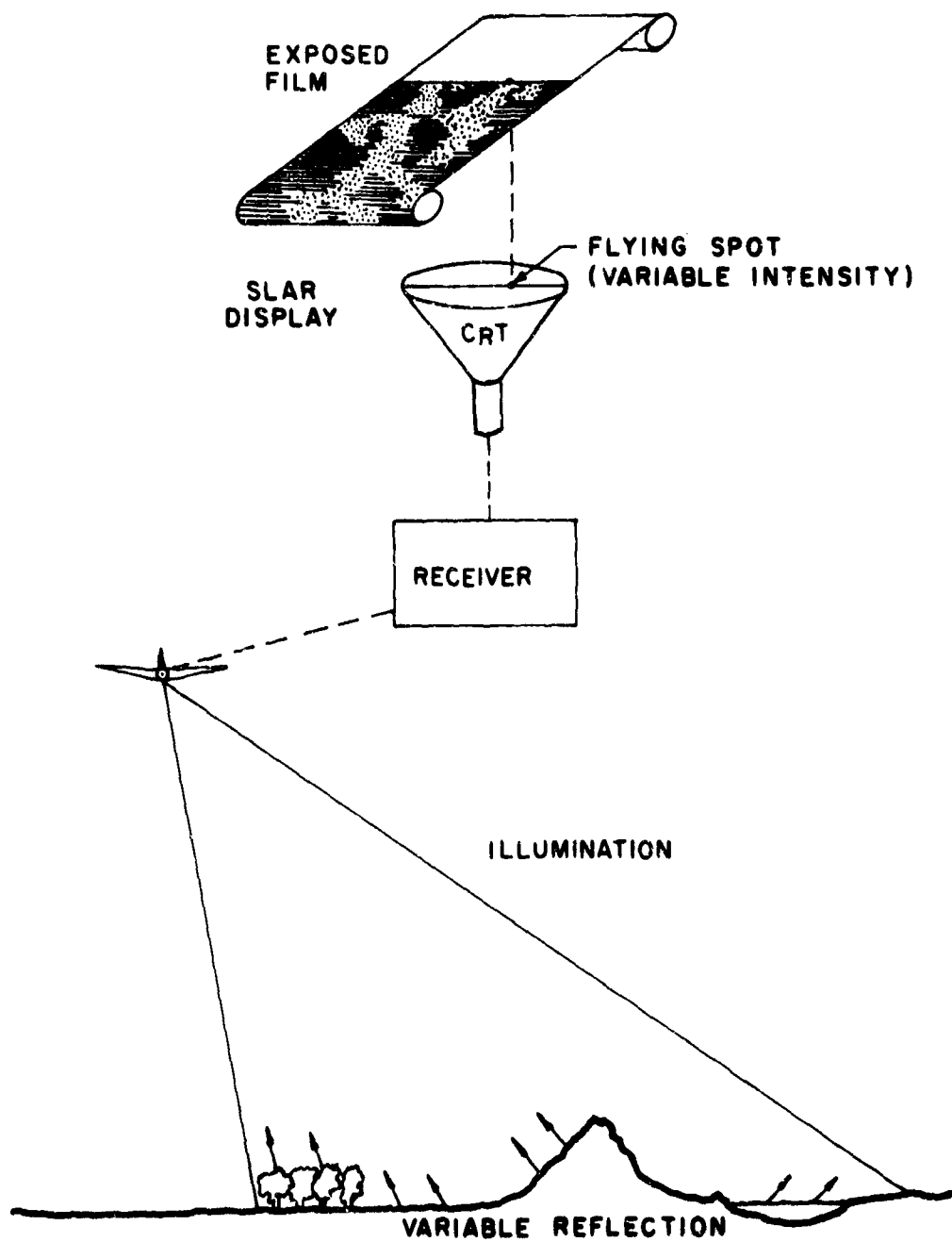


Fig. 2. Technique of producing map-like display with SLAR.

Table I. Radar Frequencies (7, 94)

Letter Code	Frequency Range (mc)	Wavelength Range (cm)
P	225 - 390	133.3 - 76.9
L	390 - 1550	76.9 - 19.3
S	1550 - 3900	19.3 - 7.69
C	3900 - 6200	7.69 - 4.84
X	6200 - 10,400	4.84 - 2.75
K (General Designation)	10,900 - 36,000	2.75 - 0.83
Ku	Approx. 12,500 - 18,000	
K	Approx. 18,000 - 26,500	
Ka	Approx. 26,500 - 40,000	
Q	36,000 - 46,000	0.83 - 0.65
V	46,000 - 56,000	0.65 - 0.54

equal return intensities (68). This is explained by the manner of imaging on the CRT. The greater the amount of reflected energy returned to the radar antenna, the brighter and larger in diameter will be the corresponding spot on the CRT. Also, the reflection from one object can interfere with and obscure the reflection from another. Thus, should one of two adjacent spots on the CRT be very bright, it could obscure the other. This problem is accentuated when the image is a terrain surface made up of multiple, reflecting surfaces. It is likely that the resolution of a radar terrain image, as previously defined, will not be a constant value over any particular image.

Moore (68) has suggested that a distinction should be made between resolution and detectability. Although it may not be possible to resolve two objects 100 feet apart, one of the objects, if it is a good reflector, may be detectable even though it is only 1 foot in diameter. Thus, the ability of an object or portion of terrain to reflect radar energy influences its detectability. Since the reflectivity of an object or terrain surface also affects the spot size on the CRT display, radar resolution is not a constant geometric factor.

These concepts of resolution and detectability are important in properly evaluating radar imagery for terrain analysis, engineering soils interpretation, and site selection. A SLAR image possesses the desirable characteristic of having a resolution such that very small details of the land surface are not emphasized whereas most cultural details, some being smaller than the resolution distance, are detectable because of their high reflectivity.

Radar image resolution is determined in large part by the pulse length of transmitted energy and the width of land surface illuminated by that pulse. Because of the side-looking nature of SLAR systems, resolutions in the range and azimuthal directions are independent factors. Range resolution normal to the line of flight is determined primarily by the length of each transmitted pulse of energy; while azimuth resolution parallel to the line of flight is established by the width of illuminated land surface (7, 97). Figures 3 and 4 illustrate the factors involved in determining range and azimuth resolution.

The range resolution of an image will theoretically be equal to one half the pulse length (τ). It can be seen in Fig. 3 that objects or points on a natural terrain surface separated by a distance equal to or less than $\tau/2 \cos\theta$ will produce reflections that arrive at the antenna as a continuous pulse of energy. Thus, the CRT indicator will display this return as a linear, bright line which in fact encompasses both objects or points. If the separation distance is greater than $\tau/2 \cos\theta$, a break in the two objects, or points, can be resolved. The designed range resolution of a SLAR system, being dependent on pulse length, is limited by the ability of the receiver to detect reflected energy. As the pulse length is shortened, the total amount of energy per pulse emitted by the transmitter is decreased. Thus, the reflected energy is weaker and becomes a limiting factor. Chirp radars overcome this limitation to some extent by utilizing electronic pulse compression techniques (94).

Azimuthal resolution is established by the width of terrain surface illuminated by the radar pulse (7). Figure 4 illustrates the geometry involved in establishing azimuthal resolution and also shows why it is not a constant value in the range direction. Objects, or points, on the land surface which lie within the illuminated strip are imaged as one in the azimuthal direction.

The antenna beam width is directly proportional to the wavelength of transmitted energy and inversely proportional to the length of the antenna. Assuming that the wavelength of the radar system is selected on the basis of desirable reflection characteristics, the desired azimuthal resolution must be obtained by properly designing the antenna. Two methods are commonly used to achieve high azimuthal resolution. In the case of "brute force" radar, as illustrated in Fig. 4, the antenna is simply made as large (long) as is physically possible (7). "Coherent" or "synthetic aperture" systems utilize an electronic technique to create a narrow band width. The equivalent of an extremely long antenna is synthesized by using the forward motion of the aircraft to carry the coherent radar antenna to positions along the line of flight which are treated electronically as though they were individual elements of a linear antenna array (18). In this coherent system, azimuthal resolution remains relatively constant throughout its range.

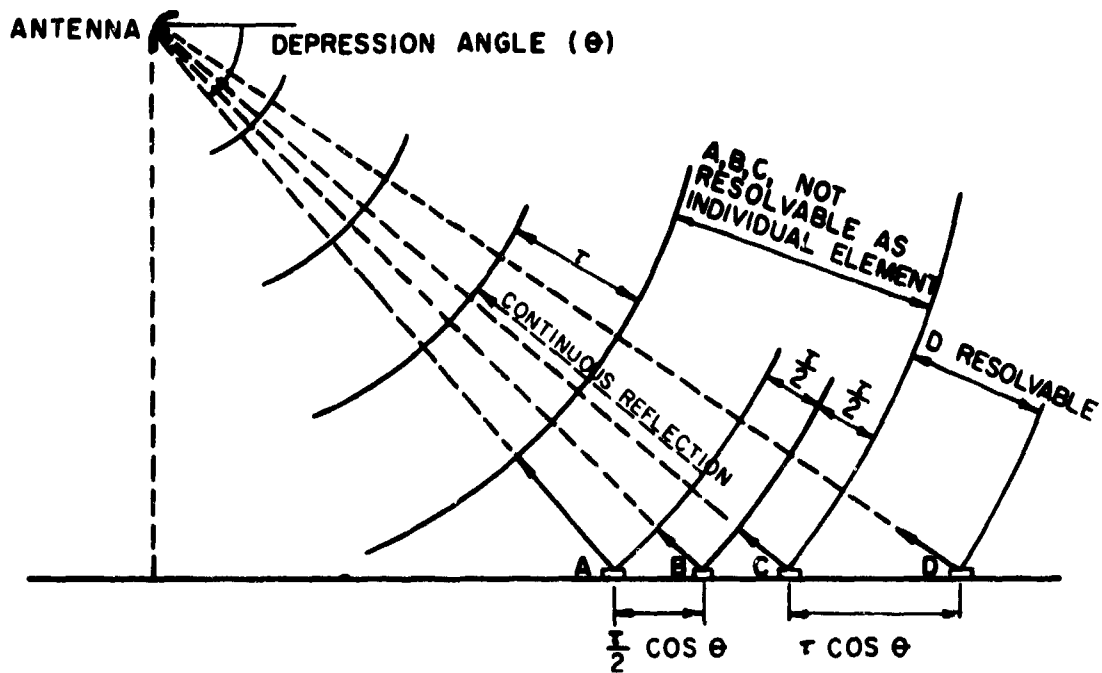


Fig. 3. Geometry of range resolution.

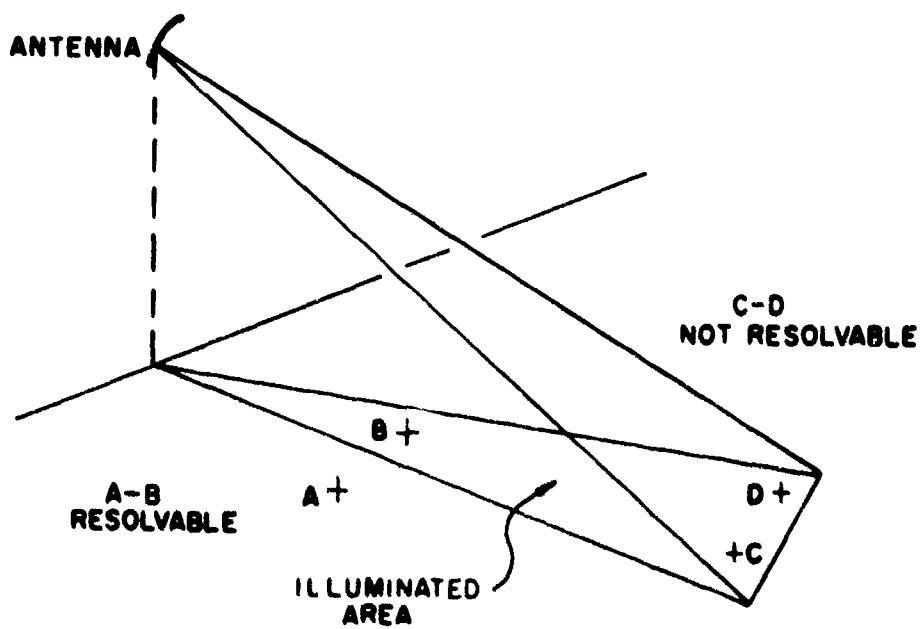


Fig. 4. Geometry of azimuth resolution.

7. Radar Image Geometry. The imaging geometry of SLAR systems is a significant factor in the design and utilization of cartographic radars as well as in terrain and soils interpretation. The interrelationship between image geometry, terrain geometry and earth curvature; image processing; and imaging aircraft instabilities produces a very complex image in terms of geometric distortion. This is a grave problem in trying to produce a geometrically accurate image for cartographic purposes, but it is not a serious handicap for the visual interpretation of terrain and soils from the imagery. When the desired product from the image is the delineation and identification of regional terrain and engineering soil types, an interpreter can sacrifice the geometric accuracy of the display without seriously degrading the value of the regional terrain and soils map. Likewise, when a preliminary map of existing cultural features is desired, the errors of positioning can be accepted for a preliminary engineering site selection study. The aspect of imaging geometry which is most important for terrain and soils interpretation is that of the side-looking nature of SLAR which produces contrasts in return as well as radar shadow. This aspect permits the estimation of terrain relief.

8. Image Presentation. SLAR images are presented in one of two ways depending on the design of the system. The slant-range display is the natural result of using actual time delays between energy transmission and reception to position individual-return, resolution cells on the cathode-ray tube. Figure 5 illustrates the effect of slant-range display on the image. The slant-range display, depicted as line XY in Fig. 5, is compressed near the ground track such that projection $A_1 < A_2$. Because the distances between targets along a slant-range sweep are a function of slant ranges and aircraft altitude, the resulting distortion is hyperbolic with maximum compression nearest the position of the ground track.

The ground-range display is an electronically modified display which more nearly approximates the true ground geometry. Line XY', in the upper portion of Fig. 5, depicts the ground-range presentation when modified by the hyperbolic waveform applied to the CRT sweep circuitry.

In the case of both the slant-range and ground-range displays, the CRT spot is delayed by an amount proportional to the altitude of the imaging aircraft. This procedure is utilized for convenience in recording the returns so that the blank area on the CRT, or "altitude hole," which develops while the radar energy is traveling toward the ground surface is minimized (Fig. 5).

9. Scales. Most SLAR images produced to date by the various imaging systems have possessed such complex geometric distortions as to negate their value for any but the most preliminary cartographic applications. Levine (58) concludes that it is impractical to generate a Mercator projection directly with a side-looking radar system and that only crude mapping can be performed with the imagery without processing

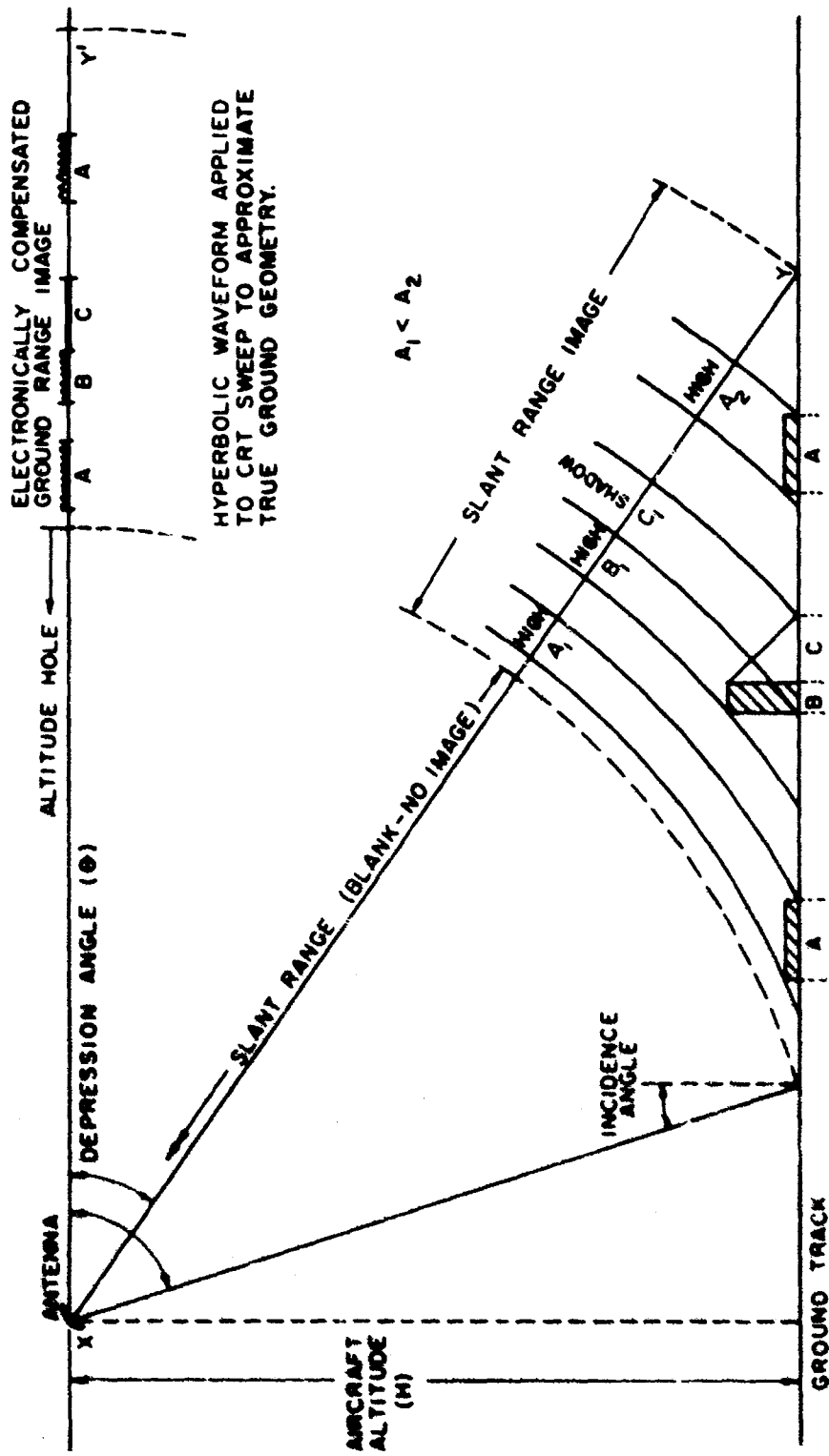


Fig. 5. Slant range image geometry.

with special equipment. Scheps (83) describes an engineering model of a side-looking radar restitutor which is said to correct for most of the geometric distortions normally found in SLAR images. This restitution, however, requires two, data-gathering flights to provide ground-position information, altitude, and the SLAR imagery. Another restitution device has been described which utilizes only optical transformations to correct for the gross image distortions (62).

Although it must be concluded that further advances in the state-of-the-art are required before SLAR imagery can be used directly for cartographic purposes, the geometric distortions which prevent the calculation of accurate regional scale ratios are not so severe as to preclude terrain and engineering soils interpretation. A cartographic application requires the precise and accurate determination of distance between points; while terrain and soils interpretation requires the evaluation of landforms, drainage systems, and those factors which together form a pattern visible on the imagery. Thus, an average image scale is sufficient for this interpretative process, and scales calculated directly from the imagery are adequate.

Just as range and azimuthal resolution are determined by different design parameters of the SLAR system, two different parameters of a SLAR imaging flight affect the range and azimuth scales. In addition to criteria of system design, range scale is affected by the imaging aircraft altitude whereas the azimuthal scale is related to the velocity of the aircraft and its relation to film speed across the face of the CRT. Although many SLAR systems are designed to produce imagery of a specified scale, inaccuracies and distortions require scale determination for each strip of imagery. When ground distances are known, average values of range and azimuthal scale can be computed as the simple ratio of image distance between two points in both the range and azimuthal direction to their corresponding ground distances. Such determinations can commonly be made using topographic maps as the representation of true ground distances with stream intersections, topographic features, or cultural features being the points common to both the image and the ground surface.

If true ground distances are not known, the relationship between radar image geometry, aircraft velocity, and image distances can be utilized to calculate approximate range and azimuthal scales. A knowledge of image display design parameters is required for such calculations. Figure 6 illustrates those parameters used in image scale calculations. Azimuth scale, being related to imaging aircraft velocity, can be calculated with the equation

$$S_A = \frac{D_A}{V_t}$$

where S_A is the scale ratio parallel to the ground track; D_A is the film distance between

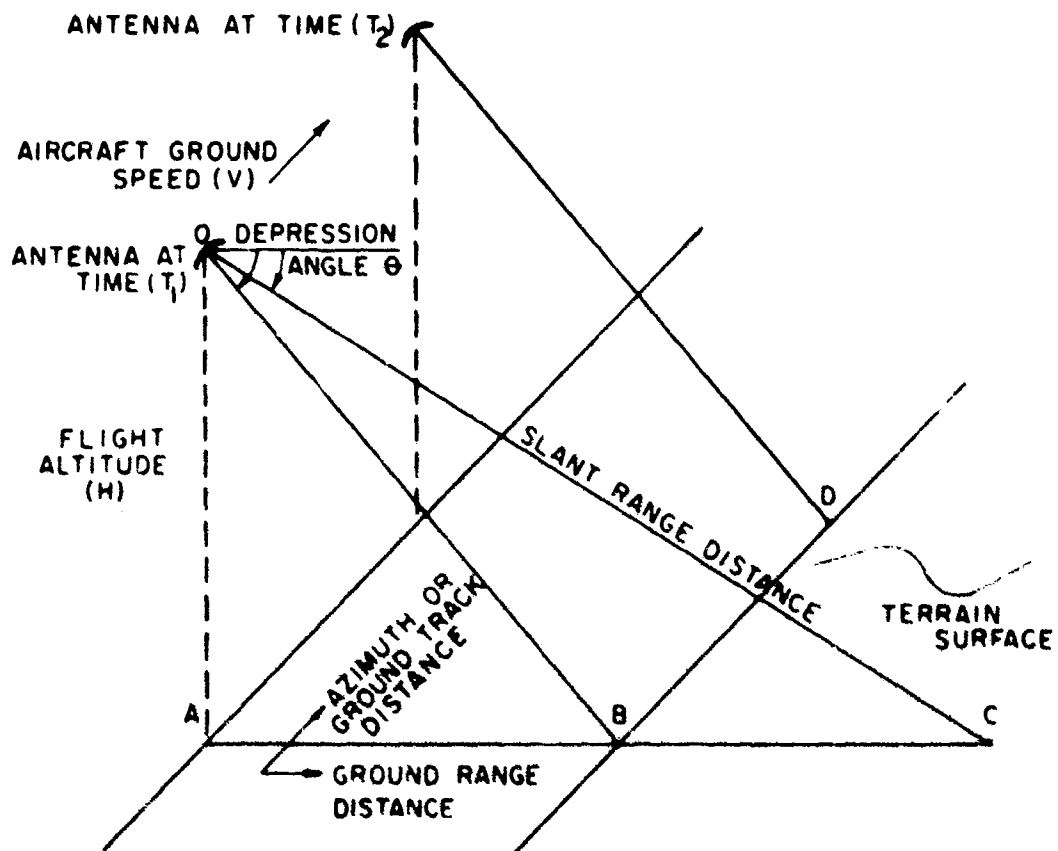
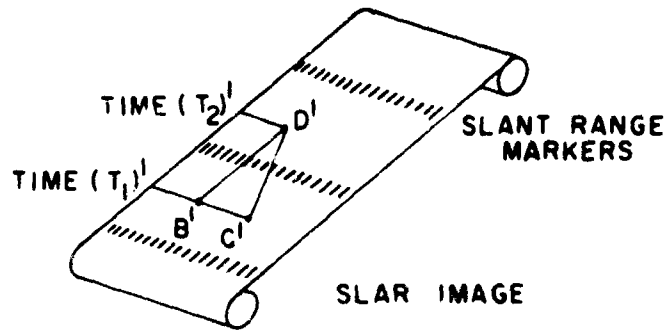


Fig. 6. Image scale geometry.

two points in the direction parallel to the ground track; and Vt is a calculated ground distance where V is equal to aircraft ground speed and t is equal to time of flight between the two corresponding points on the ground. With respect to Fig. 6,

$$S_A = \frac{\overline{B'D'}}{V(t_2 - t_1)}$$

Accurate time and aircraft ground speed data required for this calculation are often recorded along the margin of the imagery.

Ground-range scale, related to aircraft altitude, can be calculated with the equation

$$S_R = \frac{D_R}{D_G}$$

where S_R is the scale ratio perpendicular to the ground track; D_R is the distance on the image between two points in the direction perpendicular to the ground track; and D_G is a ground distance calculated from the aircraft altitude-slant range relationships

$$D_G = \sqrt{(\text{Slant Range})_2^2 - H^2} - \sqrt{(\text{Slant Range})_1^2 - H^2}$$

with slant ranges being the straightline distance between the radar antenna and the points in question and H being the aircraft altitude. Slant-range distances can be calculated directly from the SLAR image if system display parameters are known. SLAR images have slant-range markers superimposed upon them from which the slant-range distance to a point can be determined. Each marker as depicted in Fig. 6 represents an incremental increase in the slant-range distance to a point positioned at that marker. The actual distance represented by the markers is a function of the system design. Aircraft altitude is usually recorded in a data block in the margin of the image. With respect to Fig. 6,

$$S_R = \frac{\overline{B'C'}}{\sqrt{(OC)^2 - H^2} - \sqrt{(OB)^2 - H^2}}$$

Distance OC is calculated from the slant-range markers superimposed on the image.

Under optimum conditions of system operation, the ground-range presentation should exhibit ground range and azimuthal scales which are equal and uniform throughout the image. With similar optimum conditions, the slant-range display will have a uniform azimuthal scale but a nonuniform, ground-range scale which varies

proportionally with the hyperbolic relationship between slant range and aircraft altitude. Thus, at best, only an average of ground-range scale can be directly obtained from limited areas of the slant-range display.

Normally, aircraft ground speed, flying altitude, and system parameters cannot be considered to be constant throughout a flight even though the CRT sweep can be designed to account for earth curvature, atmospheric effects, or an above-sea-level reference plane. Furthermore, these factors cannot be expected to vary in a predictable, systematic manner. Consequently, ground range and azimuthal scales can be expected to vary independently and should be considered valid only over limited areas. If there is not a great difference between ground range and azimuthal scales, the two may be averaged so that a single scale can be utilized. If there is a great difference between ground range and azimuthal scales, the only recourse for general scaling is to trace the range and azimuthal projections of a required line and compute the distance as the hypotenuse of a right triangle. With respect to Fig. 6, the ground distance CD could be calculated by solving the relationship

$$CD = \sqrt{(BD)^2 + (BC)^2}$$

where BD and BC are determined from image distances $\overline{B'D'}$ and $\overline{B'C'}$ divided by their respective scale ratios.

10. Terrain Elevations. Terrain elevations theoretically are determined from SLAR images. Theoretical expressions relating the height of terrain features to their radar shadows exist as do radar parallax equations. Unfortunately, the information necessary for accurate height determinations is seldom provided. The complexities involved in obtaining true height determinations are of such magnitude that the only practical means of evaluating terrain relief are with the use of simplified approximations of radar shadow equations. Radar parallax measurements require at least two radar flights over the subject area with the area being imaged from different elevations or from opposite sides. There have been no reported instances where extensive areas have been covered by SLAR imagery of suitable quality for accurate radargrammetric measurements. It is anticipated, however, by several researchers (50, 54, 55, 83) that future advances in the state-of-the-art will eliminate many of the problems experienced with present radargrammetric research.

The basic geometry involved in determining terrain heights from monoscopic radar shadow measurements is illustrated in Fig. 7. The height of a terrain feature such as A in Fig. 7 is calculated from the equation

$$H_t = H_r - (H_r - H_s) \frac{S}{S_s}$$

where

H_t = target height above reference plane

H_r = altitude of antenna above reference plane

H_s = elevation of terrain above reference plane upon which is cast the radar shadow

S = slant range to top of topographic feature (calculated from slant-range markers)

S_s = slant range to edge of shadow (calculated from slant-range markers).

When ground range imagery lacking slant-range markers is used, the equation becomes

$$H_t = H_r - (H_r - H_s) \left(\frac{R^2 + H_r^2}{R_s^2 + H_r^2} \right)$$

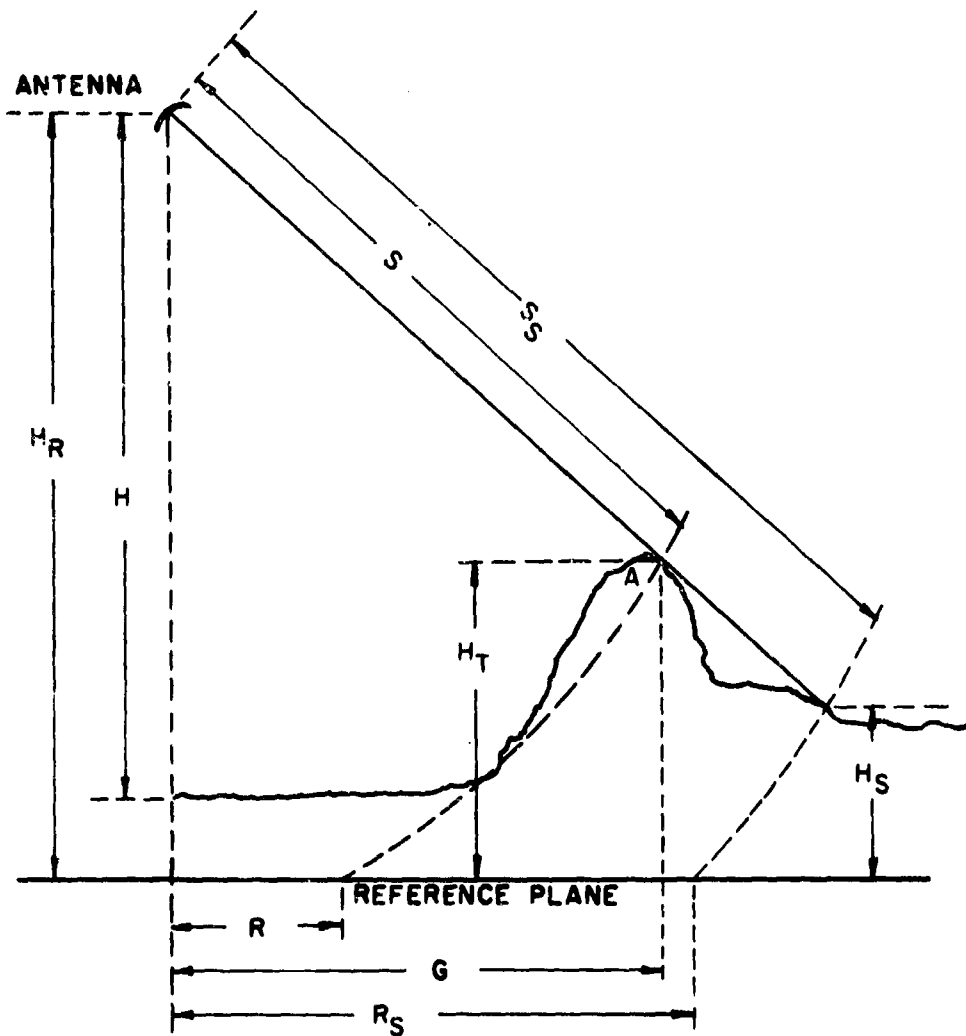
where

R = ground-range distance to top of topographic feature (measured from image)

R_s = ground-range distance to edge of shadow (measured from image).

It can be seen from Fig. 7 that the parameters H_r and H_s would be very difficult to determine without prior field information. Thus, to reduce the problem to that of solving for one unknown, terrain height imaged on one SLAR strip, it is commonly assumed that the reference plane coincides with the general terrain surface ($H_s = 0$) and that this surface also is at zero altitude with respect to the imaging aircraft. The terrain feature height equation reduces to $H_t = H(1 - G/R_s)$ for ground-range displays lacking slant-range markers, or $H_t = H(1 - S/S_s)$ for slant-range displays, where H is aircraft altitude, G is the horizontal distance from the ground track to the terrain feature, and the other symbols are as shown in Fig. 7. The errors introduced by this simplified, terrain-height equation are usually within the limit of accuracy of planimetric scales. Unacceptable errors will occur if the radar shadow is cast upon a surface which does not approach the horizontal.

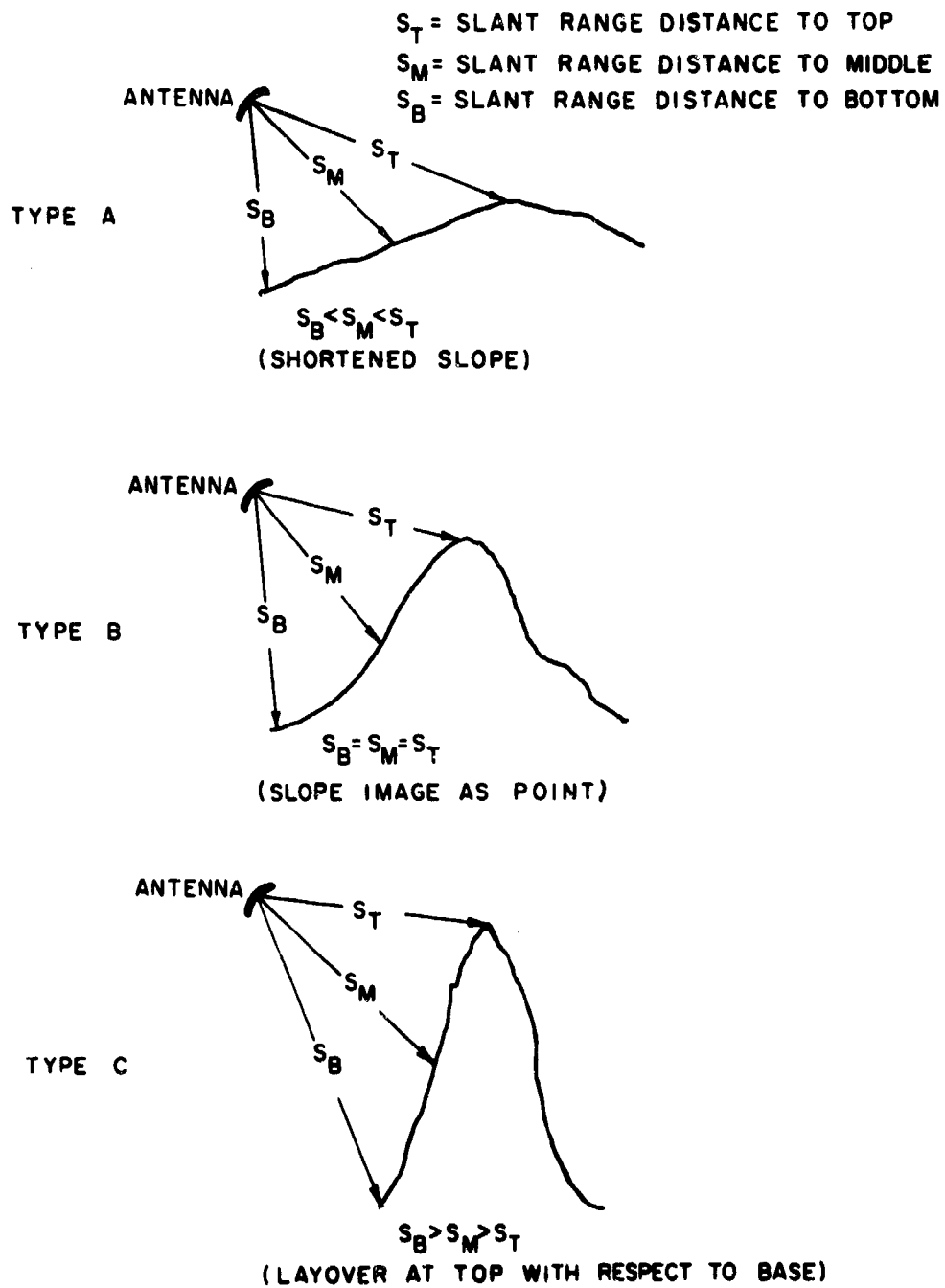
The nature of radar imaging is such that the position of resolution elements on the CRT is determined solely by the time interval between transmission of energy



AFTER GOODYEAR AEROSPACE CORPORATION (37)

Fig. 7. Terrain elevation geometry.

and its reception at the antenna after having been reflected by a surface. This fact accounts for several types of image distortion directly related to the height of terrain features. The types of distortions illustrated in Fig. 8 are all produced as the result of the imaging geometry and its relationship to ground slopes. A terrain feature of type A, with a gentle slope facing the antenna, is imaged with its surface shortened proportionately to its slope. Type B terrain features with surfaces all of an equal distance from the antenna are imaged as point features. The slope of type C terrain features is such that the crest is closer to the antenna than the base and a severe distortion occurs. In



AFTER GOODYEAR AEROSPACE CORPORATION (37)

Fig. 8. Terrain feature types.

such cases, the top of the terrain feature is imaged at a position on the film nearer the ground track than is the base. This results in a "layover" of the top of the feature with respect to its base.

The previously discussed distortions which result from the effect of the terrain itself, along with inaccuracies resulting from system deficiencies, prevent a reasonable determination of terrain elevations in most cases. Only in the case of a simple terrain (e.g., a regularly shaped high mountain on a flat plain) and high-quality imagery can determinations of terrain elevations from monoscopic SLAR imagery be considered to be reliable.

Flight-line configurations which will produce images with a stereo capability are illustrated in Fig. 9. The opposite-side configuration requires flight lines which are parallel while the same-side configuration utilizes flight lines at different elevations. Although a certain degree of error can be tolerated in flight-line configuration, it appears that flight-line positioning and geometric image distortions have prevented the realization of an operational stereo radar program. Such a program awaits further advances in the state-of-the-art in both the imaging systems and the navigational controls of the imaging aircraft.

11. Radar Equation. The relationship commonly used to define the average received pulse power of a nonimaging radar system is given by the radar equation (2)

$$P_r = \frac{\sigma G^2 P_o \lambda^2 [f(\theta, \phi)]^4}{(4\pi)^3 R^4}$$

where

P_r = average received pulse power (watts)

σ = radar scattering cross section

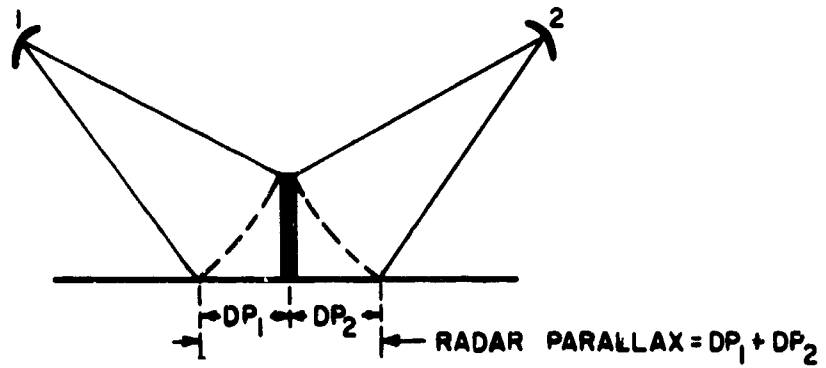
G = maximum antenna gain

P_o = transmitted power

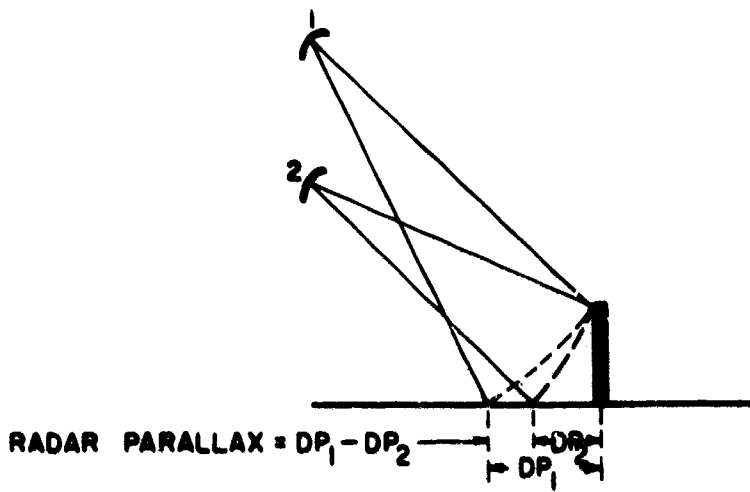
λ = wavelength of transmitted energy

$f(\theta, \phi)$ = normalized one-way antenna voltage pattern
(θ = depression angle, ϕ = antenna beam width)

R = distance between antenna and target.



(A) OPPOSITE SIDE CONFIGURATION



(B) SAME SIDE CONFIGURATION

AFTER RAYTHEON / AUTOMETRIC (7)

Fig. 9. Stereo configurations.

Although the uncalibrated SLAR imagery used for this study could not be evaluated in terms of the quantitative parameters of the radar equation, it is of value to qualitatively assess those factors of the equation which are affected primarily by the illuminated terrain. In doing so, some insight into the significance of SLAR images (which are actually 2-dimensional plots of radar cross section per resolution cell as a function of range and ground-track distance) may be gained.

Cosgriff, Peake, and Taylor (16) have shown that the parameters of the general radar equation can be grouped as being parameters of target, imaging geometry, and system. Properties of the target, which in this case is terrain, are given in terms of the radar-scattering cross section (σ). Transmitted power (P_0), wavelength (λ), and maximum antenna gain (G) are functions of system design; while depression angle (θ), normalized one-way antenna voltage pattern [$f(\theta, \phi)$], and distance between the radar antenna and target (R) are functions of the radar-imaging geometry.

The radar-scattering cross section (σ) is a measure of the ability of a target to produce a radar return, or reflection. It is defined as equivalent to the area of an isotropic scatterer which would produce a radar return at the antenna equal to that from the target. Cosgriff, et al., (16) and Moore (68) have described the parameters which determine the radar-scattering cross section. These parameters include the dielectric and conducting properties of the terrain surface, the roughness, and the geometric shape as determined by local and regional slopes. The specific effect of each of these parameters on the average radar-scattering cross section is significantly influenced by the wavelength and polarization of the incident electromagnetic energy as well as by the incident angle of that energy as determined by the geometric relationship between the antenna and the terrain surface. Various polarizations are produced by the design of the SLAR antenna by which the transmitted microwave energy is constricted to oscillation in a specific plane. Polarization of the incident energy is not directly accounted for in the radar equation but influences the values of the scattering cross section.

12. Scattering Theories. Although an analysis of the mathematics of existing terrain-scattering theories is beyond the scope of this study, it is necessary for a proper understanding of radar reflection to evaluate, in a qualitative sense, the assumptions upon which several scattering theories are based. The existing radar-scattering theories, in general, can be grouped into two categories (104). Theories of the first group postulate a relatively simple mathematical model to describe a reflecting surface and proceed with a rigorous solution of the scattering and reflection from that surface. Theories of the second group describe a surface in terms of measurable, experimental parameters and proceed to solve the problem of scattering and reflection from that surface. In general, the theories of the first group provide good solutions to the problem of reflection and scattering from the hypothesized surface, but the surface models do not adequately describe any actual terrain surface. Theories of the second group encounter

difficult problems when subjected to rigorous solutions, but their results can be more easily related to actual terrain surfaces.

For distributed targets, such as terrain, the size of the terrain feature illuminated depends upon the antenna beam width (ϕ) and the pulse length (τ). Thus, radar cross section values as defined in the general radar equation are dependent upon radar parameters as well as terrain parameters. In order to normalize the measured, reflected power to a value which is independent of the radar parameters, Goidstein divided the radar cross section area (σ) by the area illuminated by the radar (A) to obtain the dimensionless parameter σ_0 , where $\sigma_0 = \sigma/A$ (35). This parameter, σ_0 , valid when scattering properties are uniform over an illuminated area, has been extensively utilized as the measured quantity in experimental radar backscatter (non-imaging) studies (38, 39, 60). One research group (Ohio State University Antenna Laboratory) has used a parameter, γ , modified from σ_0 for experimental measurements (16). For their purpose, the radar cross section (σ) is divided by the projection of the illuminated area normal to the radar beam direction to obtain γ such that $\gamma = \sigma_0/\sin\theta$, where θ is the depression angle of the incident radar energy. Both the normalized radar cross section (σ_0) and the normalized echo area (γ) are expressed in decibel units which are equal to the logarithm to the base 10 of the ratio of transmitted and received powers as defined in the radar equation.

Many scattering models have been proposed by several researchers (9, 16, 38, 104). Of these, two "complete" models have been reasonably successful in predicting backscatter from specific types of natural terrain (16). The smooth-surface model assumes a terrain surface to be locally smooth, with random irregularities much less than a wavelength in depth. In addition, the regional slope of the surface is assumed to be much less than unity. The second model is based on scattering from thin, lossy² cylinders such as grass or weeds. The assumption is that the individual blades or stems scatter like long, thin, lossy cylinders having a maximum diameter much less than a wavelength. It is also assumed that none of the incident energy penetrates to the ground surface.

The smooth-surface model explains the variation of normalized radar cross section (σ_0) with depression angle (θ) reasonably well for smooth surfaces such as concrete and asphalt roads when the proper ground constants are chosen. The variation of σ_0 with surface roughness is also explained for relatively smooth surfaces. The thin, lossy cylinder model theory agrees generally with a measured dependence of σ_0 with the inverse of wavelength (λ) for some specific types of vegetative cover. Also, the variation of σ_0 with depression angle is reasonably well described for properly chosen ground constants.

2. lossy - A target which dissipates microwave energy.

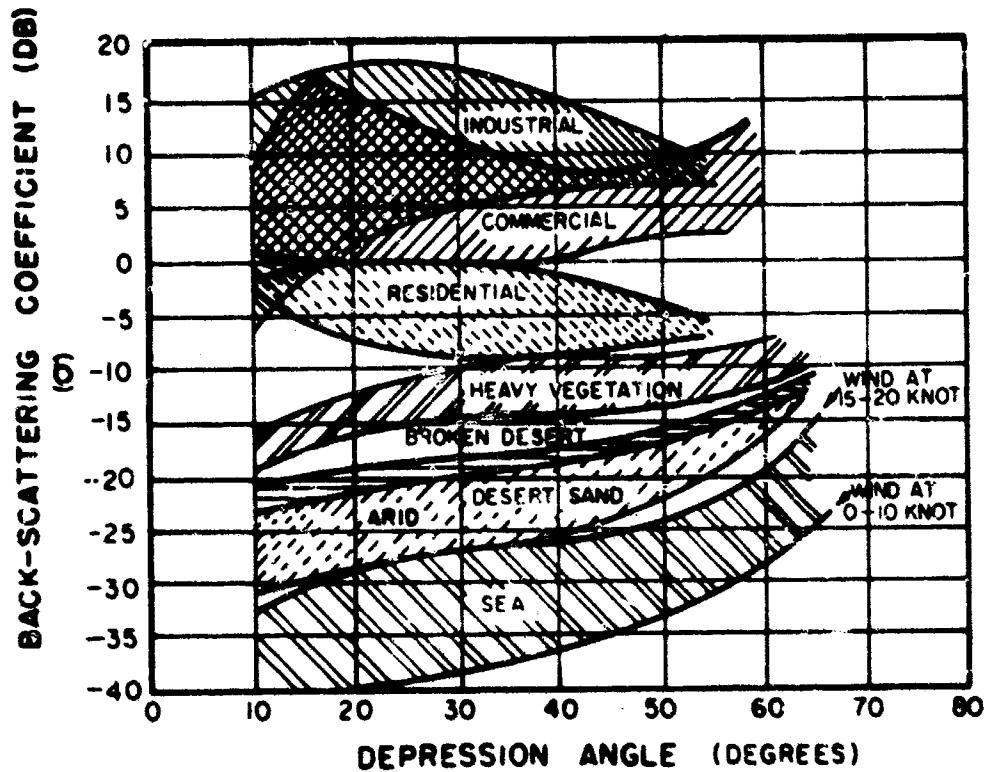
Although all of the experiments concerned with the development of scattering models have dealt with non-imaged radar backscatter data, the general conclusions resulting from all of these studies should qualitatively apply to a study of SLAR image interpretation.

Essentially, all radar backscatter experiments show that relatively smooth surfaces (roughness less than one-half the wavelength of the incident microwave energy) produce a normalized radar cross section (σ_0) of large magnitude at a vertical angle of incidence which rapidly decreases to low values for grazing incidence. Rough surfaces, on the other hand, produce smaller values of σ_0 at the vertical, but the decrease in σ_0 toward grazing incidence is less. Thus, at intermediate angles of incidence, σ_0 is larger for rough surfaces than for smooth surfaces. Furthermore, the theories generally agree that backscatter of near-vertical incident energy is caused by roughness having a large horizontal scale and relatively small slopes whereas backscatter of energy at near grazing angles is caused by roughness having a small horizontal scale and relatively steep slopes. A transition occurs between the two extremes.

Figure 10 shows the variation in σ_0 with respect to depression angle for a variety of terrain and target types. These measurements were made by the Goodyear Aerospace Corporation with an X-band, nonimaging, airborne radar system (36). Figure 11 illustrates the dynamic range of the terrain parameter (γ) as measured by Cosgriff et al. (16) for various terrain types. Although there is no quantitative relationship between σ_0 and γ values and corresponding imaged terrain types as seen on the uncalibrated SLAR imagery used for this study, a general relationship between high σ_0 or γ values and lighter image tones can be expected.

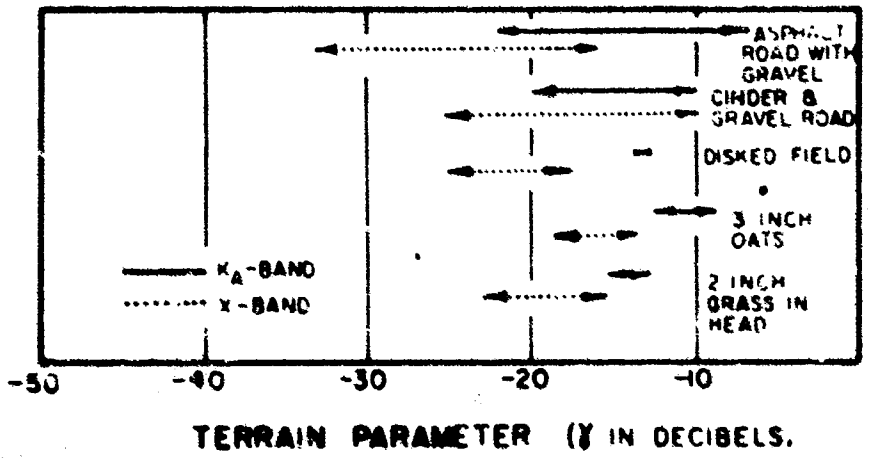
Although radar re-radiation is known to be affected by the electrical properties of illuminated terrain, it is concluded that present experimental and theoretical studies have only partly explained the effect of surface conditions on radar scattering. The effect of terrain surface electrical properties has been recognized and evaluated for specific, relatively simple conditions but has not been satisfactorily accounted for in "complete" terrain backscatter models.

It has been observed and partially substantiated by limited experimentation that for any given wavelength in the radar portion of the electromagnetic spectrum, the depth of penetration varies inversely with the relative dielectric constant of the material and directly with wavelength (19, 104). Thus, at appropriate wavelengths, penetration could be expected to be relatively greater in dry materials than in wet materials. All other factors remaining constant, the normalized radar cross section (σ_0) apparently decreases with decreasing dielectric constant of illuminated material (16, 19).



(COURTESY AMERICAN SOCIETY OF PHOTOGRAMMETRY)(97)

Fig. 10. Variation of backscattering coefficients at X-band.



AFTER COSGRIFF ET AL. (16)

Fig. 11. Dynamic range of terrain parameter at K- and X-band.

The previous discussion of radar theory, while having limited application to qualitative SLAR image interpretation, does present a general concept with which interpretations should agree. Thus, visually defined SLAR image tones should be related to radar cross sections so that lighter tones generally represent higher decibel values of σ_0 or γ while darker tones represent lower σ_0 or γ values.

13. General Considerations of the Reliability of SLAR Imagery as a Record of Terrain Reflectance Data. A SLAR image must be evaluated in terms of its capability to present a reliable display of terrain reflectance data. The SLAR image is essentially a 2-dimensional plot of radar reflectivity. The image consists of numerous resolution cells each of which represents a radar cross section (σ) value for a specific portion of the imaged terrain. Consequently, the degree to which the image represents the true distribution of reflectance from terrain depends upon the relationship between the image tone of each resolution element and corresponding actual (σ) value as well as the relative geometric position of each resolution element.

Each resolution element represents an average value of radar cross section for a portion of terrain whose area is determined by the resolution of the radar system. The SLAR system records a statistical sampling of fluctuating reflection signals. Constructive and destructive interference of reflected energy can further modify signals. Thus, a group of resolution elements defining a tone on a radar image represents a mean radar cross section that can change with time. For visual interpretations, however, the manner in which the reflected signals are recorded is more significant than their statistical fluctuations. The CRT of a typical SLAR system cannot record all signal levels with equal discrimination (56). The CRT and associated electronic components possess the capability of displaying maximum differences between high- or low-intensity signals. Thus, if most of the available film-density range is used to record differences between low-level return signals, high-level, strong returns are compressed into a small-density range. Conversely, if instrument gain is set to discriminate between high-level, strong returns, density separation at low levels is lost. In other words, either high or low returns are "clipped" and recorded at one density level. Most natural terrain surfaces produce relatively low returns and are best recorded when there is maximum, low-level signal separation.

The relative, geometric position of each resolution element is determined by the electronic measurement of range distance to each area contributing a return. In addition to the previously discussed image distortions caused by the geometry of the terrain, distortions arise resulting from improper instrument settings, equipment malfunctions, and aircraft instability (7, 56)

If the SLAR system is not properly adjusted to account for aircraft altitude, drift, and ground speed, the resulting image will not display the terrain in its proper

2-dimensional form. If the altitude control is set lower than the actual aircraft altitude, a blank area will be displayed at the beginning of the CRT sweep. On the other hand, if the altitude control is set too high, the relative position of the resolution elements will be expanded at the beginning of the CRT sweep. If the drift-compensating device on a SLAR system is improperly set, the resulting image will be distorted. As an example, rectangular fields might appear as parallelograms (7). The aircraft, ground-speed control determines the rate at which the recording film passes across the face of the CRT display. If the film speed is too fast relative to aircraft ground speed, the resolution elements will be expanded in the azimuthal direction. Conversely, if the film speed is too slow, the resolution elements will be compressed.

Erratic aircraft movements will produce image distortions (56). Turning, yaw, pitch, rapid change in flying altitude, and roll contribute to this problem. Relatively slow changes in aircraft heading will produce either compression or expansion of the image depending upon whether the antenna scans the terrain too fast or too slow. Yaw, a rapid, unplanned change in aircraft heading, can cause the antenna to scan the same portion of terrain twice, thus producing a double image. Rapid rocking up and down or pitch of the aircraft can result in redundant imaging or, in some cases, loss of image of a portion of the terrain. Rapid changes in aircraft altitude can cause the blurring of image segments. Roll of the aircraft can result in the uneven illumination of terrain.

Equipment malfunctions do not necessarily produce geometric image distortions but do degrade the appearance of SLAR imagery. Momentary camera stoppages will result in thin, dark lines which cross the image normal to the flight-line direction. Streaking parallel to the flight-line direction may be caused by defects in the phosphor coating of the CRT. Antenna lobing can also produce horizontal streaks across a SLAR image. This degradation is caused by the uneven illumination of the terrain.

Faded or washed-out images are the result of an insufficient return signal. A weak magnetron, producing insufficient power for illumination, can cause this degradation as can heavy cloud cover. In the case of SLAR systems normally considered for the mapping and interpretation of terrain features, only dense thunderheads would significantly attenuate the radar energy.

III. PREVIOUS INVESTIGATION

14. Earth Research. The use of radar images for purposes other than military target identification apparently was first recognized and exploited by Lieutenant H. P. Smith in 1947 (84). While stationed in Greenland with the Army Air Force, he noticed the similarity of background clutter in Plan Position Indicator (PPI) radar scope

photographs to the shape of the terrain in the area. He made a map of the northwestern coast of Greenland from the PPI radar scope photographs which turned out to be an order of magnitude better than the existing charts. Smith prepared a report on the subject which was turned over to the U. S. Geological Survey. With this inception, other government agencies began to consider the potential of radar imagery as a useful display of terrain data.

Most of the early research and development projects concerned with radar images had as their objective an advance in the state-of-the-art of PPI radar mapping and charting (24, 37, 85, 99). Although much of the radar mapping and charting research has been "classified," investigations involving PPI radar systems, and in recent years SLAR systems, have continued and are occasionally reported in the open literature (46, 50, 54, 55, 59, 62, 83). Although not of primary concern for this study, the subject of radar mapping and charting or "radargrammetry" is well covered in the text *Radargrammetry* (58) or the 3rd edition of the *Manual of Photogrammetry* (97).

One of the earliest discussions on the use of radar images for interpreting terrain features reported in the open literature was an article in *Photogrammetric Engineering* by Pamela Hoffman (41). In this article, keys were presented as an aid for determining the nature of terrain features. A qualitative analysis of PPI radar scope photographs indicated that city areas and regions of rugged relief produced the highest radar return (brightest tone). Metal surfaces were responsible for the greatest reflection while wood structures, earth features, and vegetation produced the minimum discernible image. It was recognized that the size of individual terrain features contributed to the strength (or brightness) of the image. Features that could act singly or as a group to form corner reflectors produced the highest (brightest) returns. The majority of hydrographic features appeared as no return (dark tone) areas on the scope. Smooth water reflected radar energy away from the antenna while islands, reefs, and sand bars appeared as high returns within the dark areas. Swamps appeared as low-return (dark) features while areas of high relief were presented on the scope in a manner similar to a shaded relief map. The scope appearance of open, low-relief areas was described as being indeterminate ground clutter. Although some cultural features were indicated, it was not possible to interpret terrain slope features, vegetation, or microrelief.

The qualitative evaluation of PPI radar scope photographs for use in the interpretation of natural-terrain features continued until the early 1960's. Hoffman (42, 43) reported on progress in radar image interpretation in which the technique of interpreting radar scope photographs was compared to conventional, airphoto interpretation. The procedure was based on the recognition and evaluation of variations in return intensity. The size, shape, pattern, tone, texture, shadows, and environment of terrain features as expressed on a radar scope were considered the major factors to be analyzed.

Although few radar characteristics of specific terrain features were presented, an approach toward radar interpretation was established.

Feder (25, 26, 27, 28) stressed the potential qualitative and quantitative uses of PPI radar scope photographs. Without offering specific techniques for application, his articles suggested that subsurface soil and rock compositions, moisture, and metallic contents and temperatures could be determined from radar imagery. It was also indicated that the textures of surficial terrain materials down to gravel sizes could be read directly from the radar while the texture of finer substances could be inferred. Feder's conclusions concerning the penetration of the terrain surface and subsequent interaction with soil and rock by the radar energy were based on qualitative image observations as well as controlled radar backscatter experiments. More recent research has indicated that such potentials are overly optimistic when attributed to short-wavelength radar imagery.

The characteristics of SLAR imagery were first introduced in the open literature in the late 1950's. As was the case of PPI radar, early research involving SLAR was concerned with mapping and charting developments (13, 17, 54). Although reference was made to the interpretability of SLAR imagery by several authors during this time (11, 15, 71), it was not until 1962 that the potential of SLAR imagery for terrain and geological studies was stressed in the open literature. The First Symposium on Remote Sensing of Environment held at the University of Michigan in 1962 apparently initiated interest in radar with many researchers.

Parker (73) and Smith (95) reviewed the nature of remote sensing by radar at this symposium and presented potential applications, and Scheps (83) reviewed the history of radar geology. Fischer (32) presented a paper on the application of radar to geological interpretation and made reference to a study in which a densitometer profile was constructed from a SLAR image for purposes of geological interpretation. A later report (97) of this same investigation concluded that, in a New Mexico study area, materials could be differentiated into three groups on the basis of their signal-return intensity. These groups, in order of decreasing return, consisted of: (1) igneous rocks and drifting sands; (2) ferruginous sandstone; and (3) limestone, siltstone, gypsum, and soils. The different levels of return intensity were illustrated with a densitometer profile and corresponding geologic cross sections. Fischer also showed that some structural features visible on the radar were not visible or, in some cases, poorly visible on corresponding conventional photographs.

15. Research from 1962 to 1965. During the period from 1962 to 1965, numerous articles were published which stressed the potential application of SLAR images to terrain and geological mapping studies. Feder (29, 30, 31) continued to stress the potential of radar to penetrate the earth's surface and "read" subsurface compositions

and conditions. The conclusions derived by Feder, however, were based on theoretical capabilities rather than the analysis of experimental data. Bienvenu and Pascucci (11) and Simons and Beccasio (92) reported for the Autometric Corporation on the use of SLAR imagery for engineering geology and geoscience purposes. Without establishing a specific interpretation technique, they demonstrated the capability of applying conventional airphoto-interpretation techniques to SLAR images. They were able to recognize landforms, drainage, and map geology by inference from the SLAR images. Leonardo (56) reported on the capability and limitations of remote sensors and considered radar as one of several sensors which as a group could contribute to the collection of useful terrain data.

In 1965, it became apparent that the bulk of research on SLAR image interpretation was concentrated within a few research groups. Reports and articles describing research efforts by the Autometric Corporation; University of Kansas, Center for Research in the Engineering Sciences; U. S. Geological Survey; National Aeronautics and Space Administration; Goodyear Aerospace Corporation; Cold Regions Research and Engineering Laboratory; and several individuals became available in the open literature. Most of these documents reported on research sponsored by either the Department of Defense or the National Aeronautics and Space Administration.

In 1965, the Autometric Corporation released a comprehensive report on the "Geoscience Potentials of Side-Looking Radar." (7) The imagery from unclassified radar systems was evaluated. One of these systems was the AN/APQ-69 (X-band, 3.2 cm wavelength). A summary of the conclusions derived from that qualitative study follows:

a. Surface Drainage. Mapping of surface-drainage features from radar imagery was relatively straightforward even though recognition of microdrainage was made difficult if not impossible by the small scale and low resolution of the imagery. Drainage mapping was significantly easier in mountainous areas than in relatively flat areas where it was sometimes impossible to map more than the primary drainage.

b. Cultural Features. Cultural features identified on the radar mosaics used in the study did not approach the anticipated level of interpretation. This was attributed to the experimental nature of the imagery being studied. It was indicated, however, that considerably more cultural detail could be extracted from imagery obtained from equipment whose gain setting was relatively low.

c. Regional Lineation Pattern. Regional lineations were identifiable as mappable units on radar imagery of moderate-to-high relief areas. In low-relief areas, a greater dependence was placed on the use of drainage patterns to infer the existence of

lineations. It was shown that lineations mapped from radar imagery reflect prevailing regional tectonic trends.

d. Agricultural Land Use. It was possible to obtain reconnaissance-level interpretation of land use and distributions from radar imagery. Such interpretations were made primarily by inference from relief, drainage patterns, and geographic association.

e. Regional Vegetation. With the exception of mountainous areas, it appeared possible to map regional vegetation conditions. Such mapping was produced primarily by inference.

f. Surface Configurations. Good, qualitative, regional, surface-configuration information was mapped monoscopically on the basis of distinctive, landform characteristics. Such information included relief classes, slope, and type of ground profile. It was suggested that a reliable presentation of the dominant surface condition could be made if the mapped units were large in proportion to the scale of the imagery.

g. Geology. Radar imagery proved to be of value for the interpretation of geologic structure and lithology in mountainous regions where drainage patterns and relief could be used for inference. In plains and basins where bedrock is often overlain by deep surficial deposits, radar imagery was best used as an adjunctive tool. A table of relative Ka-band return values associated with various geological materials was presented as a guide. Some examples include: (1) weak returns – sand, silt, clay, shale, marl, chalk; (2) moderate returns – gravel, glacial drift, limestone, diabase, basalt; and (3) strong returns – sandstone, granite, rhyolite, gneiss, and schist. These values represented observed conditions on the imagery and were not evaluated in terms of the actual physical or chemical conditions producing the return.

h. Physiography. Regional physiographic units could be clearly and accurately identified and delineated although micro-terrain features were less distinguishable if at all apparent.

i. Surficial Materials. Surficial materials were inferred from interpretations of regional geology, physiography, drainage, land use, and vegetation. It was stressed, however, that the interpretation of surficial materials must take into account the fact that returns are affected by such factors as wavelength of the energy and physical and chemical properties of the target.

j. Ice. It was demonstrated that regional ice interpretation is possible from radar imagery. Sea ice features associated with the physical processes of formation, growth, drift, and disintegration were identifiable.

Following the report of the Autometric research, Beccasio and Simons (8), Simons (91), and Holmes (44) reported on further applications of SLAR image interpretation to terrain studies. Beccasio and Simons (8) and Simons (91) discussed the interpretability of SLAR imagery as presented in the Autometric Report, while Holmes (44) applied the results of the Autometric Report to the mapping of engineering materials. Although specific interpretation techniques were not presented, examples of imagery and final maps of interpreted materials were illustrated.

Results of research conducted at the University of Kansas, Center for Research in the Engineering Sciences, became available in the open literature in 1965. Many papers advising the scientific and engineering communities of the state-of-the-art of SLAR image interpretation have been introduced into the literature since that time.

Reports by Ellermeier, et al. (23), Rouse, et al. (80), Simonett, et al. (88, 89), Simonett (87), and Moore (68) and papers by Pierson, et al. (75), and Kirk and Walters (45) discussed the potential use of SLAR image interpretation for a variety of purposes including Arctic and Antarctic studies from space; geoscience investigations including the determination of geologic structure; and reconnaissance vegetation and soil mapping.

Dellwig, et al. (20) reported on preliminary studies of K-band radar imagery obtained over Pisgah Crater, California. It was tentatively concluded that: (1) AA and Pahohoe lava at the study site could not be isolated on the radar imagery; (2) faults traced on photos of the Pisgah Crater area could not be isolated on the imagery; and (3) in the Lavic Lake playa area, relatively high surface roughness and relatively greater moisture content of the surface soil both correlated in a general way to high radar returns. Deficiencies of the imagery for interpretive purposes were attributed to the wavelength of the system. Later studies of the Pisgah Crater area involving multiple polarized K-band SLAR imagery were reported by Dellwig and Moore (21), Ellermeier, et al. (22), and Gillerman (34). Dellwig and Moore found that differences in return on like- and cross-polarized SLAR imagery could be used qualitatively to differentiate alluvial materials and bedrock. Without offering specific interpretation techniques, they suggested that multiple-polarized SLAR imagery could be used to differentiate between sources of alluvial material, differentiate rock types in areas of apparent similarity, and absolutely identify rock type on the basis of contrasts in return from various combinations of polarized radar. Ellermeier, et al. presented empirical evidence to support the theory that a measure of surface roughness and, to some extent, composition could be obtained from the analysis of multiple-polarization radar. They found evidence that lineation and structural orientation as well as variations in terrain composition were more apparent in cross-polarized rather than direct-return imagery. A study by Gillerman designed to evaluate the apparent relationship between the glass content of rock and its appearance as a low-return feature on cross-polarized K-band SLAR

imagery concluded that surface roughness, degree and type of vegetation, and perhaps age of the rock were contributing factors to the low return. Further investigation into the phenomena was suggested.

16. Recent Research. More recent work at the University of Kansas, Center for Research in the Engineering Sciences, has consisted of developing techniques for SLAR image enhancement designed to aid the interpretation of natural and agricultural vegetation. Morain and Simonett (69, 70) reported on methods for the interpretation of vegetation from radar imagery which included the use of an image discrimination and enhancement combination and sampling system (IDECS). This system employed tri-color image combinations, the generation of probability density functions, and a data space sensor. A study of K-band radar imagery was made of the Horsefly Mountain area in Oregon and was supported by field investigation.

Probability/density curves measured with a flying-spot scanner and tabulated with a pulse height analyzer were evaluated for a variety of vegetation types. Each curve exhibited some variation in shape. It was concluded that the dissimilar shapes represented differing interactions between the radar energy and the plant communities (and bare soil). It was suggested that specific vegetation types could be identified on the basis of these changes in curve shape. A further conclusion was presented that the radar image contains subtle differences which the unaided or untutored eye at first sight cannot distinguish.

Simonett et al. (90) reported on the potential of SLAR as a remote sensor in agriculture. Crop and soil parameters of about 400 fields near Carden City, Kansas, were measured and statistically correlated with average film density values for those same fields. Imagery (K-band) used for the study was obtained from three late summer and autumn flights and was like-polarized although not calibrated.

Results of the statistical experiment indicated that percent ground cover, crop height, surface geometry, and crop and soil moisture content significantly affected radar-return intensity. Some fields, notably sugar beets and bare soil, could be identified with an acceptable probability of accuracy from the images. Others were discriminated with less certainty.

This study was the first of a series aimed at evaluating the potential of multi-frequency, poly-polarized radar imagery for extracting information on agricultural crops.

Leighty (52), McAnerney (63), and Prentice (76) have reported on SLAR image interpretations performed in conjunction with the research activities of the U. S. Army Cold Regions Research and Engineering Laboratory, Hanover, New Hampshire.

Leighty analyzed AN/APQ-56 SLAR imagery with respect to Arctic terrain interpretation. A quantitative assessment of tonal patterns was considered to be impractical so a qualitative interpretation technique was presented. This technique included the consideration of each of the following factors:

- (1) Observation and qualitative evaluation of tonal contrast.
- (2) Geometric arrangement of tones (patterns).
- (3) Consideration of aircraft aspect and its relation to the radar image.
- (4) Delineation of pattern boundaries.
- (5) Mental reconstruction of a feature that is most compatible with the observed image.

It was concluded that:

- (1) SLAR imagery can be interpreted for terrain information.
- (2) The interpreter must utilize his experience to a greater extent when viewing SLAR imagery as opposed to conventional photographs.
- (3) Techniques used to interpret photographs are valid for radar images.
- (4) More information must be derived by inference from radar images than from photographs.
- (5) SLAR imagery scale can be varied to meet specific requirements.
- (6) The relative signal levels in decreasing order of magnitude were reflected from snow, glacial ice, soils and rocks, lake and sea ice, and open water.

McAnerney and Prentice presented examples of interpreted SLAR imagery obtained over South Dakota and Minnesota. McAnerney introduced a simplified method of estimating the height of an object from its radar shadow. This and a discussion of a deductive process similar to that used in airphoto interpretation led him to conclude that a trained interpreter could describe the physiography, geology, and soil of a land surface and provide a reasonable assessment of the geography of a populated region through the interpretation of SLAR imagery. Prentice presented specific examples of pattern differences between the radar imagery and airphotos of an area in the vicinity of Willmar, Minnesota. It was concluded that, in order to obtain optimum

imagery interpretation, an interpreter must possess knowledge of the imaging system as well as understand the physical properties of the components of the imaged scene.

As the National Aeronautics and Space Administration (NASA) became involved with remote sensing, SLAR imagery was distributed to a number of earth scientists for evaluation. This resulted in many articles stressing the potential of SLAR as an aid to geologic mapping from orbital satellites (3, 4, 5, 6, 49, 51). In addition, the work of the U. S. Geological Survey in evaluating SLAR imagery was reported by Reeves and Kover (77) and Kover (47). In a summary of Geological Survey Research in 1966 (100), individual investigations of SLAR imagery of the San Andreas fault zone, Hart Mountain area in Oregon, Oregon coast, High Cascade Range in Oregon, and Jackson Hole, Wyoming, were briefly described.

U. S. Geological Survey researchers found that structural geologic and topographic features were recognizable on SLAR imagery. Several fault zones were distinguished which had not been clearly recognized in the past. It was reported that, in some cases, terrain was effectively "defoliated" on SLAR imagery. Although specific rock types were not identifiable, unconsolidated materials were found to be distinguishable from consolidated materials.

The results of investigations presented in the U. S. Geological Survey Review of Research were in abbreviated form and did not include examples of imagery or specific interpretation techniques.

Simpson (93) and Rhodes and Schwartz (78) reported on the potential of SLAR as a geographic tool, and Carnegie and Laver (12) included SLAR as one of several useful sensors in multiband remote sensing for forest and range inventories. Although these articles did not include specific SLAR interpretation techniques, the applications were illustrated with examples of imagery.

Wise (103) reported on a study to evaluate the potential of K-band SLAR imagery for geologic mapping. Although specific SLAR interpretation techniques were not presented, a SLAR image strip of the Harrisburg, Pennsylvania, area was annotated and illustrated. It was concluded that vegetative and cultural patterns were the most prominent elements. Geologic contacts appeared as more subtle changes in topographic grain, relief, or as changes in forest cover, field shape, or orientation. Reflections from steep slopes, small gulleys, elongate meander patterns, and linear forest patterns accentuated some dikes and small fracture zones. It was concluded that some of the lineations seen on the SLAR imagery were "pseudo-geologic" features caused by fence lines and field boundaries. The author stressed caution in geologic interpretation from the imagery.

Rib (79) reported on SLAR as one of many sensors used in a multi-sensing technique for detailed engineering soils mapping. It was concluded that the K-band SLAR imagery available for that study was of value for landform determination but of little value for interpreting glacial soils because all soils appeared dark on the imagery. However, the resolution of the imagery was poor and this limited its value. It was suggested that K-band radar images may be of more value for interpreting bedrock and residual soil conditions.

Rydstrom (81, 82) discussed the interpretation of local geology with respect to the qualitative evaluation of intensity of return. It was concluded from continuing studies underway at the Goodyear Aerospace Corporation that the strength of a return signal is more acutely sensitive to surface roughness and geometric configuration of an imaged object than it is to compositional material. Furthermore, the return differences caused by physical configurations were found to be sufficient to mask the lesser return variations attributable to material types.

Several interpretative procedures were found to be unique to radar imagery interpretation during the course of the Goodyear Study. Because of the unidirectional illumination of terrain by radar, small variations in surface relief such as drainage details or fault scarps were accentuated by return contrasts. Specular reflective surfaces of fine-textured materials such as clay, silt, or sand were found to be imaged as no-return areas, while coarser surfaces created a textured, higher return. Terrain geometry was found to produce a significantly high return in the case of limestone and some lavas where natural dihedral and trihedral reflectors formed as the result of weathering and erosion.

Meyer (65) has reported on one of the most recent SLAR studies in which calibrated radar data were statistically correlated with ground-truth data. Computational techniques were devised to compare the effect of various crop conditions and ground parameters with corresponding radar backscatter coefficients measured from calibrated SLAR imagery. Reference film densities appeared as "gray scale" wedges on the image film.

Results of the study indicated that a calibrated radar system is useful for extracting terrain information from radar imagery. The type of crop and, in some cases, crop condition had the most significant effect on the radar backscatter coefficient at similar depression angles. For the range of soil types found in the Phoenix, Arizona, test area, the soil type did not significantly affect the amount of reflected radar energy.

It was recommended that further work include the construction of a calibrated test range similar in part to the radar geology test area described by Shepard (86) which contains patches of various types of rock buried to various depths in

Willcox Playa in Arizona. Density readings of imagery obtained over the Willcox test area indicated that some of the patches could be detected, but an analysis of the data was not undertaken.

It is apparent that the majority of SLAR image terrain investigations reported in the open literature have not included the measurement of ground-truth parameters. In fact, the only calibrated radar terrain study reported in open literature has been that by the Goodyear Aerospace Corporation. The approach used for the interpretation of SLAR imagery has been the same as that used for conventional airphoto-interpretation. Although a general technique for radar interpretation encompassing a systematic procedure for the extraction of terrain information has not been developed, specific radar patterns have been illustrated with examples by many investigators.

IV. RESEARCH APPROACH

17. Introduction. Information concerning terrain parameters, including engineering soil groups, is not directly measurable from, or directly observable on, any form of remote sensor display. With conventional aerial photography, soils information is interpreted by means of a logical deductive and inference process based upon the evaluation of the pattern elements of tone, texture, and form as seen on stereo models. Because SLAR imagery also records and exhibits patterns, though not necessarily the same patterns as seen on aerial photography, it was a primary objective of this study to develop an engineering soils interpretation technique based on the concept of pattern analysis. This entailed the definition and evaluation of SLAR image patterns and their correlation to corresponding engineering soil types and land surface conditions. Qualitative and quantitative analyses were undertaken to explain the appearance of SLAR images in terms of terrain parameters which could be correlated with corresponding engineering soil conditions.

Chronologically, the investigation included a detailed literature survey of techniques presently utilized for the interpretation of SLAR imagery followed by the selection of representative samples of imagery for study. A systematic technique for interpretation of engineering soils information from SLAR imagery evolved as the SLAR imagery was qualitatively analyzed. An evaluation of quantitative methods for extracting terrain data from the imagery led to a model which can be used to predict terrain roughness with parameters measured from monoscopic SLAR imagery.

18. Acquisition of Imagery. No SLAR imagery was obtained from flights designed specifically for this study. Because SLAR is a relatively new sensor, most operational sensors are in a stage of continuing modification. Furthermore, there are no commercial systems available at this time. Consequently, study imagery was selected

from imagery obtained for purposes other than this investigation. Although ample footage of imagery was available, the variety of terrain and engineering soil types evaluated was limited and essentially pre-determined.

Both "classified" and "unclassified" samples of imagery were obtained for use in this investigation. ETL arranged visits to Goodyear Aerospace Corporation, Akron, Ohio; Autometric Corporation, Alexandria, Virginia; Rome Air Development Center, Rome, New York; and the Willow Run Laboratories, Ypsilanti, Michigan. SLAR imagery was obtained from all of these sources. All samples of film were copies of the original. Although it was requested that the film be the closest generation to the original quality, many samples of imagery were significantly degraded from original quality. Most of the SLAR image samples consisted of positive or negative transparencies. Some positive prints were selected in cases where the film negatives could not be copied or where only a single print was available.

Table II summarizes the general specifications of SLAR imagery used in this investigation. The form of each initial image from which all working copies were made is described as negative transparency, positive transparency, print, etc. Included is the location of each imaged study site and a brief description of the climatic condition during the day of each flight.

19. Qualitative Analysis of SLAR Imagery. The qualitative analysis or evaluation of interpretability of SLAR imagery was accomplished as a 2-phase procedure. The first phase consisted of interpreting terrain conditions and engineering soil types from each image without the benefit of any ground-truth information. Although this first phase necessarily required the use of conventional airphoto techniques of pattern recognition, every attempt was made to identify and describe patterns unique to SLAR imagery. Emphasis was placed on the evaluation of the basic elements of image tone and texture as seen on the photograph of the SLAR display. These elements were then related to the grosser patterns of drainage, topography, and, ultimately, geomorphic landform. No conscious effort was made to relate the various pattern elements to specific causal factors at this early stage of analysis. Although an interpretation of probable engineering soil conditions was made, it was of secondary importance to the cataloging of SLAR image pattern elements.

The second phase of the qualitative analysis had as its purpose the determination of the relative importance of all previously defined SLAR image pattern elements as predictors of engineering soil types. Pattern elements were qualitatively correlated singly and in groups with parameters of the terrain from which the elements were recorded. An attempt was made to explain the significance of each pattern element in terms of the interaction of the radar energy and the illuminated terrain surface. A SLAR, image-interpretation technique was developed which provides for a systematic

Table II. SLAR Image Study Sites

Location	Image Description	Approximate Scale	Date and Flight Condition
Humphrey's Peak Flagstaff, Arizona	UNCLASSIFIED - Multiple Polarized K-band SLAR, Negative Transparency Good Quality Imagery	1:196,300	November 5, 1965 Clear
Phoenix, Arizona	UNCLASSIFIED - Multiple Polarized K-band SLAR, Negative Transparency Poor Quality Imagery - washed out	1:173,600	November 8, 1965 Clear Ground Temperature Range 52-81° F
Phoenix, Arizona	CLASSIFIED - X-band	1:480,000	
Willcox, Arizona	UNCLASSIFIED - Multiple Polarized K-band SLAR, Negative Transparency Good Quality Imagery	1:149,400	November 8, 1965 Clear Ground Temperature Range 34-76° F
Willcox, Arizona	CLASSIFIED - X-band	1:475,000 1:427,500 1:522,500	
Yuma, Arizona	CLASSIFIED - K-band	Multiple Samples Variable Scales	
Little Rock, Arkansas	CLASSIFIED - X-band	1:450,000	
Fort Collins, Colorado	UNCLASSIFIED - Mono-Polarized K-band SLAR (AN/APQ-56) Negative Transparency Good Quality Imagery	1:400,000	August 20, 1957 Cloudy, Trace Precipitation 0.33 inch Precipitation on August 17, 0.22 inch on August 18, 1957 Temperature Range 56-78° F
Elgin AFB, Florida	CLASSIFIED - X- and K-band	1:111,000 1:69,400 1:402,500	
Lafayette, Indiana	UNCLASSIFIED - Multiple Polarized K-band SLAR, Flight 82 - Negative Transparency	1:172,800	September 14, 1965 Cloudy, Trace Precipitation Ground Temperature 64-83° F
	Flight 86 - Negative Transparency	1:108,720	October 7, 1965 Cloudy, .15 inch Precipitation Ground Temperature 48-64° F
	Flight 126 - #1 Positive Transparency #2 Positive Transparency #3 Positive Transparency	1:201,600 1:184,100 1:209,500	July 26, 1966 July 26, 1966 July 26, 1966 Clear Ground Temperature Range 64-92° F
	Good Quality Imagery		

Table II (cont'd)

Location	Image Description	Approximate Scale	Date and Flight Condition
Northern Illinois and Indiana	CLASSIFIED - X-band	1:487,000	
Kentucky Lake Area, Kentucky	UNCLASSIFIED - Mono-polarized K-band SLAR (AN/APQ-56), Negative Transparency Good Quality Imagery	1:375,000	November, 1957 Flight Condition Unknown
Eastern Kentucky	CLASSIFIED - X-band	Multiple Samples Variable Scales	
Mt. Airy, Maryland	UNCLASSIFIED - Multiple Polarized K-band SLAR, Negative Transparency Good Quality Imagery	1:105,000	October 5, 1965 Clear Ground Temperature Range 33-53° F
Vicksburg, Mississippi	UNCLASSIFIED - Multiple Polarized K-band SLAR, Negative Transparency Good Quality Imagery	1:97,400	November 10, 1965 Cloudy, Trace Precipitation Ground Temperature Range 59-69° F
Watertown, New York Area	CLASSIFIED - X- and K-band	Multiple Samples Variable Scales 1:47,100 - 1:457,000	
Woods County, Oklahoma	CLASSIFIED - K-band	1:200,000	
Harrisburg, Pennsylvania	UNCLASSIFIED - Multiple Polarized K-band SLAR, Negative Transparency Good Quality Imagery	1:187,500	July 20, 1965 Trace Precipitation on July 19, 1965 Ground Temperature Range 62-83° F
"Haystack Region," Puerto Rico	CLASSIFIED - X-band	1:50,000	
Texas Point, Texas	UNCLASSIFIED - Multiple Polarized K-band SLAR, Negative Transparency Good Image Quality	1:172,800	November 9, 1965 Cloudy, 0.25 inch precipitation Ground Temperature Range 64-76° F
Salt Lake City, Utah	UNCLASSIFIED - Multiple Polarized K-band SLAR, Negative Transparency Good Quality Imagery	1:125,000	October 20, 1965 Clear, Trace Precipitation on October 19, 1965 Ground Temperature Range 34-63° F
Jackson Hole, Wyoming	UNCLASSIFIED - Multiple Polarized K-band SLAR, Negative Transparency Good Quality Imagery	1:172,500	October 21, 1965 .08 Precipitation on October 20, 1965 Ground Temperature Range 19-54° F
Laramie, Wyoming	CLASSIFIED - X-band	1:703,100	

evaluation of each image pattern significant for the determination of a representative engineering soil type.

The preliminary and detailed phases of qualitative image investigation required certain mechanical procedures for ease of data extraction. Positive transparencies were oriented so that radar shadows had their tips pointed toward the interpreter. Magnifying lenses and various scales were utilized for the routine procedure of scale ratio determination. The SLAR image transparencies, of course, were viewed on a light table. Frosted acetate overlays were extensively used to record pattern boundaries and to trace drainage and transportation networks.

20. Quantitative Analysis of SLAR Imagery. It was hypothesized that two aspects of an uncalibrated SLAR image were potentially capable of being quantified. Radar image texture, being a function of the distribution of individual resolution elements as well as their return values, was evaluated as being a potentially common link between images from uncalibrated radar systems. Radar shadow size and shape, being a function of system geometry and terrain relief, were evaluated as parameters for the prediction of terrain roughness.

The SLAR image texture experiment was an attempt to relate the shape of a probability density curve (histogram of tone values) to visually defined image textures. Probability density curves were obtained by recording the signal output of a Macbeth densitometer with a Packard multichannel analyzer. Textural correlations were performed visually and statistically.

A terrain-roughness model composed of measured parameters from SLAR images was derived statistically. Radar shadow sizes and shapes were measured from monoscopic SLAR images and correlated with a calculated terrain roughness expressed as the log of Fisher's dispersion factor "K" (33, 40, 98).

21. Collection of Ground-Truth Information. In order to carry out the detailed study phase of the qualitative analysis and the quantitative experiments, it was necessary to collect ground-truth information for each study site. Information concerning the geologic history, topography, and terrain relief; engineering and pedological soil types; geology; vegetation; and cultural activity was required for each area imaged by the various SLAR systems. Because all of the SLAR imagery utilized was obtained prior to the inception of this investigation, field measurement of transient factors such as soil-moisture content, agricultural crop types, and areas of bare soil was not justified as a means of obtaining correlative data. It was necessary to accept more general information in the form of qualitative estimates based on field observation or the results of previous studies.

Most of the ground-truth information was extracted from pertinent literature. Table III lists the general sources of information found to be of value in establishing the ground truth necessary for the analyses performed during the course of this investigation. Some study sites were defined more adequately than others. Literature relating to the ground truth of the study sites located in Arizona, for example, was not plentiful. For this reason, and as an interim check of the reliability of the developing interpretation technique, the Wilcox study site was field checked. It was possible to make field observations at the Phoenix and Humphrey's Peak study sites. Field observation of specific terrain conditions was also utilized for the determination of ground truth within the Northern Indiana and Illinois study sites.

Table III. Ground-Truth Information Sources

Source No.	Item	Source (Location)
Engineering Information		
1	Engineering Soil Maps	Arizona & Indiana
2	County Drainage Maps	Arizona & Indiana
3	"The Origin and Distribution of United States Soils"	CAA - Purdue University, 1946
4	<i>Highway Engineering Handbook</i> , K. B. Woods (ed.)	McGraw-Hill, Inc., 1960
Topographic Information		
5	Topographic Maps (Scales - 1:250,000, 1:62,000, 1:24,000)	U. S. Geological Survey
Geologic Information		
6	Geological Quadrangles	U. S. Geological Survey
7	Preliminary Investigation Maps	U. S. Geological Survey
8	Professional Papers	U. S. Geological Survey
9	Maps, Bulletins, & Reports	State Geological Survey
10	Water Resources Reports	U. S. & State Geological Survey
11	Bulletin	Geological Society of America
12	<i>Physiography of the Western United States</i> N. M. Fenneman	McGraw-Hill, Inc., 1931
13	<i>Physiography of the Eastern United States</i> N. M. Fenneman	McGraw-Hill, Inc., 1938
Pedologic Information		
14	Agricultural Soils Maps	U. S. Dept of Agriculture
15	<i>Soils and Men - Yearbook of Agriculture</i>	U. S. Dept of Agriculture, 1938
Inferred Information		
16	Airphoto Mosaics & Stereo Pairs	Federal & State
17	Unpublished Research Reports & Theses	--
18	Field Observations	--

Table IV summarizes the ground truth and environment established for each of the study sites displayed on SLAR imagery. Each summary represents the information that is contained in the specific maps and overlays made for correlation with each SLAR image during the detailed qualitative analysis phase of the investigation.

V. QUALITATIVE ANALYSIS OF SLAR IMAGERY

22. Introduction. The feasibility of interpreting terrain and cultural features from photographic or image displays of land surfaces has been established through the application of airphoto interpretation to a variety of engineering and military problems. The concept has been based primarily on the analysis, by inference and deduction, of pattern elements. It was hypothesized from the beginning of this investigation that a group of patterns unique to specific terrain conditions and engineering soil types is visible on SLAR imagery and available for use in a systematic interpretation technique. By relating specific SLAR image patterns to the radar energy-terrain surface interaction producing each pattern, it was anticipated that the interpretation technique would produce results which would complement or, in some cases, be superior to that information available from conventional aerial photography.

Qualitative analysis consisted of a 2-phase research approach. A preliminary evaluation of SLAR imagery was undertaken as a means of identifying, describing, and cataloging fundamental pattern elements. This was followed by a detailed evaluation phase in which a select group of repetitive patterns was described in terms of its component elements. These patterns were then related to genetic and morphologic landforms and ultimately to engineering soil types. The results of both phases of qualitative analysis led to development of a systematic interpretation technique for the extraction of engineering soils information from SLAR imagery.

23. Evaluation of Pattern Elements. Two parameters can be observed on and described from SLAR imagery. The tone (radar return) of individual and groups of resolution elements and image texture formed by the distribution of resolution elements of varying return values are unique to SLAR imagery. All SLAR image patterns were found to be a function of these pattern elements. The evaluation of pattern elements consisted of the identification, description, and cataloging of variations of the elements of tone and texture.

a. Analysis of Element of Tone. The element of tone was evaluated at two levels. Individual or small groups of resolution elements with unusually high or low return values form "discrete" tonal elements which can be related to specific cultural features or local features of natural terrain surfaces. In addition to discrete tonal elements there exists an "average" or "representative" areal tone which tends to indicate the

Table IV. Study Site Ground Truth and Environment

Location	Physiographic Province	General Physiography	General Geology	Vegetation and Culture
Humphrey's Peak Area North of Flagstaff, Arizona	Grand Canyon and Datil Sections: Colorado Plateaus	High Block Plateaus Uplifted and Dissected Volcanic Landforms	Volcanic Necks, Cinder Cones, and Multiple Flows, Dissected Sedimentary Plateaus, Unconsolidated Material Derived Primarily from Volcanic Material	Desert Brush and Grass, Ponderosa Pine at Higher Elevations, Little Evidence of Cultural Activity
Phoenix, Arizona	Sonoran Desert Section: Basin and Range	Ranges Formed as the Result of Regional Faulting and Uplift, Basins Filled with Erosional Products	Eroded, Faulted Sedimentary, Igneous, and Metamorphic Mountains Surrounding Alluvial Valley, Unconsolidated Materials in Fans, Aprons, and Valleys, Material Sizes Gradational to Sand and Silt in the Valley	Irrigated Crops in Alluvial Valley, Unirrigated Areas Support Sparse Desert Brush and Grass, Mountain Areas Support Little Vegetation, Significant Cultural Features in Irrigated Areas, Little Culture in Desert
Willcox, Arizona, Area	Mexican Highland Section: Basin and Range	Dissected and Severely Eroded Block Mountains, Intermont Basins, and Desert Plains	Eroded Sedimentary and Metamorphic Mountains Flanked by Alluvial Fans, Aprons, and in Some Cases Pediments, Willcox Playa a Major Feature of Site	Sparse Desert Brush and Grasses, Significant Cultural Features Only Near Small Town of Willcox, Arizona
Yuma, Arizona	Sonoran Desert Section: Basin and Range	Ranges Formed as the Result of Regional Faulting and Uplift, Basins Filled with Erosional Products	Eroded Sedimentary and Metamorphic Mountains, Numerous Alluvial Fans and Aprons	Sparse Desert Brush and Grass, Little Evidence of Cultural Activity
Little Rock, Arkansas	Mississippi Alluvial Plain Section: Coastal Plain	Flood Plains Bordered on East by Dissected Upland	Fine Grained Unconsolidated Flood Plain Deposits, Dissected Loessal Upland on Eastern Edge of Study Site	Heavily Vegetated Woods and Swamp Vegetation in Flood Plain, Some Agriculture, City of Vicksburg and Transportation Networks
Fort Collins, Colorado, Area	Colorado Piedmont Section: Great Plains Front Range Section:	Late Mature to Old Elevated Plains, Complex Mountains with Intermont Basins	Fine Grained Unconsolidated Material in Plains Area, Sedimentary and Metamorphic Mountains in Western Portion of Study Area	Agriculture in Plains Area, Several Small Towns and Associated Transportation Networks in Study Area

Table IV (cont'd)

Location	Physiographic Province	General Physiography	General Geology	Vegetation and Culture
Elgin AFB, Florida	East Guir Coastal Plain Section: Coastal Plain	Young to Mature Belted Coastal Plain, Numerous Estuarine Deltas	Weakly Consolidated Sediments, Fine Grained Alluvium in Stream Valleys	Heavily Vegetated, Woods, Brush, Grass, and Some Agriculture Moderate Cultural Activity
Lafayette, Indiana	Central Till Plains: Central, Arctic, and Eastern Lowlands and Plains	Till Plains with Ground Moraine and Multiple Terraces and Outwash Along Glacial Sluiceway	Primarily Till Deposits with Some Interbedded Outwash Sands and Gravels, Multiple Gravel Terrace and Outwash Deposits Along Wabash River	Predominant Agricultural Activity, Woods and Brush Along Streams and in High Relief Areas, City of Lafayette and Smaller Towns in Area
Northern Indiana and Illinois	Central Till Plains: Dissected Loessal and Till Plains: Central, Arctic, and Eastern Lowlands and Plains	Glacial Deposits, Primarily Till Plain in East, Significant Dissection and High Relief Near Mississippi River	Till Plains in Eastern Portion of Area, Becoming Dissected and Loess Covered to West, Some Outwash and Lacustrine Deposits	Predominant Agricultural Activity, Woods and Brush Along Streams and in High Relief Areas, Numerous Small and Moderate Sized Towns and Associated Transportation Networks
Kentucky Lake Area, Kentucky	Highland Rim Section: Interior Low Plateaus	Young to Mature Plateau of Moderate Relief, Karst Topography North of Kentucky Lake	Primarily Limestone Bedrock or Interbedded Sedimentary Rock, Alluvial Valleys Filled with Silt	Little Agricultural Activity, Some Woods and Pasture Land, Little Cultural Activity Except Around Lake
Eastern Kentucky	Cumberland Section: Appalachian Plateaus	Mature Plateau and Mountain Ridges on Eroded Open Folds	Folded, Eroded Sedimentary Rocks, Alluvial Stream Valleys	Little Agricultural Activity, Woods and Brush in High Relief Areas, Little Cultural Activity
Mt. Airy, Maryland	Piedmont Uplands and Lowlands Section: Piedmont	Dissected Plain of Sedimentary and Metamorphic Rock with Moderate Relief, Some Residual Ridges of Resistant Rock	Primarily Metamorphic and Resistant Sedimentary Rock, Some Linear Ridges of Quartzite and Conglomerate, Igneous Intrusive Ring Dike Features in Western Portion of Study Area	Mixed Agricultural and Wooded Plots, Higher Relief Areas Wooded, Several Small Towns and Associated Transportation Facilities in Study Area
Vicksburg, Mississippi	Mississippi Alluvial Plain Section: Mississippi Loessal Upland Section: Atlantic and Gulf Coastal Plain	Flood Plain and Associated Old Age Stream Geomorphic Features, Dissected Upland in Eastern Portion of Study Area	Fine Grained Alluvial Sediments in Flood Plain, Loessal Upland Bordering Flood Plain on East	Predominant Woods and Swamp Vegetation in Flood Plain with Agricultural Activity in Protected Areas, Woods and Brush in High Relief Portion of Loessal Upland

Table IV (cont'd)

Location	Physiographic Province	General Physiography	General Geology	Vegetation and Culture
Watertown, New York, Area	Central and Eastern Lakes and Lacustrine Plains Section: Central, Arctic and Eastern Lowlands and Plains	Moraines with Moderate Relief, Till, Outwash and Lacustrine Plains	Till, Outwash, Lacustrine and Glacio-Fluvial Deposits of All Types	Agricultural Activity to Varying Degrees Depending upon Relief, Some Woods and Swamp Vegetation
	Mohawk River Valley and New York State Glaciated Section: Appalachian Plateaus	Mature, Glaciated Plateaus with Varying Degrees of Dissection	Glacially Eroded Limestone, Shale and Sand Stone Bedrock and Glacial Deposits	Several Major Towns, Villages and Associated Transportation Facilities are in Study Area
Woods County, Oklahoma	Ozage Plains Section: Great Plains	Old Scarred Plains, Slightly Inclined Strata, Entrenched Streams	Sedimentary Rocks Consisting Primarily of Shale, Alluvial Material in Stream Valleys	Predominantly Agricultural Vegetation, Brush in Eroded or Waste-land Areas, Little Cultural Activity
Harrisburg, Pennsylvania	Pennsylvania, Maryland, and Virginia Section: Ridge and Valley	Even Crested Ridges of Eroded, Folded Rock, Valleys of Moderate to Low Relief Formed on Rocks of Low Resistance	Folded, Resistant Sedimentary Rock in Northern Portion of Study Site, Weakly Resistant Shales and Limestone Forming Valleys, Metamorphic and Igneous Intrusive Rock in Southern Portion of Study Site	Woods and Brush Cover on Steeply Sloping, High Relief Areas, Intense Agricultural and Cultural Activity in Valleys, Harrisburg, Pennsylvania, and Associated Transportation Facilities Dominate Southern Portion of Study Site
"Haystack" Region, Puerto Rico		Karst Topography, "Haystack" Mounds of Resistant Limestone Rock	Limestone Bedrock with Residual Clay Soil and "Haystack" Limestone Features	Lush Vegetation, Some Agricultural Activity, Numerous Small Villages
Texas Point, Texas	West Gulf Coastal Plain Section: Atlantic and Gulf Coastal Plain	Young Coastal Plain, Numerous Lakes and Swamps and Estuarine Deltas	Weakly Consolidated, Fine-Grained Sediments	Swamp Vegetation, Little Agricultural or Cultural Activity
Salt Lake City Area, Utah	Great Basin Section of Closed Basins: Basin and Range	Isolated Dissected Block Mountains Separated by Aggraded Desert Plains, Beach Ridges Along Eastern Coast of Great Salt Lake	Primarily Unconsolidated Sand, Silt and Clay and Evaporite Deposits	Sparse Vegetation, Eastern Portion of Study Area Contains Suburbs of Salt Lake City and Associated Transportation Facilities

Table IV (cont'd)

Location	Physographic Province	General Physiography	General Geology	Vegetation and Culture
Jackson Hole, Wyoming	Yellowstone Section: Middle Rocky Mountains	Glacial Valley Surrounded on Three Sides by Glacially Eroded Mountains, Glacio-Fluvial Deposits in Valley Alpine Glacial Features in Mountains	Glacial Till and Multiple Glacio-Fluvial Terraces in Valley, Sedimentary Igneous and Metamorphic Mountains	Alpine Vegetation in Mountains, Woods and Grass in Valley, Little Cultural Activity in Area Except for Town of Jackson, Wyoming
Laramie, Wyoming	Wyoming Basin Section: Great Plains, Front Range and Western Section: Southern Rocky Mountains	Complex Mountains with Intermont Basins	Sedimentary, Igneous and Metamorphic Mountains, Alluvial Basins	Sparse Vegetation, Some Woods in High Relief Areas, Little Cultural Activity Except Town of Laramie, Wyoming

general reflecting characteristics of a regional terrain surface. Although the image of such a regional area might contain significant discrete tonal elements, it will also show a general tone level indicative of its representative return. With few exceptions, the discrete tonal elements are significant for the delineation and identification of cultural features, radar shadow areas, and specular and cardinal reflecting surfaces whereas an estimate of average areal tone is of significance for the interpretation of regional terrain conditions.

Discrete tonal elements are significant only when their tone values produce a marked contrast with the average areal tone. Consequently, they usually are defined by their very light or very dark tone value with respect to their surroundings. The lack of calibration of the imagery used for this investigation prevented the use of transmission or reflection density values as consistent indicators of tone. Thus, only qualitative descriptive terms are used.

The actual size of a discrete tonal element displayed on a SLAR image is a function of the resolution of the system, the size and shape of the target, and the reflecting ability of the target. High returns representing high degrees of reflectivity appear as light tones on the positive prints used as illustrations in this report. Low returns appear as dark tones. Figure 12 illustrates the basic tonal contrasts which form discrete tonal elements. The relation of specific discrete tonal elements to cultural and terrain features is presented in this figure and is discussed in further detail in the Appendix.

Identifying and describing average areal tone is not as simple as recognizing high or low tones of discrete tonal elements. A combination of varying tone values must be qualitatively evaluated and an estimate made of the value of the most representative tone. The tone of each resolution element, in fact, represents a measure of the radar cross section of that portion of the terrain surface illuminated by the radar system. Ideally, the value of the radar cross section should be measurable in terms of the surface roughness and complex dielectric constant of the illuminated terrain. However, lacking a suitable theory for the reflective character of natural, vegetated terrain surfaces and lacking calibrated radar imagery, it is necessary to utilize the element of average areal tone simply as one of the pattern elements rather than as a quantitative measure of a specific terrain parameter.

Table V contains general terrain conditions, geologic material types, types of vegetation, and a qualitative description of the tonal range (return values) normally found associated with them on SLAR imagery. For purposes of delineating and interpreting regional engineering soil types, an interpreter must evaluate some or all of these tone values to arrive at an estimate of average areal tone. To effectively utilize average areal tone as a pattern element for engineering soils interpretation, it is also

Table V. Terrain Factors and Representative Tonal Ranges
(Factors Are Not Mutually Exclusive)

Factor	Reflection Characteristic	Tonal Range
Topographic		
Flat Surface	Specular Reflection if Surface is Smooth, No Return	Dark Tones
Sloping Surface Facing Antenna	Relatively High Return Due to Orientation Effects	Medium to Light Tones
Sloping Surface Facing Away from Antenna	Relatively Low Return Due to Orientation Effects	Medium to Dark Tones
Geologic		
Rough Surfaces (> 1 Wavelength)	Diffuse Reflection, Medium to High Returns	Medium to Light Tones
Smooth Surfaces (< 1 Wavelength)	Specular Reflection if Surface is Flat, No Return Reflection Influenced by Topographic Effects	Dark Tones Lighter Tones Produced by Orientation Effects
Natural Corner Reflectors Produced in Bedrock by Weathering	Maximum Reflection of Incident Energy Back to Antenna, High Return	Very Light Tones
High Surface Moisture Content	Greater Reflection with Increasing Values of Dielectric Constant, Higher Returns with Higher Moisture Contents if Water Does not Produce a Smooth Surface	Medium to Light Tones
Low Surface Moisture Content	Lower Returns with Decreasing Values of Dielectric Constant	Medium to Dark Tones
Vegetation		
Trees, Woods, and Forests	Diffuse Reflection, High Returns	Light Tones
Brush	Higher Returns with Increasing Dielectric Constant in Humid to Subhumid Areas, Brush with Higher Moisture Content Produces Greater Degree of Reflection	Light Tones, (Medium to Dark Tones in Arid Environment)
Natural Grass, Weeds	Diffuse Reflections, Medium to Low Returns, Dry Vegetation Produces Less Reflection Than Lush, Moisture-Rich Vegetation	Medium Tones in Humid to Subhumid Areas (Dark Tones in Arid Environment)
Broad Leaf Crops, Crops with Naturally High Moisture Content	Diffuse Reflection, High Returns	Light Tones
Small Leaf Crops	Diffuse Reflection, Medium Returns	Medium Tones



ELEMENTS RESULTING FROM SPECULAR REFLECTION OF
RADAR ENERGY FROM SMOOTH WATER SURFACES



ELEMENTS RESULTING FROM THE EFFECT OF
RADAR SHADOWING



ELEMENTS RESULTING FROM THE SPECULAR REFLECTION
OF RADAR ENERGY FROM SMOOTH MAN-MADE SURFACES



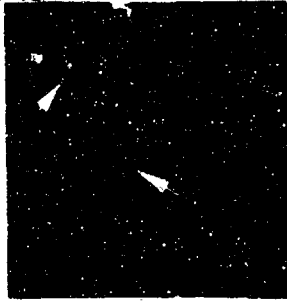
ELEMENTS RESULTING FROM THE DIRECT REFLECTION OF
RADAR ENERGY FROM CULTURAL AND LOCAL TERRAIN FEATURES

Fig. 12. Discrete tonal elements.

LIGHT AVERAGE AREAL TONE



**SLOPE FACING
ANTENNA, ROUGH
SURFACE**



**RELATIVELY FLAT
SURFACE, ROUGH
VEGETATION**



**TERRAIN WITH
HIGH RELIEF**

MEDIUM AVERAGE AREAL TONE



**RELATIVELY FLAT
SURFACE, LIGHTER
TONED RECTANGLES
PRODUCED BY GRIDS**



**RELATIVELY FLAT
SURFACE, GRASS
COVERED**



**MODERATE RELIEF,
DESERT VEGETATION**

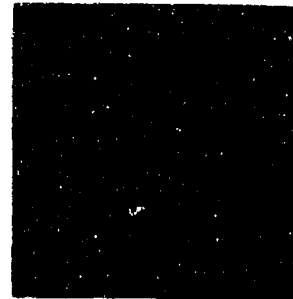
DARK AVERAGE AREAL TONE



**RELATIVELY FLAT,
SMOOTH SURFACE
NO VEGETATION**



**RELATIVELY SMOOTH
SURFACE, ARID
ENVIRONMENT**



**RELATIVELY FLAT
SURFACE, CROPS
HARVESTED**

**NOTE: ALL AVERAGE AREAL TONES MUST BE
EVALUATED IN TERMS OF THEIR RELATIVE
VALUES.**

Fig. 13. Average areal tones.

necessary to assign relative values of importance to each unit of the surface producing a different tone. For example, with engineering soils interpretation as an ultimate goal, the relatively light tones of several wood lots would be of less importance to the determination of an average areal tone than the light tones of portions of the land surface facing the antenna of the radar system. The very low tone of one cultivated field is of less significance for the interpretation of regional conditions than is the medium tone of a surrounding grass- or crop-covered plain. Although the average areal tone determination can seldom be directly correlated with a specific engineering soil type, it can be used advantageously in concert with other pattern elements as an indicator of regional land-surface condition. As complexity and variability of tones increase, the size of the regional area for which a determination of average areal tone is useful decreases.

Figure 13 illustrates the range of average areal tones found to have practical usefulness as pattern elements. Each illustration is annotated to indicate the general condition producing the average areal tone value.

b. Analysis of Element of Image Texture. The distribution and tone (return value) of individual resolution elements form an image texture. While the average areal tone of a portion of a SLAR image tends to indicate the capability of the corresponding terrain surface to reflect microwave energy, image texture yields evidence of variability of reflection within that unit. While SLAR image patterns are recognized as distinct, geometrically ordered (or disordered) contrasts in reflectivity on a macro-scale, image texture is a measure of the microvariability of reflecting surfaces and as such becomes an element of the larger scale pattern.

Image textures can be recognized as being smooth, grainy, or speckled in order of increasing coarseness or variability when viewed on a SLAR image without the benefit of magnification. Because SLAR image textures are affected by the dynamic range of tone values allowed by the CRT display device as well as by the resolution of the SLAR system, the evaluation of these factors must be taken into account when interpreting the significance of image texture. Furthermore, the evaluation of image texture as presented in this discussion cannot be extended to those textures as seen on images enlarged greater than three times because of the effect of the grain of the photographic medium of display. When the SLAR image texture of enlarged images is evaluated, the actual appearance of smooth, grainy, or speckled image textures becomes coarser with an increase in enlargement. The evaluation of texture described herein is based on original-scale imagery.

SLAR image texture is used as the pattern element which indicates the homogeneity of the reflective nature of each portion of terrain exhibiting a characteristic texture. Contrasts in image texture and contrasts in discrete and average areal tone permit the identification and delineation of patterns which can be inferred as the

unique expression of specific terrain conditions. Because of the dependence of image texture on the distribution of tones, this pattern element is less affected by the lack of image calibration than is image tone itself. Within the limits of extremely high or low SLAR system gain settings, the appearance of image textures remains relatively consistent from one image to another regardless of variation of absolute tone value resulting from external factors.

Evaluation of smooth, grainy, and speckled image textures takes into account the effect of each individual resolution element as a component of the resultant texture. There exists, in addition, a "second order" texture which approaches the level of a pattern. There are, in some cases, groups of resolution elements which together tend to form a texture with dimensions an order of magnitude larger than the previously defined textures. These "second order" textures might be considered as "macro-textures" as opposed to smooth, grainy, or speckled "micro-textures." It is believed that "macro-textures" are probably undefined patterns. This tends to introduce some degree of inconsistency in the development of the SLAR interpretation technique. However, because these undefined patterns which often appear as gross textures do tend to aid in the delineation of pattern boundaries, they are included with the discussion of texture.

The "second order" texture hereafter defined as a macro-texture can be recognized and described as having a rough, irregular appearance. It is formed by the random association of groups of resolution elements showing varying tone values. The significance of macro-texture as a pattern element lies in its indication of random variability of terrain or vegetative reflectivity. The macro-texture exhibits only the appearance of rough, irregular tonal distribution where it exists on an image.

Figure 14 illustrates SLAR image textures and the macro-texture utilized as elements of patterns significant for engineering soils interpretation. An evaluation of factors producing these pattern elements and the relation of these pattern elements to the interpretation of engineering soils are discussed in the analysis of specific SLAR image patterns.

24. Detailed Analysis of SLAR Image Patterns. The inference of engineering soil types from radar image patterns is based upon a hierarchical scheme of deduction and analysis. A series of components, individually and as groups, provides evidence for the inference of engineering soil types. Characteristic associations of the elements of tone and texture form patterns of drainage, topography, and land use. The previously mentioned patterns in various associations allow the interpretation of genetic and morphologic landforms. Genetic landforms, in this context, are defined as the repetitive expressions of the topography of the earth's surface, including relief and slope, that reflect the geomorphic processes involved in their development as well as the engineering



SMOOTH IMAGE TEXTURES



GRAINY IMAGE TEXTURES



SPECKLED IMAGE TEXTURES



ROUGH, IRREGULAR MACRO-TEXTURES

Fig. 14. SLAR image textures.

soil or parent material of which they are composed. By analyzing the interpreted landforms in terms of their component patterns and pattern elements, it is possible to deduce the most probable associated engineering soil type. Morphologic landforms do not by themselves reflect a specific geomorphic process.

A detailed analysis of SLAR image patterns consisted of the evaluation of the patterns of drainage, topography, and land use in terms of tone and textural elements. Following identification and description of SLAR image patterns, the manner in which they were associated to form SLAR displays of genetic or morphologic landforms was evaluated.

a. SLAR Image Patterns of Drainage. The particular design or geometric relationship formed by a group of individual streams within an area is referred to as a drainage pattern. It is generally recognized that drainage patterns can reflect the influence of such geologic factors as inequalities in rock hardness, structural controls, and the recent geologic and geomorphic history of an area. The term "drainage pattern" does not imply that component streams will always be filled with water. In arid regions, the drainage pattern is often only the expression of surface swales or low areas which carry water during times of rainfall.

The analysis of drainage pattern for the interpretation of conventional aerial photographs has been well defined (66, 67). Parvis (74) has presented, perhaps, the most comprehensive adaptation of drainage-pattern analysis for airphoto interpretation purposes.

Drainage patterns extracted from SLAR imagery for the interpretation of engineering soil types are of the same order of significance as they are for conventional airphoto interpretation. However, the appearance and general level of detail of drainage patterns imaged by SLAR are different. Instead of relying on topographic form as seen in a stereoscopic airphoto model, the SLAR image patterns of drainage must be recognized as unique associations of discrete tonal elements. Table VI lists those conditions which usually produce discrete tonal elements which may as a group form SLAR image displays of drainage pattern.

McCoy (64) has indicated that first-order streams as defined by Strahler (96) are often not interpretable from SLAR images because of scale and resolution. This situation, confirmed during the course of this investigation, tends to degrade the value of drainage-pattern analysis for the interpretation of local terrain conditions but has little effect upon the evaluation of regional conditions. Regional drainage densities (Σ stream lengths/area) can be estimated.

Table VI. Discrete Tonal Elements Related to SLAR Image Drainage Pattern

Discrete Tonal Element	Condition Producing Element
Thin, sinuous and/or discontinuous lineation of no return, dark tone	Specular reflection from water surface
Thin, sinuous and/or discontinuous lineation of radar shadow, dark tone	Areas absent of any return because of the blocking of radar illumination, stream entrenchment, high-relief topography, and dense, high-riparian vegetation could produce this situation
Thin, sinuous and/or discontinuous medium to high-return elements contrasting with surroundings, medium to light tones	Medium to high returns from riparian vegetation or surface formed by a stream bank facing the SLAR antenna
Thin, sinuous and/or discontinuous lineation formed as a field boundary, Contrasts between light medium and dark average areal tones	Irregular field boundary necessitated by an adjacent, low-order stream
Discontinuous lineations formed as contrasts between relatively large-scale units of medium to high return and radar shadow, contrast between light tones and radar shadow	High-relief topography from which radar shadows are of large areal extent; contrast with high return from slopes facing antenna is great

Figure 15 illustrates some of the basic drainage patterns as portrayed on SLAR imagery. Such patterns, usually traced on plastic overlay sheets during the course of an image analysis, are developed as the result of integrating all of the discrete tonal elements (Table VI) inferred to be related to the drainage system.

b. SLAR Image Patterns of Topography. The capability of evaluating topography by viewing stereo SLAR image models has not been perfected. Consequently, the interpretative element of topographic form utilized for airphoto interpretation is not yet applicable. In the case of monoscopic SLAR images, the qualitative analysis of topography of cross-sectional shape of terrain is truly dependent upon pattern recognition. Evaluation of topographic conditions from SLAR imagery is, of necessity, less precise in terms of estimated dimensions than is the interpretation of topography from stereoscopic, airphoto models.



DENDRITIC



RECTANGULAR



TRELLIS



PINNATE



PARALLEL



CRESCENTIC



BRAIDED



DISTRIBUTARY

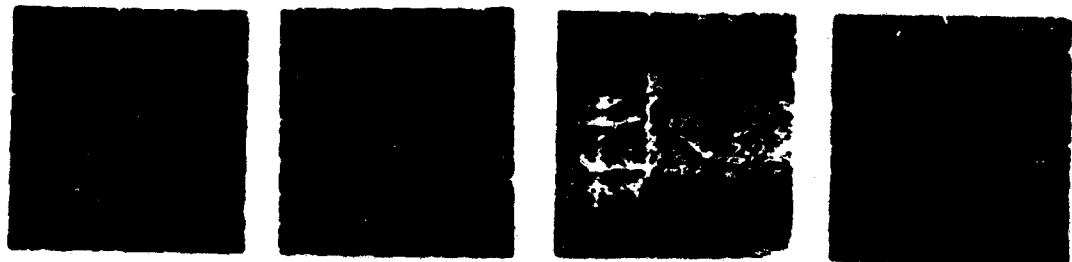


NO PERCEPTIBLE CHANNELS

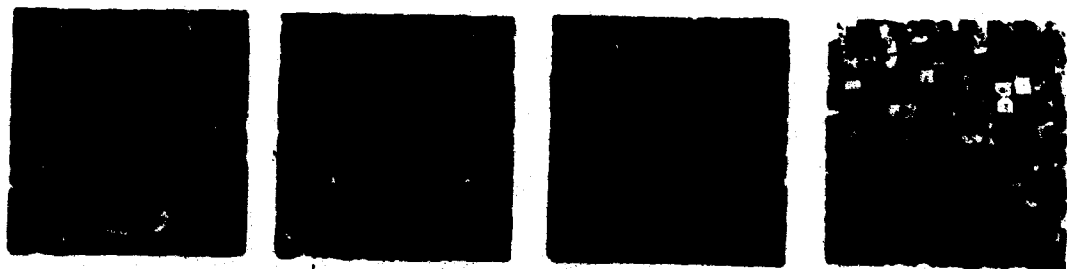
Fig. 15. Basic patterns of drainage.



RELATIVELY HIGH RELIEF



RELATIVELY MODERATE RELIEF



RELATIVELY LOW RELIEF

Fig. 16. Patterns of topography.

Discrete tonal elements, average areal tones, and image textures individually and in combination form patterns of topography. The pattern of drainage itself makes a further contribution. In general, discrete tonal elements provide evidence of high relief or abrupt changes in topographic form, whereas average areal tones and textures must be evaluated for the interpretation of more subtle topographic features.

Correct assessment of topographic form is vital to the interpretation of engineering soil types. The determination of genetic and morphologic landforms is greatly dependent upon the analysis of topography. The visual effect of combinations of return elements which allow the determination of specific topographic conditions is herein defined as "patterns of topography."

Conditions of high relief are portrayed on SLAR imagery in the form of radar shadows. Higher topographic features generally produce shadows which are longer in the range direction. Light-toned areas produced by slopes facing the SLAR antenna are commonly found associated with the radar shadows. The overall roughness of imaged terrain affects the distribution of shadows with a greater frequency of shadow occurrence characteristic of rougher terrain.

Areas of moderate relief produce SLAR image shadows of smaller size. In such cases, patterns of drainage may be indicators of relative relief. High-drainage densities are generally associated with higher relief areas. There is, however, less contrast between shadow and light-toned areas on imagery obtained from moderate-relief areas.

Low-relief areas generally produce no radar shadow or light tones because of topographic effects. Contrasts in tone and texture are normally the result of variations in local surface roughness.

Occurrence and distribution of wooded areas sometimes offer indirect evidence of relief and topographic forms. Trees normally will be found growing in areas not suitable for agricultural activity. Agricultural field shape offers still another indirect line of evidence with regular, rectangular field boundaries normally associated with relatively flat land.

Relative relief is illustrated in Fig. 16. General conditions of slope and topographic form appear as a function of radar shadow, average areal tone, and image texture. The recognition of significant topographic forms by an interpreter is entirely dependent upon a knowledge of geologic and geomorphologic processes.

c. SLAR Image Patterns of Land Use. Specific patterns of agriculture, natural vegetation, and cultural activity are considered patterns of land use. Agricultural

and natural vegetative patterns are composed primarily of the elements of average area tone and texture. Cultural patterns are usually individual or geometrically regular assemblages of discrete tonal elements. Patterns of land use, although valuable to the interpretation of landform and, ultimately, engineering soil type, are very sensitive to the geographic region being interpreted and attain a maximum degree of usefulness when evaluated by an experienced interpreter. Farming practices which, to a large extent, determine agricultural patterns are not consistent throughout the world. A knowledge of the causes of different farming practices may allow an interpreter to relate agricultural patterns to landform and engineering soil type. Similarly, natural vegetative communities vary with climate and soil. In the case of specific cultural features, a knowledge of design criteria may contribute to utilization of cultural patterns in the interpretation of engineering soil types. Density of cultural features can often be related to general topographic conditions when other evidence is not available.

Agricultural patterns significant for the interpretation of SLAR images consist primarily of field shapes. Rectangular fields are indicative of relatively flat terrain while irregular shapes interspersed with wood lots indicate rough terrain. Contour farming which produces curvilinear field boundaries is indicative of rolling terrain with moderate relief. Strip farming is indicated on SLAR imagery by narrow, banded tonal contrasts and is indicative of subhumid to arid climatic environments.

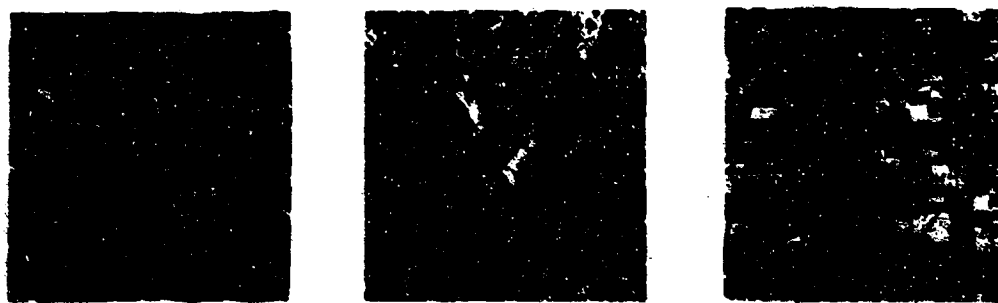
Cultural patterns, previously illustrated in Fig. 12, are generally composed of discrete tonal elements. Smooth, man-made surfaces such as highways, airfields, or urban streets appear on SLAR imagery as dark-toned lineations. Man-made corner reflectors such as railroads, buildings, or other structures appear as very light toned elements on SLAR imagery. Their identification requires the recognition of characteristic geometric assemblages of returns (tones).

Patterns of agricultural land use representative for portions of the United States are illustrated in Fig. 17. Table VII lists general radar characteristics of selected cultural features.

25. Interpretation of Landforms. Interpretation of genetic and morphologic landforms found within an area imaged by SLAR immediately precedes the interpretation of probable engineering soil types. When a genetic landform can be inferred to exist with reasonable certainty, an engineering soil type and probable land surface condition can be deduced. A specific geologic process is inherent in a genetic classification. Conversely, if only a morphologic landform can be inferred, much more dependence must be placed upon evaluation of the significance of each pattern element and the patterns of drainage, topography, and land use which they form. For example, a flood plain can be directly inferred to contain unconsolidated, relatively fine-grained alluvium while a plain may contain a variety of unconsolidated or consolidated geologic



**RECTANGULAR FIELD PATTERNS
BOUNDARIES NOT INFLUENCED BY TERRAIN**



**FIELD SHAPE AND DISTRIBUTION OF
BOUNDARIES INFLUENCED BY TERRAIN**



STRIP FARMING



**NO AGRICULTURAL
ACTIVITY**



**NO AGRICULTURAL
ACTIVITY**

Fig. 17. Patterns of land use.

Table VII. Radar Characteristics of Cultural Features

Cultural Feature	Return	General Radar Image Characteristic Pattern
Urban Area	Very high	Linear and rectangular grid patterns produced by intersecting streets; clusters of high-return spots from buildings
Suburban Area	Medium to High	Linear and rectangular grid produced by intersecting streets; few high-return clusters
Highways - improved	Very low	Linear traces, generally smooth curves
Highways - unimproved	Very low, in general, but similar to return from adjacent terrain	Linear traces, possibly sharp curves, and poor alignment
Railroads	Very high	Linear traces; very gentle curves
Power Transmission Lines	Very high	Beaded pattern resulting from reflection from individual towers
Bridge Structures	Very high	Usually individual high-return spot or short, linear trace
Airport runways; supporting structures	Very low high to very high	Linear traces, X-pattern, clusters of high-return spots
Industrial Area	Very high	Clusters of high returns in localized area
Agricultural Area	Variable high to low	Rectangular blocks with uniform return; variation in return from block to block; contour farming produces fields which tend to parallel existing topography

materials. Commonly, it is through evaluation of the regional association of several landforms that a genetic classification may be derived.

Genetic landforms usually show a characteristic, well-defined, and delineative shape characterized on a SLAR image by a topographic pattern. Morphologic landforms, conversely, feature such general topographic characteristics, that could have been formed by numerous geologic processes. A list of genetic and morphologic landforms encountered and recognized by inference during this investigation follows:

Genetic Landforms	Morphologic Landforms
Loess Plain	Valley
Dune	Basin
Ground Moraine	Lowland
Ridge Moraine	Plain
Outwash Plain	Plateau
Coastal Plain	Hill
Lacustrine Plain	Mountain
Playa Plain	Ridge
Alluvial Fan	Terrace
Alluvial Apron	•
Fluviatile Plain	
Flood Plain	
Glacio-Fluvial Terrace	
Beach Ridge	
Beach	
Arcuate Delta	
Estuarine Delta	
Anticlinal Mountain	
Synclinal Mountain	
Monoclinial Ridge	
Cinder Cone	
Lava Flow	

Many of these landforms are shown in the example interpretations illustrating the systematic interpretation technique, and all are described in terms of their SLAR image appearance in the Appendix.

26. Interpretation of Local, Land-Surface Conditions. "Local, land-surface condition" as used in the context of this report refers to local conditions influenced by soil moisture content, soil texture or particle size, or the surface roughness of bedrock.

Local, land-surface conditions are the most difficult terrain parameters to extract from SLAR imagery and are also subject to the greatest amount of error. Because of the complexity of terrain-reflecting surfaces, a specific land-surface condition can seldom be directly inferred from the appearance of a small portion of a SLAR image. The local, land-surface condition must be interpreted through re-evaluation of the pattern elements of tone and texture after a regional landform has already been established. The regional association of patterns is very important in establishing a geologic setting in which specific, local, land-surface conditions can exist.

Realizing that SLAR image displays of different local, land-surface conditions are not mutually exclusive, an interpreter can qualitatively analyze the pattern elements of discrete tone, average areal tone, and texture in terms of a probable microwave energy-terrain surface interaction. Thus, general relationships between surface roughness and the resulting radar cross section can be utilized advantageously. These relationships have been discussed in Section II of this report and described in Table V.

27. Systematic SLAR Image Interpretation Technique. An interpretation technique has been developed which involves the systematic analysis of pattern elements and patterns followed by an interpretation of landform and, ultimately, engineering soil type. The technique is illustrated in the flow diagram of Fig. 18. As can be seen in the diagram, the technique is not a direct procedure in which each step, when completed, is eliminated from further consideration. Although the technique generally progresses from identification of pattern elements to interpretation of landform and inference of engineering soil type, the interpreter must continually re-evaluate the significance of each pattern and its elements in light of an increasing level of knowledge. Each new bit of evidence extracted from the imagery calls for the re-evaluation of all previously determined evidence. For example, the inference that a linear, dark-toned, discrete tonal element is a radar shadow may prove inconsistent with a subsequent inference that the landform expressed by regional patterns is a playa plain. The inference that a relatively large, irregularly shaped, dark-toned area is a lake may be inconsistent with a subsequent landform interpretation of a high-relief mountain system showing evidence of existing in an arid environment. Thus, as evidence leading to the interpretation of landforms and engineering soil types is accumulated, it must be fitted into a logical analysis of a realistic terrain situation. Evidence which is not consistent with a logical analysis must be re-evaluated or discarded as uninterpretable.

A descriptive discussion of landforms, their general SLAR image characteristics, and probable associated engineering soil types is presented in the Appendix. Included is a discussion of the inferred microwave energy-terrain surface relationship which produces the patterns utilized in the technique. The procedure of interpretation is demonstrated by several examples in the summary of this section.

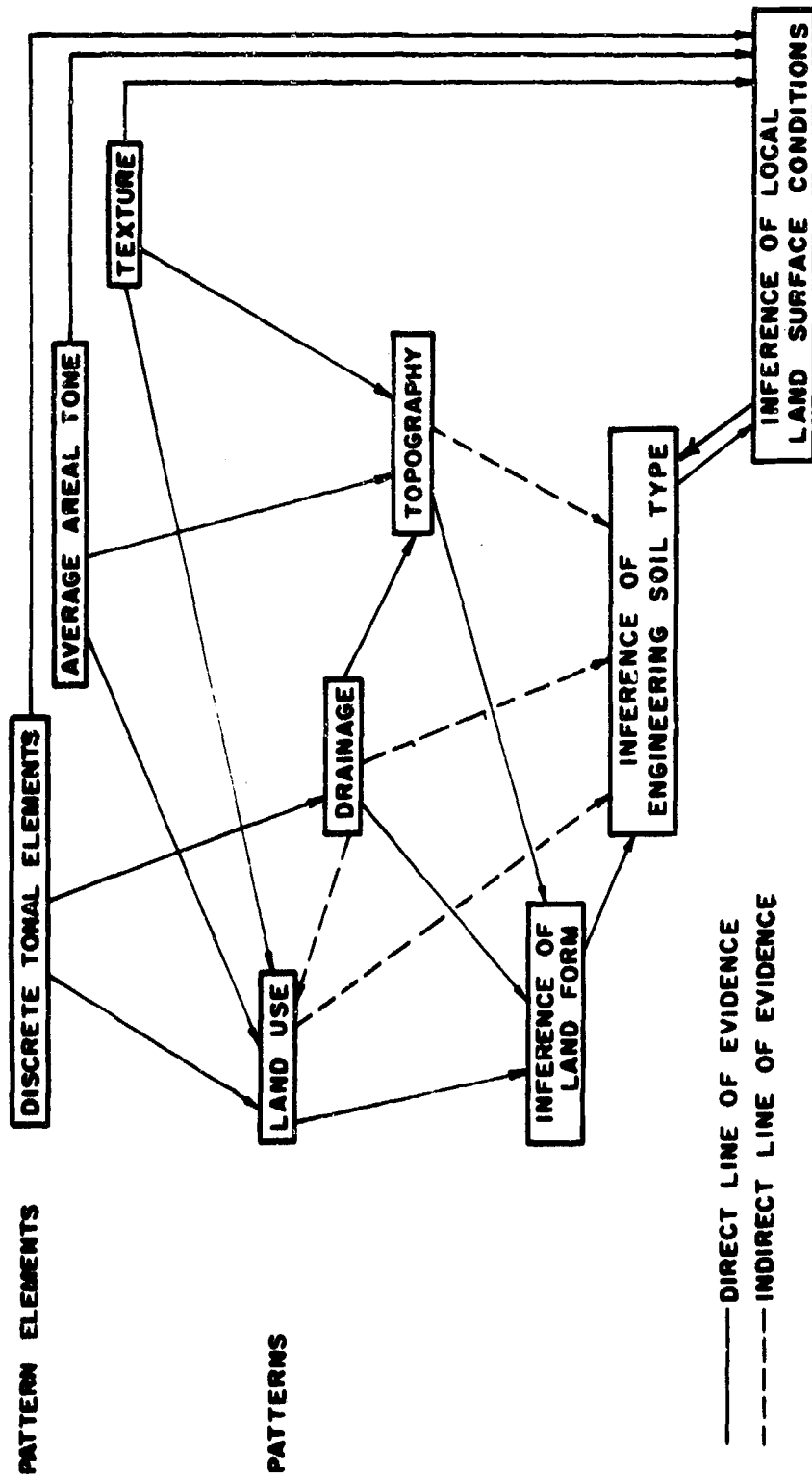


Fig. 18. Systematic interpretation flow diagram.

28. Effect of System Design, Image Resolution, and Degradation on Interpretation. It was observed during the qualitative analysis of a variety of SLAR images that images showing the greatest range of tone values allowed the most accurate and complete interpretations of engineering soil type. Although regional terrain conditions and engineering soil types were interpretable from all images, satisfactory determination of local, land-surface condition was limited to imagery with a wide, dynamic range of tone values. In terms of general system types, this was evidenced by the fact that "brute force" SLAR imagery, with a wide dynamic range of tone values, was more satisfactorily interpreted than was "synthetic aperture" SLAR imagery. In the case of "synthetic aperture" SLAR imagery, dynamic range was lost because of incoherent, reflected power fractions received by the system (97). The state of polarization of the unclassified, multiple polarized, K-band imagery did not appear to be a significant factor for qualitative, regional interpretation.

Image resolution did not appear to be a critical factor in interpretation of regional engineering soil types. Although resolution naturally affects the general appearance of an image, the pattern elements, patterns, and inferred landforms were of such a scale that resolution only affected the determination of local, land-surface conditions. Resolution of the imagery was, in fact, considered an attribute for regional interpretation in that the complex and almost infinite detail of minor, land-surface facets and vegetative cover as seen on small-scale, monoscopic, conventional photography was not recorded.

Degradation of SLAR imagery because of geometric infidelity was found to be of serious consequence only if the regional patterns of drainage, topography, and land use were severely distorted because of aircraft instability. Normal distortion caused by slant range display of imagery did not affect interpretation of engineering soil types although delineated boundaries had to be adjusted to check with ground truth. The fact that this distortion is predictable considerably lessens its detrimental effect.

The effect of degradation of SLAR imagery by atmospheric attenuation could not be properly assessed. Only one strip of K-band imagery obtained during a heavy thunderstorm was used in the investigation. In that case, only a small portion of the image was uninterpretable.

29. Evaluation of the Systematic Interpretation Technique. Two groups of Purdue University graduate students participating in an advanced course concerned with interpretation and mapping of engineering soil types from aerial photography evaluated the systematic SLAR image interpretation technique. One group was given SLAR image negative transparencies for interpretation. The members were provided with a very brief description of the SLAR concept. No interpretation guides or keys were provided.

The second group was provided with SLAR image positive prints for interpretation. This group received a reasonably detailed description of SLAR systems as well as an interpretation guide and textual keys similar to those described in this report. Each group spent about 4 hours interpreting SLAR imagery.

Although it was not intended to conduct a documented performance test with these groups of students, it was anticipated that an estimate of the value of the systematic interpretation technique would be forthcoming. Taking into consideration the varied educational and employment experiences of the members of each group, the following observations were made:

a. Interpretations made with the benefit of the interpretation guide and textual keys were more consistent in terms of inferred parameters. All interpretations made by the group were comparable in that a similar set of criteria was used for the deductive process.

b. Although both groups were able to correctly delineate most major landforms displayed on the various images, the group provided with a guide and keys tended to produce a somewhat more detailed regional interpretation of engineering soil types.

c. The group provided with an interpretation guide and keys was able to document each interpretation with reasonable inferred evidence obtained from the SLAR imagery. The other group could not explain the deductive process used for interpretation.

d. The group provided with an interpretation guide and keys was able to correctly infer the general climatic environment, types of vegetative cover, and regional topographic relief associated with each SLAR image. The other group was able to infer only general climatic environment and gross relief from the SLAR imagery.

30. Comparison Between SLAR Image and Aerial Photograph Interpretation.
The SLAR image interpretation technique was adapted from the airphoto approach of recognizing and evaluating repetitive patterns expressed by relatively homogeneous units of the earth's surface. Because of SLAR image scale, resolution, wavelength of operation, and monoscopic display, however, several aspects of the SLAR pattern recognition technique are considerably different than the airphoto technique. SLAR image patterns are regional in scope and definition. Tonal contrasts are due to variations in roughness at a scale corresponding to the wavelength of operation. Most important is the fact that the equivalent of the airphoto pattern element of form must be inferred from radar shadow and tonal contrast on SLAR imagery.

SLAR imagery was found to be best suited for regional engineering soil studies. As SLAR image interpretations become more localized and detailed, they also become subject to a greater probability of error. Conventional aerial photographs at typical scales of 1:20,000 to 1:60,000, however, are best suited for interpretations at the level at which SLAR imagery ceases to be of value. It was found that because of the effect of averaging of return, radar imagery was an excellent tool for regional engineering soil interpretation and was more easily interpreted than were airphoto mosaics at an equivalent scale.

31. Summary of Qualitative SLAR Image Analyses. A systematic approach to the interpretation of regional engineering soil types from SLAR imagery has been developed. The technique requires identification and delineation of pattern elements; evaluation of patterns formed by the pattern elements; and ultimately, inference of landform and regional engineering soil type. The Appendix summarizes generalized correlations between SLAR image parameters and landform parameters found to be interpretable during the course of this investigation. Although this list is incomplete, it represents those terrain situations and SLAR image patterns repeatedly shown in a consistent manner on the imagery utilized for this investigation. If only morphologic landforms are inferable from a SLAR image, the interpreter must rely heavily upon the significance of regional landform associations as well as more general relationships between geomorphology and geology. Basic relationships which are most useful are the general correlations between high relief and resistant bedrock and high density of drainage and impermeable materials.

Extraction of data from SLAR images can be facilitated when a definite procedure is implemented as outlined by the systematic interpretation technique. The following data evaluation guide was developed as a means of assuring collection and evaluation of SLAR image data in a consistent manner. Figures 19 through 23 illustrate the application of the systematic SLAR image interpretation technique to K-band imagery.

Data Evaluation Guide

1. Orient image with flight line at top (shadows pointing toward interpreter).
2. Delineate areas on image overlay which exhibit a generally uniform appearance.
3. Analyze each delineated area with respect to the following pattern elements:
 - a) Discrete tonal elements
 - (1) Light tones -- geometric configuration
 - (2) Dark tones -- geometric configuration
 - (3) Radar shadow -- size, shape, and extent

- b) **Image textures:**
Extent of smooth, grainy, or speckled image textures or rough, irregular macro-texture
 - 4. **Evaluate regional drainage**
 - a) **Patterns (dendritic, parallel, trellis, etc.)**
 - b) **Delineate areas exhibiting either a lack of surface drainage or intense surface drainage**
 - c) **Estimate drainage density**
 - 5. **Evaluate topography**
 - a) **Estimate relative relief from size and shape of shadow and drainage density**
 - b) **Estimate general topographic form from average areal tonal contrasts**
 - c) **Evaluate relation of topography to vegetation and land use**
 - 6. **Evaluate effect of vegetation, culture, and land use on image characteristics**
 - a) **Identify farming practices from field shape and extent**
 - b) **Describe vegetative types (agricultural, grass, brush, or forest)**
 - c) **Determine relative location, extent, and distribution of cultural features (cities, surface transportation networks, etc.)**
 - 7. **Re-evaluate delineated areas of uniform appearance and adjust boundaries**
 - 8. **Infer genetic or morphologic landforms**
 - 9. **Infer engineering soil types (parent materials)**
 - a) **Bedrock types**
 - b) **Relative particle size or USCS classification of unconsolidated materials**
-

Fig. 19. Example Interpretation: Mississippi Valley.

Area	Regional Drainage	Regional Topography	Land Use	Special Conditions	Landform and Inferred Engineering Soil Type
A	Dissected; Outcrops and Minor Stream Proximal	Relatively Flat Terrain; Curvilinear Patterns Indicative of Low Ridges and Swale Topography	Limited Agricultural Activity; Predominantly Forest with Some Grassy Areas	Borrow Pit for Massmade Levee Adjacent to Designated Area, Tonal Contrasts Indicative of Selective Growth of Vegetation on Materials with Different Particle Sizes	Flood Plain, Ridge and Swale Type: Unconsolidated, Fine Grained Alluvium Consisting of Sand, Silt, and Clay
B	No Evidence of Surface Drainage	Flat	Rectangular Field Patterns, Some Trees Along Fence Rows	Area Protected by Massmade Levee, Field Remnants Not Affected by Topography	Flood Plain, High-Level Type: Unconsolidated, Fine Grained Alluvium Consisting of Silt and Clay
C	Dissected with Locally Pinnate Tributaries, Relatively High Density of Streams	Moderate Relief, Terrain Slightly Dissected with Very Steep Valley Walls	Limited Agricultural Activity, Predominantly Forested	Very Steep Valley Walls Indicated by Thin Shalestone and Light Tonal Elements Produced by Slopes Facing Autocans	Dissected Loess Surface: Unconsolidated, Fine Grained Eolian Material Consisting of Silt with Uniform Particle Size
D			Light Discrete Tonal Elements and Gridlike Pattern Indicative of Urban Area		

FLIGHT LINE DIRECTION



0 1 2 3 4 5
MILES

Fig. 19. Example interpretation: Mississippi Valley.

Fig. 20. Example Interpretation: Arizona

Area	Regional Drainage	Regional Topography	Land Use	Special Conditions	Landform and Inferred Engineering Soil Type
A	No Evidence of Surface Drainage	Very Flat (Area A ₁) is inferred to be Rough on a Micro-scale Thus Produced a Lighter Tone	No Evidence of Any Agricultural or Natural Vegetation	Light Toned Limitations Produced by Diffuse Reflection, NE-SW Lineation Indicative of Railroad, E-W Lineation Indicative of Trail	Plays: Unconsolidated Fine Grained Sand, Silt and Clay. Area A ₁ Inferred to be Dry, Cracked Surface Producing Diffuse Reflection
A-1	No evidence of Surface Drainage, Numerous Dark Toned Spots and Residual Spotted Heavy Textures Inferred to be Due to Pebbles, Small Lakes or Indistinct Basins	Gently Rolling with Low Relief, Surface Pitted with Basins	No Evidence of Agricultural Activity, Image Texture and Tone Indicative of Brush and Grass	Position of Area Adjacent to Plays Evidence for Inferred Eolian Origin of Deposit, Lineations Within Area Parallel to Edge of Plays	Stabilized Sand Dune Complex; Unconsolidated Eolian Material Consisting of Sand with Uniform Particle Size
C	No evidence of Surface Drainage	Curvilinear Ridge with Moderate Height	Surface Inferred to be Brush and Grass Covered	Curvilinear Feature Parallel Edge of Plays	Beach Ridge: Fluvially Deposited Sand and Fine Gravel
D	Limited Evidence of Surface Drainage, Dark Toned Areas on Image Produced by Dry Lakes and Indistinct Basins	Relatively Flat Surface	Limited Evidence of Agricultural Activity, Image Texture and Tone Indicative of Brush and Grass	Lack of Drainage Pattern Indicative of Internal Drainage	Alluvial Plains: Unconsolidated, Fine Grained Material Consisting of Fine Sand and Silt
E	Parallel, Local Distributary Patterns, Drainage Channels Accumulated on Image by Contrasting Light and Dark Toned Streaks	Gently Sloping Toned Plays, Relatively Low Relief	No Evidence of Agricultural Activity, Image Texture and Tone Indicative of Grass and Brush	Overall Dark Tone Indicative of Smooth Terrain Surface	Alluvial Apron: Unconsolidated, Fine Grained Material Consisting of Fine Gravel and Sand
F	Distributary Channels Contributing to Form Parallel Channels at Outer Margin of Area Nearst Plays	Series of Fan-Shaped Sloping Units, General Slope Away from Mountain Front Toned Alluvial Apron and Plays, Moderate Relief	No Evidence of Agricultural Activity, Limited Occurrences of Brush and Grass	Light Overall Tones Produced by Slopes Facing Antenna	Alluvial Fans: Unconsolidated Material Consisting of Some Boulders, Gravel, and Coarse Sand

Fig 20 (cont'd)

Area	Regional Drainage	Regional Topography	Land Use	Special Conditions	Landform and Inferred Engineering Soil Type
G	Distributary Drainage	Fan Shaped, Sloping Surface, Moderate Relief	No Evidence of Agricultural Activity, Brush and Grass Inferred to Exist on Slope	Light Overall Tone Due Primarily to Slope Facing Antenna, Surface Materials Inferred to be Dense Because of Unique Light Tone	Alluvial Fan: Cemented, Partially Consolidated Alluvial Material Consisting of Gravel and Course Sand
H	Dendritic Controlled in Part by Geologic Structure	Mountainous, High Relief Terrain, Linear Ridge with Sharp Crest	No Evidence of Agricultural or Natural Vegetation	Linearity of Feature and Joint Pattern Indicative of Sedimentary Origin	Bedrock Ridge: Consolidated Sedimentary or Slightly Metamorphosed Rock, Bedrock May be Calcareous If Alluvial Fan Material (Area G) Cemented
I	Dendritic	Mountainous, High Relief Regional Linear Trend	No Evidence of Agricultural or Natural Vegetation	Area Continuation of Linear Feature (Area H)	Bedrock Mountains: Consolidated Sedimentary and Metamorphic Rock
J	Dendritic	Mountainous, High Relief, Topography More Rounded Than Evidenced in Areas (h) or (i)	No Evidence of Agricultural or Natural Vegetation	No Linearity of Topographic Features	Bedrock Mountains: Metamorphic or Igneous Rock
K	Grossly Dendritic, Locally Rectangular, High Density Drainage	Hilly Topography, Moderate Relief	No Evidence of Agricultural Activity, Image Texture and Tone Indicative of Brush and Grass	Distinct, Unique Drainage Pattern Characteristic of Impermeable Material	Bedrock Hills: Consolidated Sedimentary Rock, Possibly Shale
L	Dendritic, Distinct Locally Fiminate Tributaries	Gross Surface Gently Sloping Toward Southwest, Moderate Relief	No Evidence of Agricultural Activity, Image Texture and Tone Indicative of Brush and Grass Cover	Locally Pinnate Drainage Pattern, Evidence of Erosion in Two Distinctly Different Types of Material	Alluvial Plain (Pediment Surface): Alluvial Gravel and Sand Veneer Over Sedimentary Bedrock
M	Distributary and Parallel Complex	Regional Slope Toward North, Low Relief	No Evidence of Agricultural Activity, Image Texture and Tone Indicative of Brush and Grass	Dark Toned Streaks Produced by Smooth Condition of Drainage Channel as Compared to Adjacent Terrain	Alluvial Apron: Unconsolidated Fine Grained Material Consisting of Sand and Silt

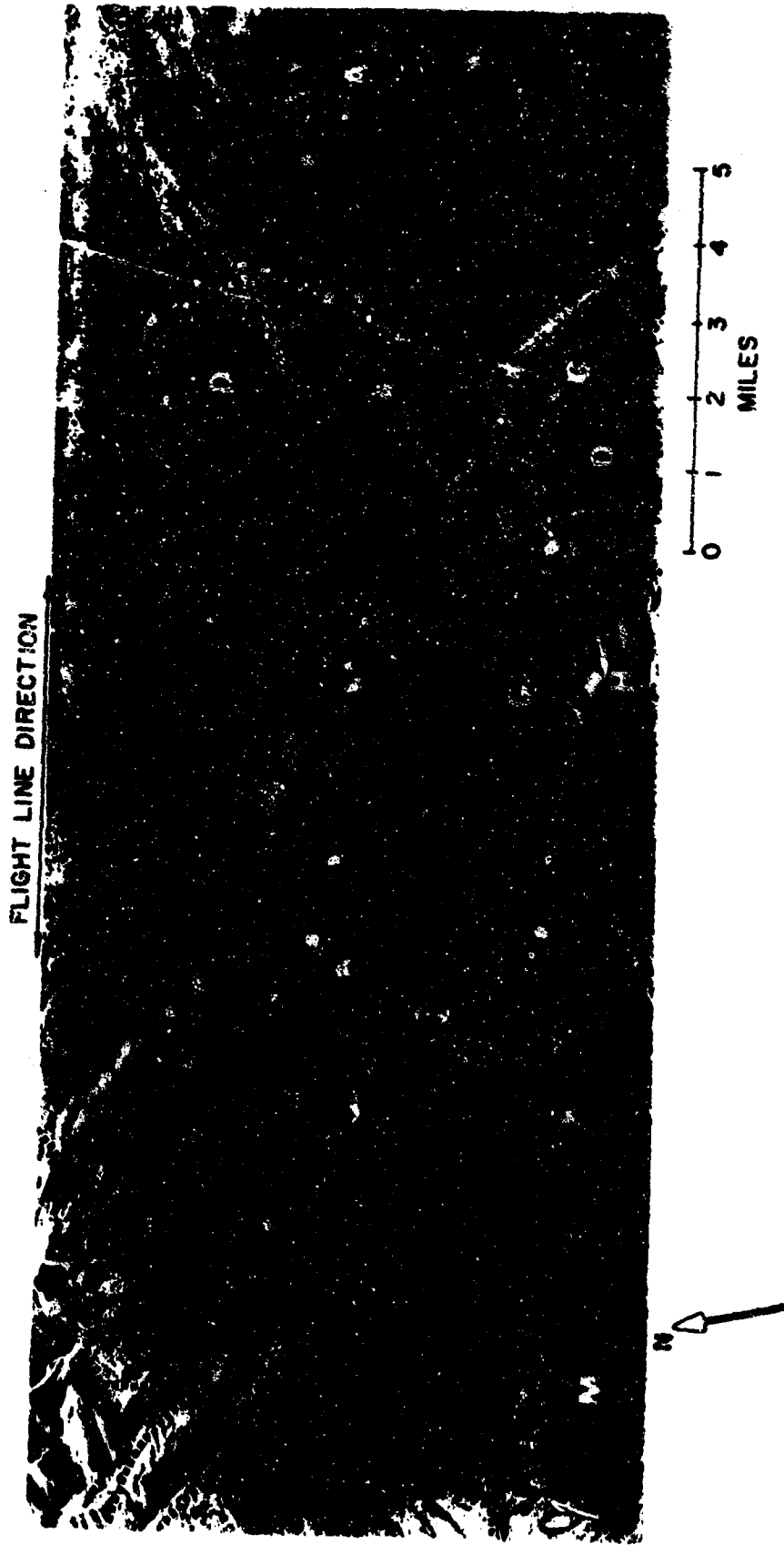


Fig. 20. Example interpretation: Arizona.

Fig. 21. Example Interpretation: Wyoming.

Area	Regional Drainage	Regional Topography	Land Use	Special Conditions	Landform and Inferred Engineering Soil Type
A	Braided	Relative Flat, No Relief	No Evidence of Agricultural Activity, Riparian Vegetation is Indicated	Braided Stream Pattern Indicative of Excessive Stream Load	Flood Plain: Unconsolidated Alluvial Material Consisting of Gravel, Sand, and Silt
B	Grossly Dendritic, Locally Deranged, Lakes in Evidence	Rolling Somewhat Irregular Topography, Moderate to Low Relief	No Evidence of Agricultural Activity, Area Predominantly Forest Covered	Area Adjacent to Glacially Eroded U-Shaped Valleys	Ridge Moraine: Unconsolidated Till, Heterogeneous Mixture of Clay, Silt, Sand, and Gravel
C	No Evidence of Surface Drainage	Flat, Multiple Scarps Indicative of Multiple Terrace Levels	Limited Evidence of Agricultural Activity, Several Poorly Defined Rectangular Fields Which Are Probably Pastures, Natural Vegetation Inferred to Consist of Grass and Low Brush	Multiple Terrace Levels Adjacent to Moraine and Glacially Eroded Mountains	Glacial Terrace Deposits: Glacio-Fluvial Material Consisting of Stratified Sands and Gravel
D	Distributary	Gently Sloping to West, Fan Shape with Relatively Low Relief	Limited Evidence of Agricultural Activity, Natural Vegetation Inferred to Consist Primarily of Grass		Alluvial Fan: Unconsolidated Alluvial Material Consisting of Sands and Gravel
E	Grossly Dendritic with Some Parallelism of Drainage Produced by Structural Control	Mountainous Terrain with Relatively High Relief, Evidence of Linearity and Structural Control Exists	No Evidence of Agricultural Activity or Extensive Natural Vegetation, Image Texture Indicative of Limited Forest Cover	Linear Tonal Contrasts Indicative of Gross Bedrock Stratification and Regional Dip	Mountains: Resistant Bedrock Inferred to be of Sedimentary Origin
F	Dendritic	Mountainous Terrain with Relatively High Relief	No Evidence of Agricultural Activity, Image Texture Indicative of Forest Cover	Area Exhibits Rounded Form with Sharp Crests Less Prevalent Than in Area (E), Some Evidence of Linearity	Mountains: Resistant Bedrock Inferred to be of Sedimentary Origin, Bedrock Perhaps Less Resistant Than That Delineated in Area (E)

Fig. 21 (cont'd)

Area	Regional Drainage	Regional Topography	Land Use	Special Conditions	Landform and Inferred Engineering Soil Type
G	Grossly Dendritic with Locally Trellis Patterns	Mountainous Terrain with High Relief, Domical Form, Evidence of Gross Stratification Present Around Periphery	No Evidence of Agricultural Activity, Image Texture Indicative of Limited Forest Cover	Planimetric Shape and Topography of Feature Indicative of Breached Anticlinal or Elongated Dome Structure	Anticlinal Mountain: Bedrock Inferred to be Resistant and of Sedimentary Origin, Core of Structure Possibly Metamorphic or Igneous Rock
H	Grossly Dendritic	Mountainous Terrain with Very High Relief, U-Shaped Valleys Inferred to be the Result of Intense Glacial Erosion	No Evidence of Agricultural Activity, Limited Forest Cover at Lower Elevations	Numerous Tributary Streams Enter Major Valleys from Steepest Slopes, Streams Controlled by a Rectangular Joint System	Mountain: Bedrock Inferred to be Very Resistant and of Igneous Origin
I			Light Discrete Tonal Elements and Gridded Pattern Indicative of Urban Area		

FLIGHT LINE ORIENTATION

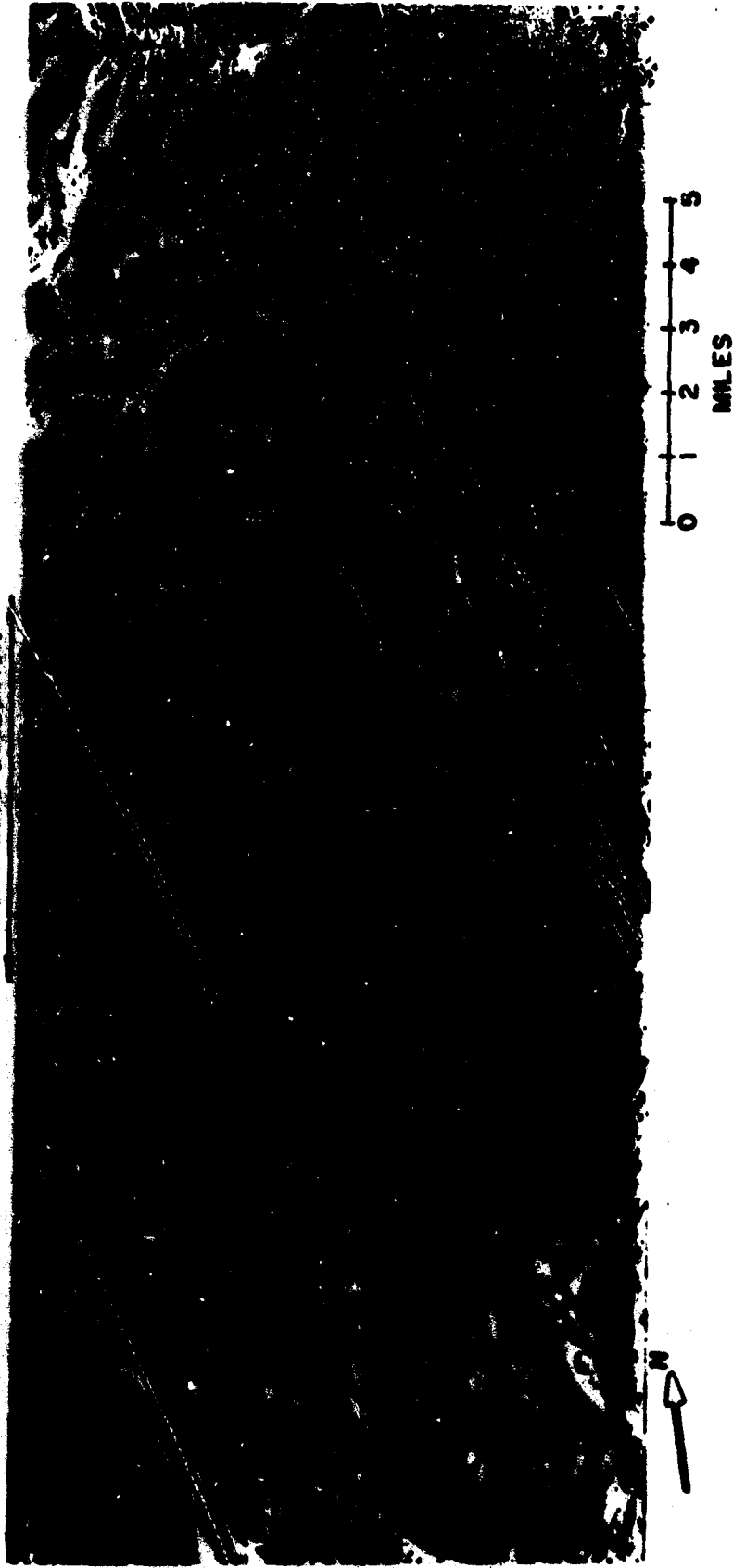


Fig. 21. Example interpretation: Wyoming.

Fig. 22. Example Interpretation: Pennsylvania

Area	Regional Drainage	Regional Topography	Land Use	Special Conditions	Landform and Inferred Engineering Soil Type
A	Meandering Major Stream and Adjacent Tributary Features	Relatively Flat, Terraces and Flood Plain Exist Adjacent to Stream. Several Islands Exist in Stream	Agricultural Activity Evident Along Flood Plain and Terraces Adjacent to River	Strong Bedrock Control Exerted on the Stream in Several Areas	Flood Plain and Fluvial Terrace Deposits: Unconsolidated Fluvial Drift Consisting of Stratified Silt, Sand, and Gravel. Islands Composed of Bedrock
B	Traills	Linear Mountain Ridges with High Relief	Predominantly Forest Covered	All Ridges Parallel and Separated by Linear Valleys	Sedimentary Bedrock Mountains: Resistant Sedimentary Rock Consisting Primarily of Sandstone
C	Dissected	Hills with Moderate Relief	Predominantly Forest Covered	Area Inferred to be Associated with Linear Ridges of Area (B) but Does Not Express Linearity	Sedimentary Hills: Relatively Resistant Bedrock Consisting of Interbedded Sandstone and Shale
D	Greenly Dissected with Locally Rectangular Patterns	Low Relief Terrain, Valleys Associated with Adjacent Linear Ridges	Extensive Agricultural Activity, Limited Riparian Vegetation and Tree Cover Adjacent to Field Boundaries	Numerous Cultural Features Scattered Throughout Area	Sedimentary Bedrock Valley: Non-resistant Sedimentary Rock Consisting Primarily of Shale
E	Greenly Dissected, Tributary Streams Effluents at Round-ary Between Delineated Areas (E) and (D), Major Streams in Area Exhibit Marked Pattern of Rectangularity	Relatively Low Relief, Valley	Extensive Agricultural Activity, Field Size Much Larger and More Regularly Shaped in This Area Than in Area (D)		Sedimentary Bedrock Valley: Non-resistant Sedimentary Rock Consisting of Limestone and Shale
F	Drainage of This Area Constitutes Part of the Regional Dissected Pattern of Area (E), Circular Nature of the Delineated Features Indicates of Annular Drainage	Hills with Moderate Relief Arranged in a Circular Shape	Predominantly Forest Covered	Circularity of Topographic Expression Suggests Igneous Intrusive Activity	Ring Dike: Resistant Bedrock Consisting of Metamorphosed Limestone and Shale or Igneous Intrusive Rock
G			Light Discrete Tonal Elements and Gridlike Pattern Indicative of Urban Areas		

PLANT LINE OBSERVATION

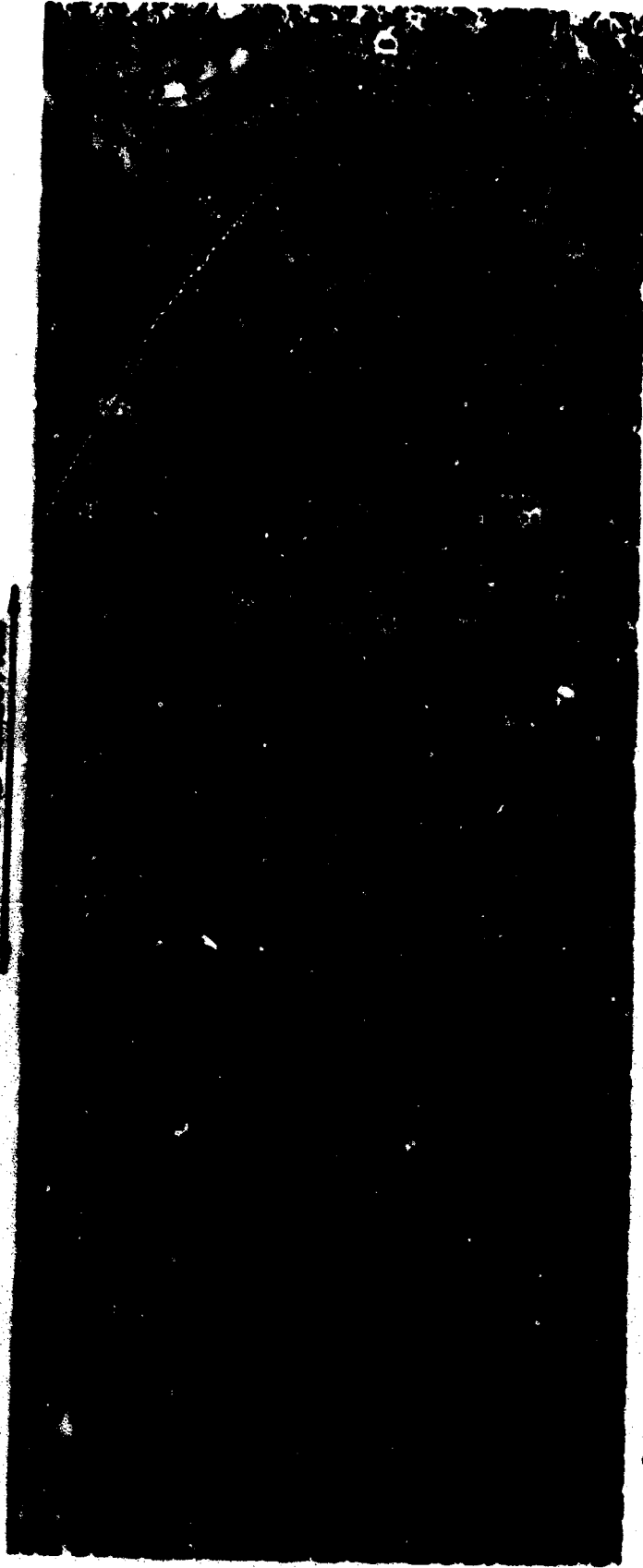


Fig. 22. Example interpretation: Pennsylvania.

Fig. 23. Example Interpretation: Northern Indiana.

Area	Regional Drainage	Regional Topography	Land Use	Special Conditions	Landform and Inferred Engineering Soil Type
A	Area Enclosed by a Major Stream, Immediately Adjacent Towns within Area Exhibit No Evidence of Surface Drainage	Relatively Flat	Extensive Agricultural Activity, Some Riparian Vegetation	Rectangular Fields Adjacent to a Major Stream Indicative of Flat Terrain Conditions	Flood Plains: Unconsolidated Alluvium Consisting of Silt, Sand, and Gravel
B	No Evidence of Surface Drainage Except at Border with Area (A)	Very Flat, Area Inferred to be at a Higher Elevation Than the Flood Plains	Extensive Agricultural and Cultural Activity, Urban Area Located within Area	Airport (Runways) Indicative of Very Flat Terrain	Terrace: Unconsolidated Glacio-Fluvial Material Inferred Because of Adjacent Land Forms, Stratified Sand and Gravel
C	Limited Evidence of Colluvial Surface Scoria, No Well Defined Drainage Pattern	Relatively Flat, Area Positioned Between Flood Plains and Upland	Extensive Agricultural Activity, Rectangular Fields	Linearities and Streaks (Scrubs) Parallel to General Direction of Stream Flow Indicative of Fluvial Deposition	Terrace or Outwash Plain: Unconsolidated Glacio-Fluvial Material Consisting of Stratified Sand and Gravel
D	Coarsely Discrete, Locally Disrupted, Several Lobe Present in Area, Highest Order Streams in Area are Undercuts	Moderate to High Relief, Evidence of Inactive Erosion Along Scarp Face, Dissected Area Bordering Flood Plains and Terrace	Limited Evidence of Agricultural Activity, Area Predominantly Forest and Brush Covered	Regional Association of Area with Upland (F) and Terrace Significant for Interpretation	Dissected Glacial Till (Possibly Ridge Moraine Deposits): Unconsolidated Glacial Till Consisting of a Heterogeneous Mixture of Clay, Silt, Sand, and Gravel with Some Erratics
E	Coarsely Discrete, Locally Disrupted, Several Lobes Present in Area, Highest Order Streams in Area are Undercuts	Moderate to Low Relief, Area Inferred to be a Topographic Trough Formed During a Period of Glacier Melting	Limited Agricultural Activity, Area Predominantly Forest and Brush Riparian Vegetation	Inferred Glacial Shallowway Regionally Associated with Adjacent Morphologic Land Forms	Glacial Shallowway within a Till Plain: Unconsolidated Glacial Drift Consisting of Poorly Stratified Sand and Gravel with Lenses of Silt and Clay, Probable Local Zones with High Organic Content
F	Limited Evidence of Surface Drainage, Disrupted Network of Drainage and Local Linearities Suggest Dish Drainage	Relatively Flat	Predominantly Agricultural, Rectangular Fields Exhibit No Evidence of Significant Topographic Influence, Limited Occurrence of Riparian Vegetation	Area Regionally Associated with Glacial Land Forms	Till Plain: Unconsolidated Glacial Drift Consisting of a Heterogeneous Mixture of Clay, Silt, Sand, and Gravel with Some Erratics
G			Light Discrete Tonal Elements and Crinkled Patterns Indicative of Urban Areas		

FLIGHT LINE DIRECTION →



0 1 2 3 4 5
MILES



Fig. 23. Example interpretation: Northern Indiana.

VI. QUANTITATIVE ANALYSIS OF SLAR IMAGERY

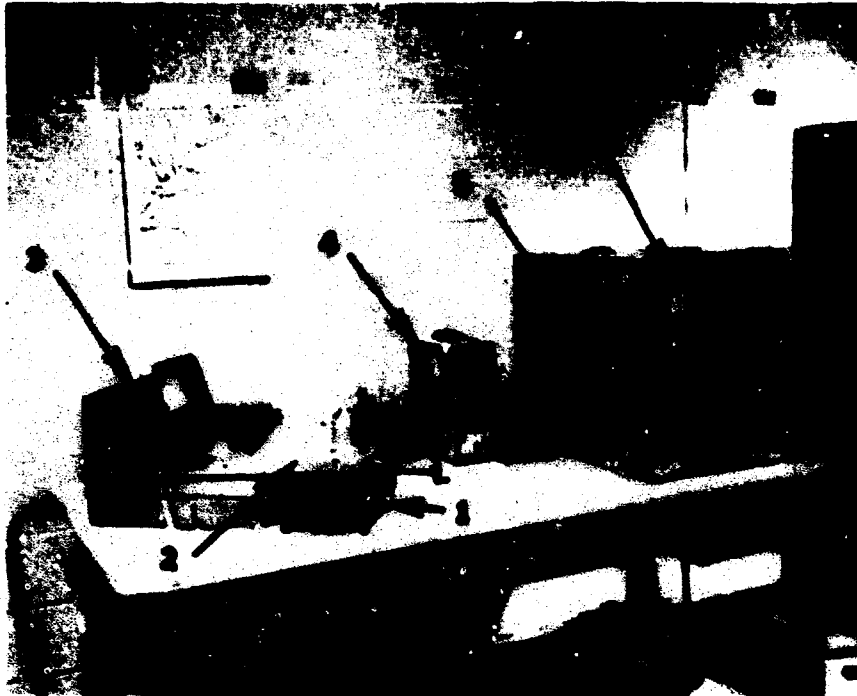
32. Introduction. It is recognized that a significant quantitative investigation into the relationship between terrain parameters and corresponding SLAR image patterns requires calibrated imagery; hypotheses for electromagnetic energy and terrain interactions; and extensive field investigation for the collection of ground-truth information. However, it is also recognized that these conditions have never been completely satisfied in previous studies and will be difficult to achieve in future investigations. Consequently, a limited investigation was made to determine which, if any, SLAR image parameters beside calibrated, absolute tone values could be quantified.

The qualitative image analysis indicated that image textures and returns produced by regional, topographic effects (shadow and very light tones) were least affected by variations in tone caused by system gain settings and photographic reproduction procedures. Thus, it was decided that an investigation into the quantification of image texture and radar shadow was warranted with their relationship to engineering soil types being the ultimate goal. Preliminary evaluation of these parameters indicated that SLAR image texture should relate most directly to areal distributions of vegetation and land-surface conditions producing a surface roughness with dimensions in the range of the wavelength of the system, whereas radar shadows should relate to large-scale roughness produced by regional, topographic conditions. The investigation of SLAR image textures and radar shadows was directed along the line previously discussed.

33. Image Texture Analysis. A previous investigation by Morain and Simonett (70) indicated that probability/density curves defining a histogram of individual tone elements within an area of SLAR imagery might be a useful measure of image texture. Other investigators (1, 53) have suggested that power spectra curves may be useful in relating SLAR image and aerial photographic data to terrain conditions. It was decided that within the limitation of equipment availability, probability/density curves of randomly sampled imaged areas should be evaluated as a measure of SLAR image texture. The hypothesis was that image texture, being a function of the distribution of tonal elements as well as their absolute tone values, should be relatively independent of system gain settings or angle of illumination.

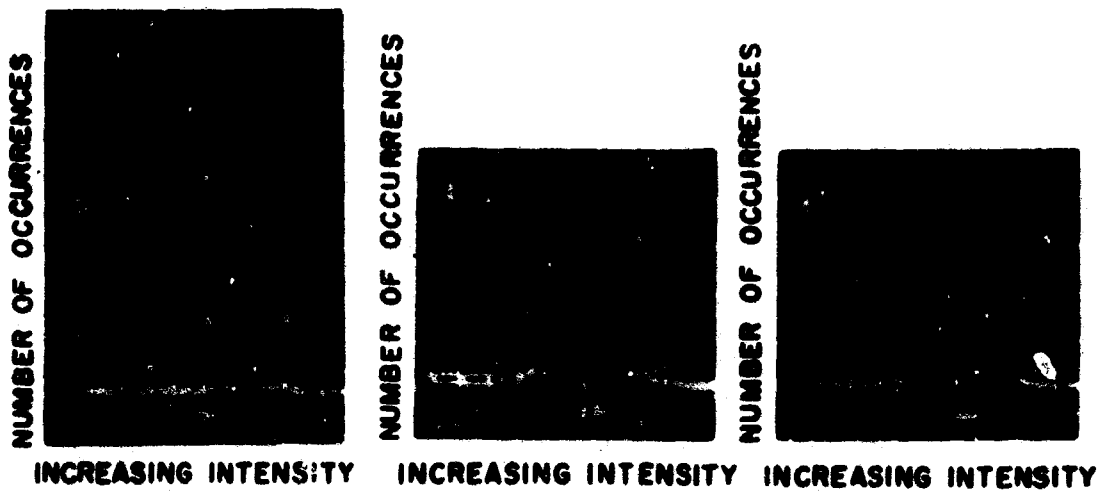
a. Selection of Sample Areas. Thirty-five sample areas were selected and delineated on SLAR image negatives representative of eight different geographic locations. Each sample area represented approximately 9 square miles of terrain. Although the sample areas were selected randomly with respect to landform type, the specific location of each area was adjusted so that only one landform type and visual image textural condition was included. All study areas were delineated on uncalibrated, K-band SLAR imagery.

b. Generation of Probability/Density Curves. Probability/density curves representing a histogram of SLAR image tonal elements within each study area were generated with a Macbeth transmission densitometer (61) coupled to a 400-channel Packard multichannel analyzer (72). Figure 24 illustrates the equipment layout used for the image texture experiment.



1. Mechanical stage with X- and Y-movement
2. Transparent plastic film carrier
3. Macbeth TD-102 transmission densitometer with 1-, 2-, or 3-millimeter aperture
4. Signal generator which feeds timing pulses to multichannel analyzer
5. Packard 400-channel multichannel analyzer
6. Cathode-ray tube from which probability/density curves were photographed

Fig. 24. Equipment for generating probability/density curves (histograms of areal tone values).



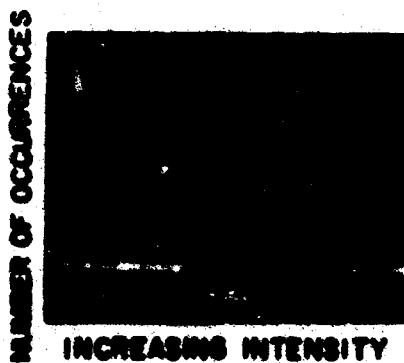
**SMOOTH IMAGE
TEXTURE**



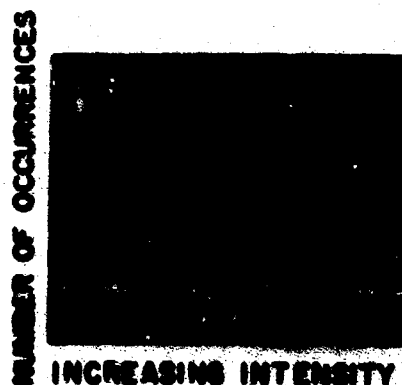
**GRAINY IMAGE
TEXTURE**



**MIXED SMOOTH AND
GRAINY IMAGE TEXTURE**



**SMOOTH IMAGE TEXTURES
WITH AGRICULTURAL PATTERNS**



**ROUGH, IRREGULAR
MACRO-TEXTURE**

Fig. 25. Representative probability/density curves obtained with 1-millimeter densitometer aperture.

A mechanical stage was adapted for use with the densitometer so that a SLAR image fixed on a plastic carrier could be moved at a relatively constant speed over the densitometer aperture. By masking the boundaries of each image study area with opaque tape, it was possible to form a grid or "mechanical raster" over the surface of the film. When the densitometer aperture was blocked by the opaque tape, density readings were significantly different than those from the film and were not included in the generation of the probability/density curves.

As each image study area was scanned by the densitometer, a continuous voltage proportional to the transmission density value was fed into the multichannel analyzer. In addition, a timing pulse which triggered the counting mechanism was fed from a signal generator into the multichannel analyzer. As the SLAR film was moved across the transmission densitometer at a speed of approximately 1.5 mm per second, density values in the form of a voltage were sampled at a rate of 50 samples per second by the multichannel analyzer. Each sampled density was then stored by the multichannel analyzer in the appropriate channel. The range of density values obtained from the films was divided into the 400 channels of the multichannel analyzer. Probability/density curves were generated with 1- and 2-millimeter densitometer apertures so, in effect, each 1-millimeter diameter tone element was counted 33 times while each 2-millimeter diameter tone element was counted 66 times. This had the effect of exaggerating the size of the probability/density curves but did not affect their relative shapes. Because imagery utilized for this experiment was uncalibrated, no attempt was made to relate specific points on the probability density curves to absolute tone values. It was curve shape that was considered to be potentially related to image texture. After each curve was generated and displayed on the multichannel analyzer oscilloscope, a Polaroid picture was taken to record the data. Figure 25 illustrates representative shapes of probability/density curves generated during this experiment and the sample areas from which they were obtained.

c. Analysis of Probability/Density Curves. The probability/density curves generated with the 1- and 2-millimeter diameter densitometer apertures were very similar in gross shape. The 1-millimeter aperture curves did, however, show more minor fluctuations because of the higher degree of resolution of tone elements. Broad, low-amplitude curves generally represented coarse, grainy image textures while narrow, sharp-peaked, high-amplitude curves were representative of smooth-image textures. Changes in absolute tone values tended to shift the curves along the abscissa rather than to change the general shape of the curves.

The first stage in the evaluation of the probability/density curves was the determination of a single-curve parameter which could be adequately correlated with visually defined image textures. Statistical curve measures consisting of X- and

Y-mean, X- and Y-variance, curve width at base (X), and peak height (Y) were calculated for the 35 curves generated with a 1-millimeter densitometer aperture and also for curves generated with a 2-millimeter densitometer aperture. In addition, an image texture was visually defined for each of the 35 sample areas. A multiple correlation analysis (101) was applied to this data with visually defined image texture being the dependent variable. This was to determine which of the several curve parameters or their X- to Y-ratio would correlate most significantly. In using the multiple-correlation technique, correlation between two variables is indicated by a number (r) which can range in value from +1 to -1. The number "1" indicates perfect correlation whereas "0" indicates no correlation. A + indicates that a direct relationship exists whereas a - signifies an inverse relationship. In analyzing multiple variables, a simple correlation coefficient such as determined for this study shows how the dependent variable changes in response to a specific, independent variable. Thus, it was possible to selectively eliminate from consideration those curve parameters which correlated least significantly with a visually defined image texture. Table VIII lists the visually defined image texture and probability/density curve parameters used in the final correlation analysis after the least significant curve parameters had been eliminated. The multiple-correlation analysis indicated that a ratio of curve base width (X) to peak curve height (Y) for curves generated with a 1-millimeter densitometer aperture correlated most significantly with visually defined image textures.

Following the correlation of curve parameters with visually defined image textures, an attempt was made to correlate the selected curve parameter (X/Y) with inferred and estimated ground-truth information related to engineering soil types. The variables utilized in this analysis are shown in Table IX with the resultant correlation matrix.

d. Interpretation of Results. It must be stressed that correlation coefficients represented in the correlation matrix of Table IX do not constitute highly significant quantitative measures. The correlation coefficients are much too low. However, considering that all data but the probability/density curve parameters are inferred, one can justifiably use the correlation coefficients as indicators of trends. Krumbein and Imbrie (48) have indicated that a correlation coefficient (r) = 0.2 or greater may be meaningful for geologic analyses involving limited samples. Assuming this is true for this experiment, the estimated percent brush, drainage density measured from the SLAR image and average areal tone of the sample area are related to the probability/density curve parameter (X/Y) in more than just a random manner. The inferred soil type and estimated percent grass or agricultural crop cover may also be loosely related to the parameter (X/Y).

It is concluded that the technique of generating probability/density curves with a macro-densitometer does not produce a curve with sufficient response to

Table VIII. Inferred Image Textures and Corresponding Probability/Density Curve Data

Inferred Image Texture*	X/Y (1-mm Aperture)		X/Y (2-mm Aperture)		X-Mean Y-Mean (1-mm Aperture)		X-Mean Y-Mean (2-mm Aperture)		X-Variance Y-Variance (1-mm Aperture)		X-Variance Y-Variance (2-mm Aperture)	
	X	Y	X	Y	X	Y	X	Y	X	Y	X	Y
3.0	0.750	0.375	2.220	1.545	2.220	1.545	2.220	1.545	0.484	0.137	0.484	0.137
2.0	0.224	0.161	1.540	1.072	1.540	1.072	1.540	1.072	0.045	0.015	0.045	0.015
1.0	0.214	0.161	1.780	1.885	1.780	1.885	1.780	1.885	0.044	0.010	0.044	0.010
1.0	0.333	0.184	1.900	1.329	1.900	1.329	1.900	1.329	0.082	0.026	0.082	0.026
5.0	0.579	0.385	2.291	1.358	2.291	1.358	2.291	1.358	0.334	0.105	0.334	0.105
3.0	0.867	0.416	2.817	1.650	2.817	1.650	2.817	1.650	0.856	0.142	0.856	0.142
3.0	0.814	0.579	2.140	1.475	2.140	1.475	2.140	1.475	0.689	0.358	0.689	0.358
3.0	1.231	0.938	2.980	2.870	2.980	2.870	2.980	2.870	2.000	0.798	2.000	0.798
2.0	0.526	0.346	2.150	1.850	2.150	1.850	2.150	1.850	0.238	0.147	0.238	0.147
2.0	0.266	0.167	1.341	0.986	1.341	0.986	1.341	0.986	0.048	0.024	0.048	0.024
3.0	0.450	0.346	1.978	1.528	1.978	1.528	1.978	1.528	0.156	0.079	0.156	0.079
2.0	0.233	0.143	1.620	1.181	1.620	1.181	1.620	1.181	0.041	0.017	0.041	0.017
1.0	0.276	0.242	1.332	1.195	1.332	1.195	1.332	1.195	0.067	0.062	0.067	0.062
1.0	0.200	0.139	2.488	1.579	2.488	1.579	2.488	1.579	0.053	0.009	0.053	0.009
3.0	0.591	0.266	1.940	1.381	1.940	1.381	1.940	1.381	0.276	0.074	0.276	0.074
3.0	0.750	0.590	2.135	1.671	2.135	1.671	2.135	1.671	0.450	0.276	0.450	0.276
3.0	0.481	0.286	2.175	1.578	2.175	1.578	2.175	1.578	0.211	0.111	0.211	0.111
4.0	0.479	0.290	1.970	1.555	1.970	1.555	1.970	1.555	0.240	0.131	0.240	0.131
5.0	1.452	1.000	3.520	2.922	3.520	2.922	3.520	2.922	2.995	1.218	2.995	1.218
1.0	0.324	0.147	1.682	1.045	1.682	1.045	1.682	1.045	0.098	0.044	0.098	0.044
1.0	0.189	0.122	1.384	1.342	1.384	1.342	1.384	1.342	0.002	0.015	0.002	0.015
1.0	0.162	0.116	1.120	0.967	1.120	0.967	1.120	0.967	0.016	0.012	0.016	0.012
5.0	2.229	1.833	3.660	3.251	3.660	3.251	3.660	3.251	7.500	3.472	7.500	3.472
3.0	0.216	0.364	1.695	1.450	1.695	1.450	1.695	1.450	0.041	0.011	0.041	0.011
2.0	0.212	0.200	1.276	1.411	1.276	1.411	1.276	1.411	0.027	0.032	0.027	0.032
2.0	0.236	0.236	1.186	1.159	1.186	1.159	1.186	1.159	0.035	0.034	0.035	0.034
5.0	0.310	0.225	1.726	1.488	1.726	1.488	1.726	1.488	0.695	0.139	0.695	0.139
4.0	0.668	0.417	2.835	2.208	2.835	2.208	2.835	2.208	0.392	0.242	0.392	0.242
4.0	0.523	0.360	2.068	1.458	2.068	1.458	2.068	1.458	0.206	0.103	0.206	0.103
4.0	0.526	0.417	2.270	1.521	2.270	1.521	2.270	1.521	0.198	0.111	0.198	0.111
4.0	1.532	0.565	3.618	3.000	3.618	3.000	3.618	3.000	0.689	0.296	0.689	0.296
4.0	1.728	0.889	4.095	2.421	4.095	2.421	4.095	2.421	4.380	1.163	4.380	1.163
4.0	0.723	0.572	3.300	2.447	3.300	2.447	3.300	2.447	0.562	0.286	0.562	0.286
4.0	2.427	1.461	6.950	5.540	6.950	5.540	6.950	5.540	6.880	3.870	6.880	3.870
4.0	2.500	1.785	8.040	6.880	8.040	6.880	8.040	6.880	9.980	5.400	9.980	5.400

* Smooth Texture = 1.0 Mixed Smooth and Grainy Texture = 3.0 Rough, Irregular Macro-Texture = 5.0
 Grainy Texture = 2.0 Smooth Texture with Agricultural Patterns = 4.0

Table IX. Correlation Matrix: Probability/Density Curve Parameter Versus Inferred and Measured SLAR Image Parameters

Variable	Description	1	2	3	4	5	6	7	8	9	10	11	12	13
1	Probability/density curve parameter (X/Y)	1.000												
2	Inferred soil type: 1 = clay, 2 = clay-silt, 3 = silt, 4 = silt-sand, 5 = sand, 6 = sand-gravel, 7 = gravel, 8 = cobbles, 9 = bedrock	0.146	1.000											
3	Estimated percent forest cover	0.100	-0.253	1.000										
4	Estimated percent brush	-0.034	0.381	0.183	1.000									
5	Estimated percent grass or crop	1.000	-0.076	-0.200	0.240	1.000								
6	Estimated percent bare soil		1.000	-0.352	-0.391	-0.363	1.000							
7	Estimated relief rank: 1 = very high, 2 = high, 3 = moderate, 4 = low, 5 = flat			-0.226	0.134	-0.523	0.329	1.000						
8	Estimated surface moisture content: 1 = very wet, 2 = wet, 3 = moist, 4 = dry, 5 = very dry			1.000	-0.712	0.030	0.590	-0.285	1.000					
9	Drainage density measured from SLAR image (F/ect)									1.000				
10	Maximum relief (Fect)										1.000			
11	Film factor: 1 = low overall tone, 2 = medium overall tone, 3 = high overall tone											1.000		
12	Estimate of geologic structural control: 1 = strong control, 2 = moderate control, 3 = no control												1.000	
13	Average areal tone value: 1 = dark - 5 = light													1.000

image conditions to be useful for the analysis of terrain parameters. The averaging effect of the 1- and 2-millimeter apertures did not produce results related to regional terrain conditions as had been anticipated. It is also concluded that this experiment demonstrates that micro-densitometers or electronic scanning devices are necessary to produce quantitative image textural data sufficient in detail to approach the classification potential of human interpreters. Although the probability/density curve parameter (X/Y) correlated significantly with visually defined image textures, the parameter could not be significantly correlated with terrain parameters which individually contribute to the formation of an image texture.

34. Radar Shadow Analysis. Because of navigational inaccuracies, SLAR image distortions, and scale changes, calculation of terrain feature heights from shadow-length measurements is not generally acceptable. It was hypothesized that, because of the very strong association between imaging geometry, terrain geometry, and resulting radar shadows, an empirical relationship should exist between radar shadow size, shape, and distribution and some measure of terrain macro-roughness. Measurements of radar shadow size, shape, and distribution were made from randomly selected locations on unclassified, monoscopic, K-band SLAR imagery and correlated by means of multiple linear regression techniques with a terrain roughness parameter calculated from topographic map data.

a. Selection of Sample Locations. SLAR image sample locations were selected randomly with respect to inferred landform type. However, each sample location was selected so that it was completely within an engineering soil type or landform boundary that could be visually delineated on the imagery. This procedure was adopted to avoid the sampling of several terrain types as one unit.

Twenty-seven of the 35 sample areas delineated for the textural experiment constituted one group of locations for the collection of areal radar shadow data. In addition, 19 sample locations from 5 different SLAR images were defined as linear traces positioned perpendicular to the imaging aircraft flight line. Shadow data collected from the linear-trace locations consisted of width and frequency of occurrence but did not include areal distribution information.

b. Collection of SLAR Image Data. Each of the 27 sample areas delineated on SLAR images represented approximately 9 square miles of terrain surface. A plastic overlay was constructed with a grid spacing of 0.1 inch. The grid spacing was kept constant for all image areas evaluated. Consequently, actual terrain distances varied with image scale. A count was made of the number of radar shadows or portions of shadows positioned under each grid intersection. In addition, very light tones inferred to result from regional slopes facing the antenna were counted. The 0.1 inch grid was chosen as a spacing that would be large enough to eliminate effects of system

resolution on data collection. This spacing was also considered within the order of magnitude of terrain macro-roughness likely to be measurable.

In the case of linear-trace sample locations, the number of inferred valleys and ridges was counted along a line of specified length. In addition, the total accumulated width of radar shadow and very light toned areas was measured and the total number of discrete shadows was counted from the linear traces.

Information collected from image areas and linear traces constituted two different sets of data each of which was correlated with corresponding terrain roughness parameters. Figure 26 illustrates the geometry involved in each of the sampling techniques and describes the manner in which data was collected. Table X is a summary of SLAR image locations utilized in the experiment and all data utilized in the multiple linear regression analyses.

c. Determination of a Terrain-Roughness Parameter. Efforts to extract a terrain-relief value representative of areal terrain roughness from a topographic map were unsuccessful. A review of literature related to quantitative terrain analysis indicated that a terrain-roughness parameter defined as Fisher's dispersion factor "K" might be a reasonable parameter for correlation with radar shadow data (33, 40, 98, 102). A computer program (VECTOR) was utilized for calculation of terrain-roughness parameters for each of the areal and linear-trace sample locations. Program VECTOR, modified by Turner and Miles (98) from work done by Hobson (40), requires as an input a rectangular array of terrain elevation readings. A set of intersecting triangular planar surfaces as defined by groups of three adjacent elevation readings is established along with normal vectors to these planar surfaces. Mean vector orientation, strength, and dispersion are then calculated. Fisher's dispersion factor is calculated as a measure of the variability or spread of the unit vectors. It is defined as $K = N-1/N-R_1$ where N = number of observations (triangles) and R_1 = vector strength. "Smooth" areas produce unit vectors with high strengths and low dispersions (high K values) while "rough" areas produce low vector strengths with high dispersion (low K values).

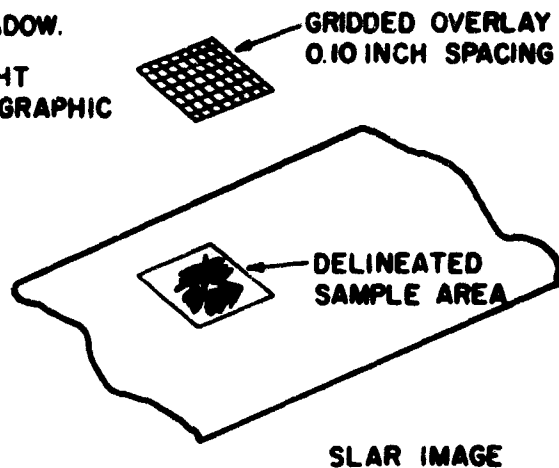
An area, corrected for image scale, was delineated on 1:62,500 topographic maps corresponding in location to each of the 27 sample areas. A rectangular grid with a 0.1 inch spacing was then used to extract terrain elevations. In cases where the delineated map area was distorted because of SLAR image distortion or scale variation, gridded elevation data was obtained from the rectangle enclosing the distorted area. The grid spacing represented 521 feet on the ground.

In the case of the 19 linear-trace sample locations, elevation data was obtained from a grid two intervals wide extending the length of the linear trace. The

AREAL GRIDDED DATA

INFORMATION COLLECTED

1. NUMBER OF POINTS OVER SHADOW.
2. NUMBER OF POINTS OVER LIGHT TONES ATTRIBUTED TO TOPOGRAPHIC EFFECTS.
3. TOTAL NUMBER OF POINTS CONTAINED WITHIN SAMPLE AREA.
4. TOTAL LENGTH OF INFERRED DRAINAGEWAYS EXHIBITED WITHIN SAMPLE AREA.



LINEAR SCAN DATA

INFORMATION COLLECTED

1. NUMBER OF INFERRED VALLEYS INTERSECTING SCAN.
2. NUMBER OF INFERRED SHADOWS INTERSECTING SCAN.
3. MAXIMUM WIDTH OF INDIVIDUAL SHADOWS.
4. TOTAL WIDTH OF RADAR SHADOW.
5. TOTAL WIDTH OF LIGHT TONE ATTRIBUTED TO TOPOGRAPHIC EFFECTS.

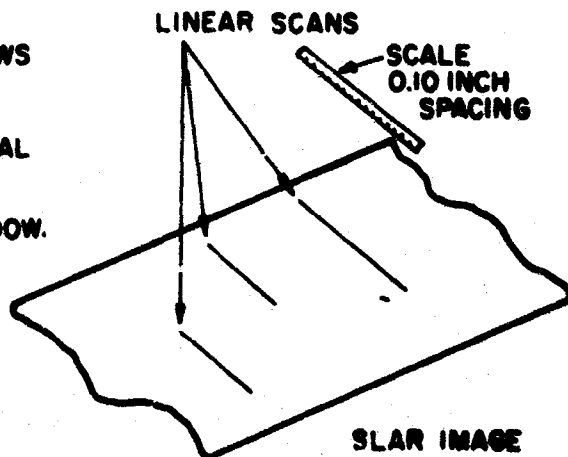


Fig. 26. Roughness experiment sampling techniques.

Table X. Summary of Sample Locations and Data Used in the Terrain Roughness Experiment

Location	Analytically Collected Data				Linear Scan Data				
	Roughness Calculated from Elevation Data		Number of Points Over Shadow +by Total Points		Roughness Calculated from Elevation Data		Number of Infrared Valleys +Total Length of Scan		Total Width of Shadow +Total Length of Scan
	K	Log K	Points Over Shadow +by Total Points	Number of Points Over High Returns +Total Points	K	Log K	Number of Infrared Valleys +Total Length of Scan	Maximum Width of Individual Shadows (Ft)	
Michigan									
Viaduct	172.0	2.23653	0.2000	0.2000	4.99	2.69749	0.00043	291.00	0.0000
Viaduct	31985.0	4.50496	0.0000	0.1000	1.83	2.21748	0.00052	390.00	0.0985
Viaduct	812885.0	5.70973	0.2000	0.0000	0.01	2.48616	0.00000	244.00	0.1045
Viaduct	2872.0	3.45678	0.0000	0.0000	0.01	2.1212.0	0.00010	0.01	0.0001
Viaduct	288.0	2.45883	0.4100	0.2000	2.99	2.99349.0	0.00010	0.01	0.0001
Maryland									
St. Alb	493.0	2.69285	0.2000	0.4000	1.46	2.51108	0.00028	1995.00	0.0974
St. Alb	267.0	2.42661	0.2000	0.2000	1.15	2.63649	0.00028	2625.00	0.1872
St. Alb	493.0	2.69285	0.2000	0.4000	1.46				
Arkansas									
Willcox	999999.0	5.99999	0.0001	0.0001	0.01	2.89998	0.00027	299.00	0.0695
Willcox	22807.0	4.35386	0.1000	0.1000	1.19	1.57000	0.00054	1494.00	0.3309
Willcox	228983.0	5.35946	0.0000	0.0000	1.26	3.59496	0.00059	1942.00	0.1601
Willcox	999999.0	5.99999	0.0001	0.0001	0.01	5.99999	0.00008	0.01	0.0001
Willcox	1643.0	3.21389	0.0000	0.1000	2.64	2.73159	0.00069	593.00	0.3740
Pennsylvania									
Harrisburg	525.0	2.72016	0.2000	0.2000	1.25	2.37880	0.00043	1875.00	0.2400
Harrisburg	41.0	1.61288	0.2000	0.1000	0.74	2.32971	0.00013	2438.00	0.1130
Harrisburg	1081.0	3.03383	0.2000	0.1000	1.76	2.55046	0.00017	1969.00	0.2440
Tennessee									
Jackson Hole	228.0	2.35816	0.0001	0.0000	0.44	4.26458	0.00007	0.1	0.0001
Jackson Hole	691.0	2.83948	0.2000	0.2000	2.26	2.94498	0.00006	104.00	0.226
Jackson Hole	2098.0	3.22066	0.4000	0.2000	3.96	1.25630	0.00032	2156.00	0.2620
Jackson Hole	22844.0	4.35731	0.0001	0.0001	0.01	5.25115	0.00012	0.01	0.0001
Jackson Hole	22844.0	4.35731	0.0001	0.0001	0.01				
Indiana									
Lafayette	4004.0	3.60274	0.0000	0.0000	0.01				
Lafayette	22844.0	4.35731	0.0001	0.0001	0.01				
Lafayette	4004.0	3.60274	0.0000	0.0000	1.02				
Lafayette	22844.0	4.35731	0.0001	0.0001	0.01				
Lafayette	22844.0	4.35731	0.0000	0.0000	0.33				
Lafayette	22844.0	4.35731	0.0001	0.0001	0.01				
Lafayette	4004.0	3.60274	0.0001	0.0001	0.01				

Note: All zero values were replaced by a relatively small value to avoid bias in the correlation analysis.

rectangular array of elevation data was three elevation samples wide. The grid spacing was 521 feet as before.

Gridded elevation data from the areal and linear trace sample locations were used as an input to program VECTOR for the calculation of Fisher's dispersion factor "K." K values and corresponding log K values for each sample site are contained in Table X.

d. Analysis of Data. Data from areal and linear-trace sample locations contained in Table X were subjected to linear multiple correlation and regression analyses. A computer program on file at Purdue University (101) was used for the analyses. In successive analyses, Fisher's dispersion factor K and log K were considered as the dependent variables while all other variables in Table X were independent variables. Each analysis yielded a correlation matrix indicating the degree of correlation between all pairs of variables and a stepwise regression in which a mathematical model for predicting K or log K was established. In the step-wise regression, variables were entered into the model in descending order of significance.

e. Interpretation of Results. Log K was found to correlate most significantly with SLAR image shadow data in the case of areally sampled data as well as linearly sampled data. However, correlations between log K and variables measured from the 27 areal samples were generally lower than correlations with data obtained from the linear traces. Error associated with the mathematical model for predicting log K from areally gridded SLAR image data was considered excessive. The technique of correlating areally gridded SLAR image data with log K was judged to be of limited value because of the loss of the direct relationship between imaging geometry, terrain feature height, and radar shadow length in the range direction.

Correlations between SLAR image parameters measured along linear traces and log K values offered considerably more promise. Table XI presents the correlation matrix involving those variables which remained after the least significant variables had been eliminated. Also included are coefficients of the two empirical models for predicting terrain roughness (K = Fisher's dispersion factor) established by the stepwise regression. Both empirical models are considered to strongly express the relationship between imaging geometry, terrain feature height, and radar shadow length.

Of the two models illustrated in Table XI, the first, containing only one variable (variable 3), appears to be the best for predicting log K. This choice was made after comparing and evaluating standard errors associated with each variable coefficient in light of the amount of variability accounted for in the regression (R^2). Model 2 with variables 2 and 3 in the equation accounts for the highest reduction in variability

Table XI. Variables Considered in Final Regression Analysis for Determination of Terrain Roughness from SLAR Imagery

<u>Variable</u>	<u>Description</u>
1	Log K = roughness parameter
2	X = number of valleys inferred from SLAR image + total length of scan
3	Y = Total width of radar shadow + total length of scan

<u>Correlation Matrix</u>			
	1	2	3
1	1.000	-0.629	-0.742
2		1.000	0.537
3			1.000

Variable 3 in Equation (Model 1)

Constant = 4.155 $R^2 = 0.55$

<u>Variable</u>	<u>Coefficient</u>	<u>Standard Error</u>	<u>Significance of Regression</u>
3	-8.273	1.815	99%

Predicting Model $\text{Log K} = 4.155 - 8.273(Y)$

Variables 2 and 3 in Equation (Model 2)

Constant = 4.582 $R^2 = 0.63$

<u>Variable</u>	<u>Coefficient</u>	<u>Standard Error</u>	<u>Significance of Regression</u>
2	-2036.518	1137.573	99%
3	6.328	2.024	

Predicting Model $\text{Log K} = 4.582 - 2036.518(X) - 6.323(Y)$

($R^2 = 0.63$), but the standard error of coefficient 2 indicates that the variable coefficient is not significantly different from zero. The variable coefficient in model 1 is significantly different from zero. With this model, 55% of the data variability is accounted for by regression ($R^2 = 0.55$).

The model $\log K = 4.155 - 8.273(Y)$, where K = Fisher's dispersion factor and Y = Total width of radar shadow along scan/Total length of scan, is considered a reasonable predicting equation in view of the multitude of unassessable conditions affecting the problem. Certain limitations of the equation are obvious. The total length of scan must be relatively large with respect to the order of magnitude of the terrain roughness. The lengths of scan utilized for this experiment ranged from about 9000 feet to 40,000 feet of actual terrain surface. Also, the equation will not produce satisfactory results if all or most of the scan is inferred to be shadow. This empirical equation is based on 19 samples and could undoubtedly be improved with further sampling from other SLAR images not available for this investigation.

Table XII presents typical landform types and corresponding measured roughness "K" values as determined by Turner and Miles (98). Also included are the landform types and corresponding "K" values calculated for this experiment.

In applying the empirical, roughness-predicting equation to SLAR image data, it is necessary to take cognizance of the standard error associated with the variable coefficient as well as the boundary values associated with the equation. It is suggested that the empirical model is best suited for defining intervals or ranks of terrain roughness as defined by $\log K$. However, data sufficient for the establishment of a meaningful confidence interval were not available. The effect of boundary values is quite apparent. If no radar shadows are seen on a SLAR image scan, the calculated roughness will be that of the constant in the equation ($\log K = 4.155$). This phenomenon can be interpreted to mean that a roughness of $\log K = 4.155$ is the limit imposed by SLAR image scale and resolution associated with samples utilized in this investigation. This limit should also be closely related to the imaging geometry associated with the SLAR system.

The empirical model for predicting terrain roughness from measured SLAR image parameters can be considered valid only for the K-band system which produced the study imagery. Imagery from other systems should produce a similar model with variable coefficients adjusted to account for imaging geometry and average scale.

f. Potential Application of the Roughness Model. The objective of this experiment was to determine the relationship between measured SLAR image parameters and a terrain-surface-roughness parameter. No attempt was made to evaluate the significance of the roughness parameter "K." However, work conducted by Hobson

Table XII. Typical Landforms and Corresponding Measured Roughness (Log K)

Terrain Type	Terrain Roughness (Log K)	
	Experiment with SLAR	Turner and Miles (98)
Escarpment		1.914
Escarpment		1.929
Sedimentary Mountain	1.255	
Metamorphic Mountain	1.279	
Sedimentary Mountain Ridge	2.326	
Sedimentary Mountains	2.550	
Hills		2.199
Hills		2.342
Hills		2.599
Dissected Loess Hills	2.217	
Dissected Loess Hills	2.436	
Dissected Loess Hills	2.637	
Metamorphic Hills	2.512	
Metamorphic Hills	2.636	
Sedimentary Hills	2.378	
Sedimentary Hills	2.732	
Drumlins		2.346
Dissected Pediment	2.896	
Ridge Moraine	2.945	
Karst Plain		2.859
Karst Plain		3.124
Plateau		3.245
Ridge Moraine and Dunes		3.461
Alluvial Apron	3.595	
Ground Moraine		4.392
Ground Moraine		4.478
Outwash Plain		4.256
Glacial Terrace	4.265	
Recent Flood Plain	4.325	
Flood Plain	6.251	
Old Flood Plain	5.378	
Playa	5.999	

(40) and Turner and Miles (98) does suggest several potential applications of the terrain-roughness parameter "K." The roughness parameter may be useful in relating terrain relief and roughness to trafficability or highway site selection problems. Turner and Miles found that log K correlated highly ($r = -0.950$) with the log of maximum triangle dip calculated by program VECTOR. Although this triangle dip would not necessarily correspond exactly to a maximum, terrain-surface slope within the sample area, there should be a reasonably high correlation between the two. The roughness parameter was found to be an indicator of maximum relief during the course of this investigation and may in the future be quantitatively related to several of the highway engineering construction costs related to topography.

VII. CONCLUSIONS

35. **Conclusions.** It is concluded from the qualitative analysis and evaluation of various SLAR images utilized in this investigation that:

a. It is possible to interpret regional engineering soil types from SLAR imagery by means of an inference technique based on recognition and evaluation of repetitive, characteristic patterns. SLAR imagery shows pattern elements of discrete tonal elements, average areal tones, and image texture which, in various combinations, form SLAR image patterns indicative of specific terrain surface conditions.

b. The extent to which inferences can be made concerning local land surface conditions such as local surface roughness or vegetative cover is governed by the dynamic range of tone values expressed on the imagery. "Brute force" SLAR imagery allows a more detailed interpretation than does "synthetic aperture" SLAR imagery.

c. No evidence of significant microwave energy penetration could be found on the SLAR imagery studied during this investigation. At the wavelengths utilized for the study imagery, the pattern elements were derived as a function of microwave reflection from the first surface of the terrain. In humid environments, the first surface is usually a vegetative surface. In arid environments, the first surface is a combination of bare soil and desert vegetation.

d. The systematic SLAR image interpretation technique developed during this investigation provides a logical basis for interpretation of engineering soil types and insures results which are consistent in derivation. The confidence with which an interpretation can be made is greatly increased if adequate field data or ground truth is available. The technique attains a maximum usefulness if used to extend knowledge from areas with known conditions.

c. The relatively small scale at which SLAR imagery is obtained and the resolution of typical imagery are considered advantageous for regional engineering soils interpretations. A synoptic view of terrain, unconfused by minor tonal contrasts, is afforded by SLAR imagery. Conventional aerial photographs at normal scales provide data necessary for detailed, local engineering soil interpretations.

It is further concluded from the quantitative analysis of various SLAR images that:

f. The shape of a probability/density curve (histogram of tone elements) generated from a SLAR image is a quantitative measure of visual image texture.

g. The shape of SLAR image probability/density curves as characterized by the ratio of base width (X) to peak height (Y) is not highly sensitive to absolute tone values and is therefore useful for extracting texture data from uncalibrated SLAR images.

h. Although a potential exists for correlating quantitative image texture data with ground-truth parameters, the image-texture parameter (X/Y) calculated from probability/density curves generated with a macro-densitometer was of no value for this purpose. The image texture parameter should be obtained from curves generated with a micro-densitometer or electronic flying-spot scanners.

i. Radar shadow measurements obtained from linear traces oriented perpendicular to the image flight line can be empirically related to a terrain macro-roughness expressed by Fisher's dispersion factor "K." The mathematical relationship, however, is valid only for the system which produced the imagery used in obtaining the parameter coefficients.

LITERATURE CITED

1. Ahmed, N. and W. W. Koepsel, 1963, "An Approach to Correlate Pulsed Radar and Photographic Data," *Technical Report EE-89*, Engineering Experiment Station, University of New Mexico.
2. Andrews, A., 1961, *ABC's of Radar*, Indianapolis, Indiana: Howard W. Sams and Co., Inc.
3. Badgley, P. C., 1966, "Planetary Exploration from Orbital Altitudes," *Photogrammetric Engineering*, Vol. XXXII (2), pp. 250-259.
4. Badgley, P. C. and R. J. P. Lyon, 1965, "Lunar Exploration from Orbital Altitudes," *Annals of the New York Academy of Science*, Vol. 123 (2), pp. 1198-1219.
5. Badgley, P. C., Fischer, W. and R. J. P. Lyon, 1965, "Geologic Exploration from Orbital Altitudes," *Geotimes*, Vol. 10 (2), pp. 11-14.
6. Badgley, P. C. and W. L. Vest, 1966, "Orbital Remote Sensing and Natural Resources," *Photogrammetric Engineering*, Vol. XXXII (5), pp. 780-790.
7. Beatty, F. D., et al., 1965, "Geoscience Potentials of Side-Looking Radar," *Raytheon Autometric Corporation*, Contract No. DA-44-009-AMC-1040(X) with U. S. Army Corps of Engineers, Alexandria, Virginia.
8. Beccasio, A. D. and J. H. Simons, 1965, "Regional Geologic Interpretations from Side-Looking Airborne Radar," *Photogrammetric Engineering*, Vol. XXXI (3), p. 507 (Abstract).
9. Beckman, P., 1965, "Scattering by Composite Rough Surfaces," *Proceedings of the Institute of Electrical and Electronics Engineers*, Vol. 53 (8), pp. 1012-1015.
10. Bienvenu, L. R., 1961, "Interpretation of Geologic Features from SLAR," *Photogrammetric Engineering*, Vol. XXVII (2), p. 488 (Abstract).
11. Bienvenu, L. R. and R. Pascucci, 1962, "Engineering Geology from SLR Records," *Raytheon/Autometric Corporation*, Alexandria, Virginia.

12. Carneggie, D. M. and D. T. Laver, 1966, "Uses of Multiband Remote Sensing in Forest and Range Inventory," *Photogrammetria*, Vol. 21 (4), pp. 115-141.
13. Claveloux, B. A., 1960, "Sketching Projector for Side-Looking Radar Photography," *Photogrammetric Engineering*, Vol. XXVI (4), pp. 644-646.
14. Colwell, R. N. (editor), 1960, *Manual of Photographic Interpretation*, American Society of Photogrammetry, Washington, D. C.
15. Colwell, R. N., 1961, "Some Practical Applications of Multiband Spectral Reconnaissance," *American Scientist*, Vol. 49 (1), pp. 9-36.
16. Cosgriff, R. L., Peake, W. H. and R. C. Taylor, 1960, "Terrain Scattering Properties for Sensor System Design (Terrain Handbook II)," *Engineering Experiment Station Bulletin No. 181*, Ohio State University.
17. Crandall, C., 1963, "Advanced Radar Map Compilation Equipment," *Photogrammetric Engineering*, Vol. XXIX (6), pp. 947-955.
18. Cutrona, L. J., Vivian, W. E., Leith, E. N. and G. O. Hall, 1961, "A High-Resolution Radar Combat-surveillance System," *Institute of Radio Engineers Transactions on Military Electronics*, Vol. MIL-5 (2), pp. 127-131.
19. Davis, B. R., Lundien, J. R. and A. N. Williamson, 1966, "Feasibility Study of the Use of Radar to Detect Surface and Ground Water," *U. S. Army Engineer Waterways Experiment Station Technical Report No. 3-727*, Vicksburg, Mississippi.
20. Dellwig, L. F., Bickford, M. E., Kirk, N. and R. Walters, 1965, "Remote Sensor Studies of the Pisgah Crater Area, California: A Preliminary Report," *CRFS Technical Memorandum No. 61-18*, University of Kansas-Center for Research Inc.-Engineering Science Division.
21. Dellwig, L. F. and R. K. Moore, 1966, "The Geological Value of Simultaneously Produced Like- and Cross-Polarized Radar Imagery," *Journal of Geophysical Research*, Vol. 71 (14), pp. 3597-3601.
22. Ellermeier, R. D., Fung, A. K. and D. S. Simonett, 1966, "Some Empirical and Theoretical Interpretations of Multiple Polarization Radar Data," *Proceedings of the Fourth Symposium on Remote Sensing of Environment, April 12-14, 1966*, University of Michigan, pp. 657-670.

23. Ellermeier, R. D. and D. S. Simonett, 1965, "Imaging Radar on Spacecraft as a Tool for Studying the Earth," *CRES Report No. 61-6*, University of Kansas-Center for Research Inc.-Engineering Science Division.
24. Esten, R. D., 1953, "Radar Relief Displacement and Radar Parallax," *Report 1294*, U. S. Army Engineer Research and Development Laboratories, Fort Belvoir, Virginia.
25. Feder, A. M., 1957, "The Application of Radar in Geologic Exploration," *Bell Aircraft Corporation Report*, Buffalo, New York.
26. Feder, A. M., 1959, "Radar as a Terrain-Analyzing Device," *Bulletin of the Geological Society of America*, Vol. 70 (12), pp. 1804-1805.
27. Feder, A. M., 1960, "Radar Geology," *Master's Thesis*, University of Buffalo (Unpublished).
28. Feder, A. M., 1960, "Interpreting Natural Terrain from Radar Displays," *Photogrammetric Engineering*, Vol. XXVI (4), pp. 618-630.
29. Feder, A. M., 1962, "Radar Geology Can Aid Regional Oil Exploration," *World Oil*, Vol. 155 (1), pp. 130-138.
30. Feder, A. M., 1962, "Programs in Remote Sensing of Terrain," *Proceedings of the Second Symposium on Remote Sensing of Environment, October 15-17, 1962*, University of Michigan, pp. 51-64.
31. Feder, A. M., 1964, "Let's Use More of the Electromagnetic Spectrum," *Transactions of the Gulf Coast Association of Geological Societies, 14th Annual Convention, October, 1964*, pp. 35-49.
32. Fischer, W., 1962, "An Application of Radar to Geological Interpretation," *Proceedings of the First Symposium on Remote Sensing of Environment, February 13-15, 1962*, University of Michigan, pp. 83-84.
33. Fisher, R. A., 1953, "Dispersion of a Sphere," *Proceedings of the Royal Society of London*, Vol. 217, Series A, pp. 295-305.
34. Gillerman, E., 1967, "Investigation of Cross-Polarized Radar on Volcanic Rocks," *CRES Report No. 61-25*, University of Kansas-Center for Research, Inc.-Engineering Science Division.

35. Goldstein, H., 1950, "A Primer of Sea Echo," *Report 157*, U. S. Navy Electronics Laboratory, Washington, D. C.
36. Goodyear Aircraft Corporation, 1959, "Final Report on Measurement of Terrain Back Scattering Coefficients with an Airborne X-Band Radar," Report GERA-463, Litchfield Park, Arizona, cited by American Society of Photogrammetry, *Manual of Photogrammetry*, Third Ed., p. 1023.
37. Goodyear Aerospace Corporation, 1964, "Coherent High-Resolution Radar Interpretation and Analysis Techniques Study (U)," (Secret Report), *Technical Documentary Report prepared for the Reconnaissance Data Extraction Branch, Rome Air Development Center, Griffiss AFB, New York*, p. 39, 41.
38. Grant, C. R. and B. S. Yaplee, 1957, "Back Scattering from Water and Land at Centimeter and Millimeter Wavelengths," *Proceedings of the Institute of Radio Engineers*, Vol. 45 (7), pp. 976-982.
39. Guinard, N. W., Ransone, J. T., Laing, M. B. and L. E. Hearton, 1967, "NRL Terrain Clutter Study: Phase 1," *NRL Report 6487*, Naval Research Laboratory, Washington, D. C.
40. Hobson, R. D., 1967, "FORTRAN IV Programs to Determine Surface Roughness in Topography for the CDC 3400 Computer," *Computer Contribution #14*, Kansas Geological Survey, Lawrence, Kansas.
41. Hoffman, P., 1954, "Interpretation of Radar Scope Photography," *Photogrammetric Engineering*, Vol. XX (3), pp. 406-411.
42. Hoffman, P., 1958, "Photogrammetric Applications of Radar Scope Photographs," *Photogrammetric Engineering*, Vol. XXIV (5), pp. 756-764.
43. Hoffman, P., 1960, "Progress and Problems in Radar Photo Interpretation," *Photogrammetric Engineering*, Vol. XXVI (4), pp. 612-618.
44. Holmes, R. F., 1967, "Engineering Materials and Side-Looking Radar," *Photogrammetric Engineering*, Vol. XXXIII (7), pp. 767-770.
45. Kirk, J. N. and R. L. Walters, 1966, "Radar Imagery, A New Tool for the Geologist," *The Compass of Sigma Gamma Epsilon*, Vol. 43 (2), pp. 85-93.

46. Konecny, G. and E. Derenyi, 1966, "Geometrical Considerations for Mapping from Scan Imagery," *Proceedings of the Fourth Symposium on Remote Sensing of Environment, April 12-14, 1966*, University of Michigan, pp. 334-336.
47. Kover, A. N., 1967, "Radar Imagery as an Aid in Geologic Mapping," *Photogrammetric Engineering*, Vol. XXXIII (6), p. 679 (Abstract).
48. Krumbein, W. C. and J. Imbrie, 1963, "Stratigraphic Factor Maps," *Bulletin of the American Association of Petroleum Geologists*, Vol. 47 (4), pp. 698-701.
49. Lancaster, C. W. and A. M. Feder, 1966, "The Multisensor Mission," *Photogrammetric Engineering*, Vol. XXXII (3), pp. 484-494.
50. Laprade, G. L., 1963, "An Analytical and Experimental Study of Stereo Radar," *Photogrammetric Engineering*, Vol. XXIX (2), pp. 294-300.
51. Leestma, R. A. and R. A. White, 1967, "Geographic Potentials of Spacecraft Imagery," prepared for the National Aeronautics and Space Administration by the U. S. Army Corps of Engineers, Fort Belvoir, Virginia.
52. Leighty, R. D., 1966, "Terrain Information from High Altitude Side-Looking Radar Imagery of an Arctic Area," *Proceedings of the Fourth Symposium on Remote Sensing of Environment, April 12-14, 1966*, University of Michigan, pp. 575-597.
53. Lenhert, D. H. and W. W. Koepsel, 1962, "Lunar Surface Characteristics Based on Radar and Photographic Data: Semi-Annual Progress Report," *Engineering Experiment Station Report PR-39*, University of New Mexico.
54. Leonardo, E. S., 1959, "An Application of Photogrammetry to Radar Research Studies," *Photogrammetric Engineering*, Vol. XXV (3), pp. 376-380.
55. Leonardo, E. S., 1963, "Comparison of Imaging Geometry for Radar and Camera Photographs," *Photogrammetric Engineering*, Vol. XXIX (2), pp. 287-293.
56. Leonardo, E. S., 1964, "Capabilities and Limitations of Remote Sensors," *Photogrammetric Engineering*, Vol. XXX (6), pp. 1005-1010.
57. Levine, D., 1956, "Standard Map Projections and the Radar Display," Goodyear Aircraft Corporation Report GERA-41, Litchfield Park, Arizona, cited by *Radargrammetry*, New York: McGraw-Hill Book Company, Inc., 1960.

58. Levine, D., 1960, *Radargrammetry*, New York: McGraw-Hill Book Company, Inc.
59. Levine, D., 1963, Principles of Stereoscopic Instrumentation for PPI Photography," *Photogrammetric Engineering*, Vol. XXIX (4), pp. 596-621.
60. Lundien, J. R., 1966, "Terrain Analysis by Electromagnetic Means: Report 2, Radar Response to Laboratory Prepared Soil Samples," *U. S. Army Engineers, Waterways Experiment Station, Technical Report No. 3-693*.
61. Macbeth Instrument Corporation, 1964, "Owner's Manual for the Operation, Maintenance, and Trouble-Shooting of the Macbeth Quantalog Densitometer, Model TD-102," Macbeth Instrument Corporation, Newburgh, New York, (unpublished information pamphlet).
62. Macchia, R. P., 1957, "Radar Presentation Resistor," *Photogrammetric Engineering*, Vol. XXIII (5), pp. 880-886.
63. McAnerney, 1966, "Terrain Interpretation from Radar Imagery," *Proceedings of the Fourth Symposium on Remote Sensing of Environment, April 12-14, 1966*, University of Michigan, pp. 731-750.
64. McCoy, R., 1968, "An Evaluation of Radar Imagery as a Tool for Drainage Basin Analysis," *Ph.D. Thesis*, University of Kansas (unpublished).
65. Meyer, W. D., 1967, "Analysis of Radar Calibration Data," *Final Report*, prepared for U. S. Army Engineer Topographic Laboratories by Goodyear Aerospace Corporation, Litchfield Park, Arizona.
66. Miles, R. D., 1963, "A Concept of Land Forms, Parent Materials, and Soils in Airphoto Interpretation Studies for Engineering Purposes," *Transactions of the Symposium on Photo Interpretation, International Archives of Photogrammetry*, Vol. 14, pp. 462-476.
67. Miles, R. D., Rula, A. A. and W. E. Grabau, 1963, "Forecasting Trafficability of Soils: Airphoto Approach," *U. S. Army Engineer Waterways Experiment Station, Technical Memorandum No. 3-331, Report 6*.
68. Moore, R. K., 1966, "Radar as a Sensor," *CRES Report No. 61-7*, University of Kansas-Center for Research, Inc.-Engineering Science Division.

69. Morain, S. A. and D. S. Simonett, 1966, "Vegetation Analysis with Radar Imagery," *Proceedings of the Fourth Symposium on Remote Sensing of Environment, April 12-14, 1966*, University of Michigan, pp. 605-622.
70. Morain, S. A. and D. S. Simonett, 1967, "K-Band Radar in Vegetation Mapping," *Photogrammetric Engineering*, Vol. XXXIII (7), pp. 730-740.
71. Olson, C. E., 1960, "Elements of Photographic Interpretation Common to Several Sensors," *Photogrammetric Engineering*, Vol. XXVI (4), pp. 651-656.
72. Packard Instrument Company, 1964, "Operation Manual for the Model 16 Pulse Height Analyzer," Packard Instrument Company, Inc., LaGrange, Illinois (unpublished information pamphlet).
73. Parker, D. C., 1962, "Some Basic Considerations Related to the Problem of Remote Sensing," *Proceedings of the First Symposium on Remote Sensing of Environment, February 13-15, 1962*, University of Michigan, pp. 7-23.
74. Parvis, M., 1950, "Drainage Pattern Significance in Airphoto Identification of Soils and Bedrocks," *Highway Research Board Bulletin No. 28*, National Academy of Sciences, Washington, D. C., pp. 36-62.
75. Pierson, W., Scheps, B. B. and D. S. Simonett, 1965, "Some Applications of Radar Return Data to the Study of Terrestrial and Oceanic Phenomena," *Proceedings of the Third Goddard Memorial Symposium on Scientific Experiments for Manned Orbital Flight, March 18-19, 1965*, Washington, D. C., pp. 87-137.
76. Prentice, V. L., 1967, "Geographic Interpretation of a Radar Image," *Annals of the Association of American Geographers*, Vol. 57 (1), p. 187 (Abstract).
77. Reeves, R. G. and A. N. Kover, 1966, "Radar from Orbit for Geological Studies," *Photogrammetric Engineering*, Vol. XXXII (5), p. 869 (Abstract).
78. Rhodes, D. C. and D. E. Schwarz, 1967, "Some Potentials and Problems in the Use of Radar Imagery in Crop Geography Studies," *Annals of the Association of American Geographers*, Vol. 57 (1), p. 156 (Abstract).
79. Rib, H. T., 1967, "An Optimum Multisensor Approach for Detailed Engineering Soils Mapping," *Ph.D. Thesis*, Purdue University (unpublished).

80. Rouse, J. W., Waite, W. P. and R. I. Walters, 1965, "Use of Orbital Radars for Geoscience Investigations," *CRES Report No. 61-8*, University of Kansas-Center for Research, Inc.-Engineering Science Division.
81. Rydstrom, H. O., 1966, "Interpreting Local Geology from Radar Imagery," *Proceedings of the Fourth Symposium on the Remote Sensing of Environment, April 12-14, 1966*, University of Michigan, pp. 193-201.
82. Rydstrom, H. O., 1967, "Interpreting Local Geology from Radar Imagery," *Bulletin of the Geological Society of America*, Vol. 78 (3), pp. 429-436.
83. Scheps, B. B., 1960, "To Measure is to Know-Geometric Fidelity and Interpretation in Radar Mapping," *Photogrammetric Engineering*, Vol. XXVI (4), pp. 637-644.
84. Scheps, B. B., 1962, "The History of Radar Geology," *Proceedings of the First Symposium on Remote Sensing of Environment, February 13-15, 1962*, University of Michigan, pp. 79-81.
85. Schreiter, J. B., 1950, "Strip Projections for Radar Charting," *Technical Paper 130*, Ohio State University Mapping and Charting Laboratory.
86. Shepard, J. R., 1966, "Radar Geology Test Area, Willcox Playa, Arizona," U. S. Army Corps of Engineers, Fort Belvoir, Virginia (unpublished information letter).
87. Simonett, D. S., 1967, "Potential of Radar Remote Sensors as Tools in Reconnaissance Geomorphic Vegetation, and Soil Mapping," accepted for publication in the 9th International Congress, International Soil Science Society, Adelaide, Australia, August, 1968.
88. Simonett, D. S. and D. A. Brown, 1965, "Spacecraft Radar as a Means for Studying the Antarctic," *CRES Report No. 61-4*, University of Kansas-Center for Research, Inc.-Engineering Science Division.
89. Simonett, D. S. and S. A. Morain, 1965, "Remote Sensing from Spacecraft as a Tool for Investigating Arctic Environments," *CRES Report No. 61-5*, University of Kansas-Center for Research, Inc.-Engineering Science Division.

90. Simonett, D. S., Eagleman, J. E., Erhart, A. B., Rhodes, D. C. and D. E. Schwarz, 1967, "The Potential of Radar as a Remote Sensor in Agriculture: 1. A Study with K-Band Imagery in Western Kansas," *CRES Report No. 61-21*, University of Kansas-Center for Research, Inc.-Engineering Science Division.
91. Simons, J. H., 1965, "Some Applications of Side-Looking Airborne Radar," *Proceedings of the Third Symposium on Remote Sensing of Environment, October 14-16, 1964*, University of Michigan, pp. 563-571.
92. Simons, J. H. and A. D. Beccasio, 1964, "An Evaluation of Geoscience Applications of Side-Looking Airborne Mapping Radar," *Raytheon/Autometric Corporation Report*, Alexandria, Virginia..
93. Simpson, R. B., 1966, "Radar, Geographic Tool," *Annals of the Association of American Geographers*, Vol. 56 (1), pp. 80-96.
94. Skolnik, M. I., 1962, *Introduction to Radar Systems*, New York: McGraw-Hill Book Company, Inc.
95. Smith, N., 1962, "Radar Technology and Remote Sensors," *Proceedings of the First Symposium on Remote Sensing of Environment, February 13-15, 1962*, University of Michigan, pp. 27-34.
96. Strahler, A. N., 1952, "Hypsometric (Area-Altitude) Analysis of Erosional Topography," *Bulletin of the Geological Society of America*, Vol. 63 (11), pp. 1117-1142.
97. Thompson, M. M. (Editor-in-Chief), 1966, *Manual of Photogrammetry*, American Society of Photogrammetry, Washington, D. C.
98. Turner, A. K. and R. D. Miles, 1967, "Terrain Analysis by Computer," *Joint Highway Research Project Report No. 31 (November, 1967)*, Purdue University, Lafayette, Indiana.
99. U. S. Air Force, 1953, "Minutes of the Third Symposium on Mapping and Charting by Radar," prepared by the Director of Laboratories, Wright Air Development Center, Wright-Patterson AFB, Ohio.
100. U. S. Geological Survey, 1966, "Geological Survey Research in 1966," *Professional Paper 550A*, U. S. Geological Survey, Washington, D. C.

101. University of California, 1966, "BMD-2R, Stepwise Regression," prepared by the Health Sciences Computing Facility at the University of California at Los Angeles.
102. Watson, G. S., 1957, "Analysis of Dispersion on a Sphere," *Royal Astronomical Society Monthly Notices*, Geophysics Supplement No. 7, pp. 153-159.
103. Wise, D. U., 1967, "A Radar Geology and Pseudo-Geology Cross Section," *Photogrammetric Engineering*, Vol. XXXIII (7), pp. 752-761.
104. Wolff, E. A., 1960, "A Review of Theories and Measurements of Radar Ground Return," *Scientific Report #1*, Electromagnetic Research Corp., Washington, D. C.

APPENDIX

GENERALIZED CORRELATIONS BETWEEN SLAR IMAGE AND GENETIC LANDFORM PARAMETERS

Loess Plain

Drainage

The gross drainage pattern is usually dendritic with locally pinnate tributaries. The pattern appears on SLAR imagery as very thin, discrete tonal elements of radar shadow and light tones from riparian vegetation. The pinnate patterns can be seen on the SLAR image.

Topography

Loess surfaces are commonly characterized by blocky, cross-sectional shapes. Stream dissection may be very intense at regional scales. Valley walls are very steep, approaching the vertical in some instances. The blocky shape of the terrain is characterized by medium to light average areal tones. Steep valley walls are expressed by very narrow, highly contrasting radar shadows.

Land Use

In humid climates, loess areas are normally covered by dense forest. This is characterized on SLAR imagery by very light tones and grainy image textures. There is normally little evidence of agricultural activity if relief is high. Those agricultural patterns that do exist tend to emphasize the pinnate drainage patterns.

Engineering Soil Type

Loess is an unconsolidated eolian drift consisting of fine-textured silt of uniform particle size. The soil is generally classified as ML or CL under the USCS.

Dunes

Drainage

Surface drainage within dunes or sand sheets is generally absent. No pattern of drainage is evident on SLAR imagery.

Topography

Dunes occur in a variety of types, with a corresponding variety of surface configurations. Specific dune shapes cannot be resolved on the imagery, but a generally rolling topography can be inferred from the existence of medium and light contrasting, average areal tones. Isolated depressions or potholes are evidenced by dark, discrete tonal elements. A sand dune complex has a characteristic speckled image micro-texture.

Land Use

Sand dunes or sand sheets rarely exhibit agricultural patterns. The speckled micro-texture may be explained by irregularly spaced zones of grass and brush which tend to grow in the more stable zones. Sand sheets which are relatively flat and free of vegetation display dark image tones because of their apparent smoothness to microwave frequencies.

Engineering Soil Type

Dunes or sand sheets consist of unconsolidated eolian material composed of coarse-textured sand of uniform particle size. The soil is generally classified SP or SM under the USCS. SM soils are more characteristic of stabilized dunes in a humid environment.

Ground Moraine

Drainage

The gross drainage pattern is dendritic with local occurrences of kettle-holes and swamps. Glacial sluiceways containing underfit streams are commonly present, and in some cases derangement of drainage occurs. Such patterns are evidenced on SLAR imagery by discrete tonal elements of shadow, light tones from riparian vegetation, or dark "no-return" tones of water bodies. Swampy areas are characterized by dark tones from water-surfaces with a surrounding light-toned border produced by swamp vegetation.

Topography

The cross-sectional shape of a ground moraine or till plain is undulating with very low relief. Consequently, no evidence of topographic relief is seen on a typical SLAR image. There are no radar shadows or fine drainage textures evident. Such a flat surface is characterized by a medium to medium-dark average areal tone.

Land Use

Ground moraines normally show a great deal of agricultural activity with numerous rectangular fields. These fields have quite variable tones and generally smooth image textures. Field boundaries are irregular only where they border a tributary stream. Scattered wood lots do occur and can be recognized by their light tones and grainy image textures.

Engineering Soil Type

Ground moraine or till plains are composed of glacial till consisting of a heterogeneous mixture of clay, silt, sand, and gravel with possibly some erratics of large boulders. These materials vary randomly vertically and laterally. The A-horizon is generally classified as CL, CH, or ML under USCS. Swampy areas usually have soils which are more silty and organic than adjacent areas (types ML and OL).

Ridge Moraine

Drainage

The gross drainage pattern is usually dendritic but can be interspersed with kettle-hole, deranged, or drainageless areas. Large masses of glacially deposited material may have radial or parallel drainage patterns. The drainage pattern is recognized on SLAR imagery as an assemblage of discrete tonal elements consisting of thin shadows, light tones produced by riparian vegetation, or "no-return" dark tones representing lakes or large streams.

Topography

Coarse-grained ridge deposits exhibit rough, crested topography with frequent basins. Finer-grained deposits produce more rolling topography with a finer stream texture. The degree of roughness of topography is evidenced on SLAR imagery by the size, shape, and distribution of radar shadows. Rough topography will exhibit a lighter average areal tone with more radar shadows than will the more gently rolling topography.

Land Use

In humid environments, ridge moraines are usually tree covered. Forestation is expressed by light tones and grainy image textures on SLAR imagery. In cases where morainic material is coarse and internally drained, woodlands are more open and, in extreme cases, are replaced entirely by open grasslands. Such grassland areas will exhibit medium to light tones with smooth image textures. An extremely pitted morainic topography will produce a rough, irregular macro-texture on a SLAR image. Ridge moraines do support agricultural activity, with fewer crops grown in the rougher areas. In some cases, field boundaries are irregular and controlled by topography. Crops are normally diversified, resulting in a wide range of SLAR image tones but all with relatively smooth image textures.

Engineering Soil Type

Ridge moraines are composed of glacial till consisting of a heterogeneous mixture of clay, silt, sand, and gravel with possibly some erratics of large boulders. These materials vary randomly vertically and laterally. There is a general correlation between till particle size and geographic location with respect to the centers of glaciation with finer materials found near the outer margin of glaciation. However, there is an even stronger correlation between till particle size and the type of bedrock from which it was derived. Thus, for regional SLAR image interpretation, little specific information can be inferred about the probable USCS classification.

Outwash Surfaces

Drainage

The gross drainage pattern is roughly parallel with a low stream density. In glacio-fluvial plains or terraces, most drainage is internal and kettle-holes are common. Well-developed stream channels will be portrayed on SLAR imagery as thin radar shadow areas or light, discrete tonal elements produced by riparian vegetation. In the absence of well-defined channels, parallelism of drainage may be expressed by medium to dark-toned streaks which may be the result of generally smoother or more moist conditions.

Topography

Outwash surfaces are generally flat to undulating and show no evidence of relief on a SLAR image.

Land Use

Many outwash surfaces are cultivated in the United States and will exhibit rectangular field patterns which are completely free of topographic influence. These patterns are evidenced by rectangular areas exhibiting a variety of tones and smooth image textures.

Engineering Soil Type

Outwash plains are composed of crudely stratified sands and gravels with occasional lenses of silt. The A-horizon will vary in classification from SP to CL.

Alluvial Coastal Plain (Swamp)

Drainage

The gross drainage pattern is fundamentally dendritic but may be deranged or reticulate near sea level. Patterns of drainage are evidenced on a SLAR image as dark, discrete tonal elements resulting from the specular reflection of energy from water surfaces or as light-toned elements produced by riparian vegetation. In many cases, contrasts in tones and textures produced by coastal vegetation will be indicative of a drainage channel. Normally, there will be few, if any, radar shadows produced by the topographic cross-section of stream channels.

Topography

The cross-sectional shape is undulating with very low relief near sea level. No radar shadows produced by topography will be evident on the SLAR image, although there may be discrete shadow elements resulting from the shadowing effect of dense vegetation. Most dark tones will be produced by water surfaces or relatively flat, smooth terrain surfaces.

Land Use

Coastal plains normally will be heavily forested in humid regions. This will be evidenced by light tones and grainy image textures on a SLAR image. Grassy surfaces will produce medium to light tones with relatively smooth textures. Agricultural activity in the coastal plain regions studied during this investigation was negligible.

Engineering Soil Type

Swampy coastal plains are composed of thinly and irregularly stratified silts and clays with some local sands. Soils will generally be highly organic in humid regions, but a specific USCS classification cannot be inferred.

Lacustrine Plain

Drainage

The gross drainage pattern is basically dendritic but in cultivated regions may be ditched or canalized. In some areas, a trunk stream may be the only natural channel. Trunk streams or canals may be recognized on SLAR images as dark tonal elements produced by specular reflection from the water surface. In some cases, light, discrete tonal elements may be produced by riparian vegetation or by direct reflection of radar energy from stream banks facing the antenna. Small ditches or tile systems in cultivated areas cannot be detected.

Topography

The cross-sectional shape is generally undulating with very low relief. No evidence of radar shadowing due to topography will be seen on a SLAR image. The average areal tone of a lacustrine plain will appear medium to dark if agricultural patterns and light crop tones are not too extensive.

Land Use

Lacustrine plains are normally cultivated in humid regions. Crop patterns are recognizable by their rectangular field boundaries. Fields will show varying tones and smooth image textures. Natural grasses will appear as medium- to low-toned areas with smooth image textures whereas scattered wood lots will be portrayed as light-toned, grainy textured areas on a SLAR image.

Engineering Soil Type

Lacustrine deposits are composed of uniform, stratified, generally fine-textured materials. Particle sizes may range from clay to coarse silts from one deposit to another. Sands are relatively rare. Soil classifications may range from OH to ML under the USCS, but specific classifications usually cannot be inferred from SLAR imagery.

Playa Plain

Drainage

The drainage pattern of a playa plain may approach that of reticulate or centripetal but a pattern of drainage is normally not evident on SLAR imagery.

Topography

Most playa surfaces are very nearly flat and as such exhibit a very dark average areal tone. Medium tones and grainy image textures may be evident on K-band imagery when the playa surface is dry and cupped by cracking.

Land Use

Playa surfaces are normally devoid of vegetation either natural or agricultural.

Engineering Soil Type

Playas normally contain finer-grained sands, silt, and clay which may be inferred to be CL or SM under the USCS.

Alluvial Fan and Apron

Drainage

The gross drainage pattern of alluvial fans is of the distributary fan type with individual channels becoming less distinct at or near the base of a fan. Radial drainage patterns may also be evident. The gross drainage of alluvial aprons is generally a combination of distributary, radial, and parallel patterns. The drainageways commonly terminate in a large trunk drainageway trending at a sharp angle (often nearly 90 degrees) to the apron channels, or to a playa. Low-order drainages of both fans and aprons are generally dendritic but distinctly elongated.

Alluvial fans and aprons develop to some extent in all climates but are most prevalent and best developed in arid regions. Thus, the drainage pattern of alluvial fans and aprons is often expressed on SLAR imagery as discrete tonal units of shadow or medium to light beaded tones from intermittent riparian vegetation. In some cases, only streaks of light or dark tone give evidence of the regional drainage. This is thought to result from significant changes in the particle size of material within the channel as compared to the surrounding terrain. Near a mountain front, light streaks will represent the reflection from large boulders in the channels; but, away from the front, the

material in a channel will be considerably smaller in size and will be represented by dark streaks.

Topography

Alluvial fans and aprons exhibit a blocky form. Topographic highs between adjacent stream channels are generally smooth although sloping away from the mountain front. Fans and aprons which face the SLAR antenna exhibit a medium to high average areal tone depending upon the degree of orthogonality of the slope with the beam of microwave energy and the surface roughness of the slope. Slopes which do not face the antenna will exhibit tones which are more representative of the local surface roughness. The general shape of fans and aprons can be inferred by recognizing a contrast in average areal tone and drainage pattern with respect to the adjacent terrain.

Land Use

Fans and aprons are rarely utilized agriculturally in the United States. Natural vegetation will commonly be concentrated along drainages and, will be expressed as light, discrete tonal elements on a SLAR image.

Engineering Soil Type

Engineering soils of alluvial fans and aprons are highly variable depending upon the type of source bedrock. Thus, an evaluation of regional landform associations must be utilized for their interpretation.

The following generalizations will often aid in the correct interpretation of alluvial fan and apron engineering soil types:

1. The steeper the slope, the coarser the engineering soil material.
2. Finest materials will be found furthest from the source of alluviation.
3. Source areas consisting of fine-grained igneous rocks produce angular fragments of gravel or cobble size as well as fine sand-silt mixtures.
4. Source areas consisting of coarse-grained sedimentary rocks produce subrounded to angular gravels as well as sand-silt mixtures.
5. Source areas consisting of fine-grained sedimentary rocks produce fine-grained materials.

Flood Plains

For purposes of airphoto interpretation, flood plains have been subdivided into environments or ridge and swale, natural levees, backswamp and abandoned water courses, and high-level flood plains. Such subdivisions help reduce the complexity of the general, flood-plain environment. A specific flood-plain feature may contain some or all of these environments and no restriction of relative size is intended. Ridge and swale, backswamp and abandoned courses, and high-level flood plains have been evaluated with respect to general SLAR image parameters.

Ridge and Swale

Drainage

The basic pattern exhibited by a ridge and swale environment is dendritic but is commonly distorted or deranged. Channels may be broadly meandering. Low-order drainage is often collinear, with drainages following arcuate swales. Patterns of drainage are usually expressed as dark, discrete tonal elements representing the specular reflection of microwave energy from water surfaces. Low-order drainages are interpretable with difficulty from contrasts in tone and texture resulting from riparian vegetation.

Topography

The cross-sectional shape is undulating but appears relatively flat on SLAR imagery. No shadows resulting from topographic effects will normally be seen. Ridges and swales may be inferred, however, from contrasts in tone and texture resulting from variations in vegetation.

Land Use

Ridge and swale areas are normally cultivated only when they are relatively old surfaces. They often support dense tree and grassy vegetation types. Only if such an area is in the process of formation would it be relatively vegetation-free. Forest vegetation will produce light tones and a grainy image texture. Grassy areas will produce medium tones and a smooth image texture while bare soil will produce medium to dark tones and a smooth image texture. Agricultural activity will be indicated on a SLAR image as elongated, rectangular field patterns exhibiting variable tones and smooth image textures.

Engineering Soil Type

Ridges normally consist of coarser material than the swales. Ridges might consist of coarse sand or, in some cases, gravel with fine sand, silt, or clay in the swales. Such inferences cannot be made on the basis of SLAR image data but may be possible through the evaluation of regional landform associations.

Backswamp and Abandoned Courses

Drainage

Gross drainage patterns are normally dendritic, but some channel bifurcation of the reticulate type may be expected. Abandoned water courses such as meander cut-offs and oxbows may be present. Patterns of drainage can be recognized as dark, discrete tonal elements resulting from specular reflection of microwave energy from water surfaces or as lineations of light or dark tones resulting from contrasts in vegetation type.

Topography

The cross-sectional shape is undulating but nearly flat. No evidence of relief in the form of radar shadow or tonal change due to topography will be seen on a SLAR image. Any contrast in tone or texture will likely result from variations in vegetation or local surface roughness.

Land Use

These surfaces are normally forested and appear as light-toned, grainy textured areas on a SLAR image. In some places, extensive areas of marsh grass and reeds may occur, especially at the ends of oxbows; and, in such instances, the corresponding SLAR image will exhibit a medium to dark tone and smooth image texture.

Engineering Soil Type

Backswamp and abandoned stream course areas are normally composed of silt and clay materials with a high organic content.

High-level Flood Plain

Drainage

Both the gross and low-order drainage pattern are normally dendritic. However, some traces of previous drainage may exist in the form of collinear or parallel patterns. In general, only the highest-order channels will be recognizable on a SLAR image in the form of discrete tonal elements resulting from specular reflection from water or high return or shadow produced by riparian vegetation.

Topography

The cross-sectional shape is undulating to blocky, normally with low relief. Such an area will exhibit no evidence of relief on a SLAR image.

Land Use

High-level flood plains are normally cultivated and subjected to intense agricultural activity. Rectangular field patterns with boundaries independent of topography can be inferred from a SLAR image. Poorly drained areas may be forested and can be recognized by a relatively light tone and grainy image texture.

Engineering Soil Type

The materials composing a high-level flood plain will generally be fine-grained but may vary from sands to clay. Specific particle sizes cannot be directly inferred from SLAR imagery. The evaluation of regional landform associations and natural vegetation may aid in the interpretation of local soil conditions.

Beach Ridge

Drainage

This landscape is usually too restricted in size to form a gross drainage pattern. Low-order drainages may exist but will seldom be recognizable on a SLAR image.

Topography

The cross-sectional shape is commonly undulating. Evidence of topographic form will consist of light average areal tones on a SLAR image if the slopes tend to face the antenna. Usually, however, evidence of relief is absent on a SLAR image. Planimetric

shapes can be recognized as tonal and textural contrasts with surrounding terrain and by evaluation of regional landform associations.

Land Use

Relatively recent beach ridges, rarely used for agricultural purposes, may support sparse grass or shrubs. Older beach ridges in humid environments may be cultivated or forest covered. In semiarid regions, beach ridges rarely support more than sparse grass or shrubs. Trees or shrubs of significant density will be displayed on a SLAR image with light tones and grainy texture. Grass, on the other hand, will produce medium to dark tones with a smooth image texture.

Engineering Soil Type

Beach ridges normally consist of coarse-grained materials ranging in size from gravel to fine sand. In all cases, radar return, due to particle size of the material alone, would be relatively low. The upper 6 to 12 inches of such materials could usually be correctly inferred to be SP--SM under the USCS classification.

Deltaic Surfaces

Drainage

Distributary drainage patterns are characteristic and may be recognized on SLAR imagery from discrete tonal elements resulting from specular reflection from water surfaces or boundaries and lineations formed by contrasting average areal tones and textures. No evidence of radar shadow produced by the cross-sectional shape of a stream channel would normally be expected.

Topography

Cross-sectional shape is gently undulating, while planimetrically a characteristic shape is formed. No evidence of relief can normally be seen on a SLAR image. An evaluation of contrast of tones and textures coupled with an analysis of adjacent landforms will often establish the planimetric shape.

Land Use

Deltaic surfaces may exhibit a variety of patterns of natural vegetation or agriculture depending upon geographic location and climatic environment.

Engineering Soil Type

Deltaic deposits normally consist of relatively fine-grained material such as sand, silt, or clay. However, the velocity of water entering a lake or sea can greatly influence the particle size of deltaic deposits. Higher velocity water may deposit coarser deltaic materials. The source of alluvial material also contributes to deltaic material sizes. Thus, an evaluation of regional landform associations is helpful in the inference of probable material sizes. In any event, deltaic deposits in humid environments will be somewhat organic.

Folded, Eroded Sedimentary Formations

Drainage

Patterns of drainage are trellis and in many cases asymmetrical. The patterns can be recognized on a SLAR image as discrete tonal elements produced by radar shadow due to topographic effects; by light tones caused by riparian vegetation or stream banks facing the antenna; or by dark tones resulting from the specular reflection of microwave energy from water surfaces.

Topography

Topographic forms consist of linear ridges and/or valleys. Resistant bedrock will form ridges while interbedded rock of less resistance will form valleys. The form can be recognized on a SLAR image from parallel traces of light tones and radar shadow. If topographic form is subdued, contrasts in image tone and texture may indicate topographic linearity.

Land Use

High-relief ridges exhibit little agricultural activity. Valleys may show patterns of cultivation in humid or subhumid environments. In humid environments, ridges are generally forest covered and exhibit a light tone and grainy image texture on a SLAR image. In any environment, slopes facing the antenna produce generally higher returns than do other surfaces.

Engineering Soil Type

Topographically, high ridges or mountains can be inferred to be resistant bedrock in humid environments. Associated sedimentary valleys can be inferred to be less resistant bedrock. Surficial soils will be characteristic of the underlying bedrock. Sandy,

granular soils will develop on sandstone; silty or clayey soils on shale; and clayey soils on limestone in a humid environment.

Volcanic Features – Cones and Flows

Drainage

Cones exhibit a radial drainage pattern. In the case of cinder cones, the drainage density will be low. Lava flows display an intensely developed, rectangular pattern. In the case of either landform, low-order drainage is generally not evident on SLAR imagery. Higher-order drainages will be evidenced as dark, discrete tonal elements of shadow. In some cases, contrasts in tone and texture produced by vegetation will be indicative of drainage pattern.

Topography

Cones are generally sharp crested and may contain calderas. The wide variety of cones can be evaluated as to probable history by their association with adjacent land forms. Flows exhibit a plain to gently undulating surface which may be quite rough at local scales. Topographic form can be inferred from SLAR imagery on the basis of radar shadow and average areal tonal contrasts. Rough lava flows exhibit very light tones and a rough, irregular macro-texture.

Land Use

Geologically youthful cones and flows generally do not support agricultural activity. Older flows and cones may exhibit patterns of cultivation in humid or sub-humid environments. Natural vegetation (trees and shrubs) will tend to grow in porous zones containing moisture and can be recognized on SLAR imagery by light tones and grainy image textures.

Engineering Soil Type

Cones may consist of igneous, extrusive, basic rock or volcanic ash, cinders, and breccia. Determination of specific parent materials can only be inferred by the density of drainage and regional association of landforms. Lava flows consist of basic, igneous, extrusive rock.

UNCLASSIFIED
Security Classification

DOCUMENT CONTROL DATA - R & D		
<i>(Security classification of title, body of abstract and indexing annotation must be entered when the overall report is classified)</i>		
1. ORIGINATING ACTIVITY (Corporate author) U. S. Army Engineer Topographic Laboratories Fort Belvoir, Virginia 22060		2a. REPORT SECURITY CLASSIFICATION Unclassified
		2b. GROUP
3. REPORT TITLE USE OF SIDE-LOOKING AIRBORNE RADAR (SLAR) IMAGERY FOR ENGINEERING SOILS STUDIES		
4. DESCRIPTIVE NOTES (Type of report and inclusive dates) Technical Report prepared by Dr. David J. Barr for USAETL under Contract No. DA-44-009-AMC-1847(X)		
5. AUTHOR(S) (First name, middle initial, last name) David J. Barr		
6. REPORT DATE September 1969	7a. TOTAL NO. OF PAGES 156	7b. NO. OF REFS 104
8a. CONTRACT OR GRANT NO. a. PROJECT NO. 4A623501A854 c. d.	8b. ORIGINATOR'S REPORT NUMBER(S) 46-TR	
8c. OTHER REPORT NO(S) (Any other numbers that may be assigned this report)		
10. DISTRIBUTION STATEMENT This document has been approved for public release and sale; its distribution is unlimited.		
11. SUPPLEMENTARY NOTES		12. SPONSORING MILITARY ACTIVITY U. S. Army Engineer Topographic Laboratories Fort Belvoir, Virginia 22060
13. ABSTRACT The report is concerned with the development and evaluation of techniques of utilizing Side-Looking Airborne Radar (SLAR) imagery for engineering soils studies. The primary objective was the development of a systematic SLAR image interpretation technique. Secondary objectives included an evaluation of methods for quantification of SLAR image textures and radar shadows. SLAR images from a variety of physiographic regions within the United States were evaluated. Systems operating at several wavelengths were represented in the study. Field checking was performed for several of the study sites. Major conclusions from the quantitative analysis and evaluation of the various SLAR images are as follows: 1. It is possible to interpret regional engineering soil types by means of an inference technique based on recognition and evaluation of repetitive, characteristic patterns. 2. "Brute force" SLAR imagery allows a more detailed interpretation than does "synthetic aperture" SLAR imagery. 3. At the wavelengths utilized for the study imagery, the pattern recognition elements were derived as a function of microwave reflection from the first surface of the terrain. 4. The relatively small scale at which SLAR imagery is obtained and the resolution of typical imagery are considered advantageous for regional engineering soil interpretations. SLAR imagery provides a synoptic view of terrain unconfused by minor tonal contrast.		

DD FORM 1473
1 NOV 60

REPLACES DD FORM 1473, 1 JAN 60, WHICH IS OBSOLETE FOR ARMY USE.

155

UNCLASSIFIED
Security Classification

14. KEY WORDS	LINK A		LINK B		LINK C	
	ROLE	WT	ROLE	WT	ROLE	WT
Side-Looking Airborne Radar SLAR Remote Sensing Terrain Analysis Soil Studies Aerial Image Interpretation						